

# *Russian Academy of Sciences*

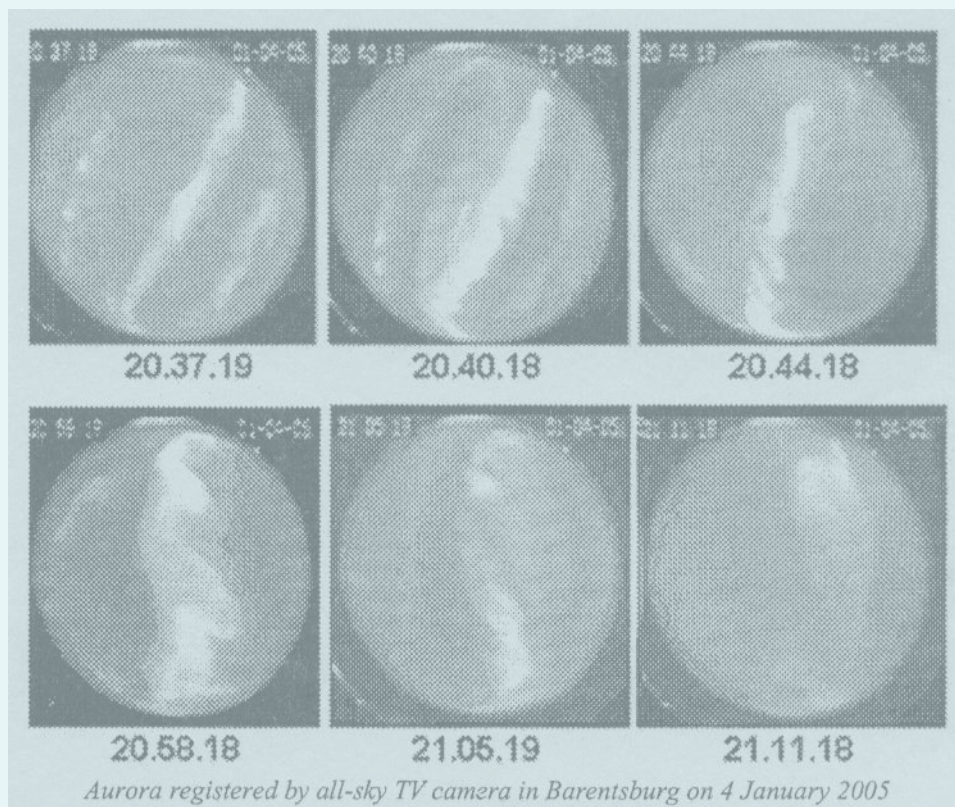
PGI -06-01-121

## PHYSICS OF AURORAL PHENOMENA

29<sup>th</sup> Annual Seminar

27 February - 3 March 2006

### Abstracts



Apatity

2006

*Russian Academy of Sciences*

KOLA SCIENCE CENTER

Polar Geophysical Institute

**PGI -06-01-121**

**PHYSICS OF AURORAL PHENOMENA**

29<sup>th</sup> Annual Seminar

Abstracts

27 February - 3 March 2006

Apatity

2006

The seminar is supported by the  
*Russian Foundation for Basic Research*  
grant 06-05-74008

The organizing committee:

Alexander Yahnin (chair)  
Boris Kozelov  
Michael Beloglazov  
Nadezhda Semenova

Addresses:

**Apatity department**

Fersman str., 14  
Apatity, 184209  
Murmansk region  
Russia

**Murmansk department**

Khalturina str., 15  
Murmansk, 183010  
Russia

The editorial board:

I.V. Golovchanskaya  
N.V. Semenova

E-mail: [seminar@pgi.kolasc.net.ru](mailto:seminar@pgi.kolasc.net.ru)  
<http://pgi.kolasc.net.ru/seminar>

## CONTENTS

### IN MEMORY OF Y. P. MALTSEV

I.I. Alexeev	Magnetic storm as it has been seen by Yuri Maltsev	15
I.V. Artamonov, E. V. Vasilyeva, A.A. Namgaladze, O. V. Martynenko	On the electric potential pattern corresponding to the Maltsev and Ostapenko FAC2 model	15
Y.I. Feldstein, L.I. Gromova, J.U. Kozyra, B.T. Tsurutani, A. Prigancova, I.I. Alexeev, A.E. Levitin, and L.A. Dremukhina	Comparative modeling (by Tsyganenko 96 and 01, and Paraboloid models) of the large-scale distortions in the geomagnetic field during the 24–27 September 1998 major magnetic storm	15
A. Levitin, L. Gromova, L. Dremukhina	Current systems of large-scale geomagnetic variations: Evolution of modeling	16
H. Lichtenegger, J.A. Morente, B.P. Besser	On the altitude dependence of Schumann resonance frequencies	16
A.A. Petrukovich, T.-L. Zhang, W. Baumjohann, R. Nakamura, A. Runov, A. Balogh	Slipping deformation of the plasma sheet magnetic structure	16
S.V. Polyakov	Boundary condition for the field-aligned current on the horizontally non-uniform ionosphere with accounting for Earth's magnetic field inclination	17

### SESSION 1. GEOMAGNETIC STORMS AND SUBSTORMS

A.V. Agapitov	Complex observations of ULF wave packets in the Earth's plasma sheet	21
N.A. Barkhatov, A.E. Levitin, O.M. Tserkovniuk	Analysis of the relation of the SYM, ASYM indices of the ring current magnetic field to the AE (AU, AL) indices	21
L. Biktash	Problems of Dst index simulation	21
L.P. Borovkov, B.V. Kozelov	Proton precipitation during a small substorm on December 16, 2004	22
R.N. Boroyev, S.I. Solovyev, V.A. Velichko, A. Du	Influence of the IMF azimuthal component on the longitudinal location of westward electrojet maximum intensity during magnetic super storms in November 2004	22
I.V. Despirak, B.V. Kozelov, A.G. Yahnin, A.A. Lubchich	The relationship of dissipation energy in the magnetotail and energy of particle precipitation during substorm	22
Yu. V. Kat'kalov, Ya. A. Sakharov, Yu. V. Fedorenko	Data acquisition systems at observatory Lovozero of the Polar Geophysical Institute as a distant segment of communication net	23
N.G. Kleimenova, O. V. Kozyreva, T.A. Kornilova, I.A. Kornilov, J. Manninen, A. Ranta, and K. Kauriste	Night-time magnetic, riometer and auroral disturbances in the late recovery phase of November 2004 superstorm	23

M.V. Klimenko, V.V. Klimenko, V.V. Bryukhanov	Numerical modeling of auroral electrojet during geomagnetic disturbances with particle precipitation included	24
I. A. Kornilov, T. A. Kornilova, O. I. Kornilov	Spatial and temporal dynamic of active polar cap arcs as a special type of breakup	24
I. A. Kornilov, O. I. Kornilov	Searching of optical effects induced by ionospheric HF heating	24
T.A. Kornilova, I. A. Kornilov, O. I. Kornilov	Distinctive features of aurora dynamics at the high latitudes during magnetic storm on January 1-7, 2005	24
B.V. Kozelov, K. Rypdal	Scaling collapse and structure functions in TV data of substorm-time aurora	25
O.V. Kozyreva, N.G. Kleimenova	Dynamics of geomagnetic pulsations, riometer absorption and auroras in the main phase of the November 2004 superstorm	25
L.L. Lazutin	Extreme magnetic storms and storm-substorm relation problems	25
A.E. Levitin, L.I. Gromova, L.A. Dremukhina, E.G. Avdeeva, D.I. Korzhan	Dst-index models: Physical and mathematical aspects of modeling	26
I.N. Myagkova, S.N. Kuznetsov, E.A. Muravieva	CORONAS-F observations of strong magnetic storm-associated electron flux variations in the outer radiation belt of the Earth	26
Thomas Penz, V.S. Semenov, M.F. Heyn, V.V. Ivanova, I.B. Ivanov, H.K. Biernat, C.J. Farrugia, F. T. Gratton	Wave structures excited in compressible Petschek-type magnetic reconnection	27
I.I. Shagimuratov, I.I. Efishov, Yu. Ya. Ruzhin, N.Yu. Tcpenitsyna	Storm-time occurrence of TEC fluctuations associated with polar patches as evidenced from GPS observations	27
M.A. Shukhtina	Quantitative geomagnetic field characteristics at geosynchronous orbit during substorm growth phase	27
V.A. Velichko, I.Ya. Plotnikov, D.G. Baishev, N.G. Skryabin, R.N. Boroyev, A.V. Moiseyev	Geomagnetic "crochet" as a predictor of an intense storm in November 2004	28
O.I. Yagodkina, V.G. Vorobjev	Auroral precipitation dynamics during magnetic storms	28
L.S. Yevlashin	Short-term variations of the intensity of H-alpha hydrogen emission of auroras in the initial period of auroral substorm	28

## **SESSION 2. FIELDS, CURRENTS, PARTICLES IN THE MAGNETOSPHERE**

I. I. Alexeev	Compressed solar wind control of the auroral oval expansion	31
N.A. Barkhatov, A.E. Levitin, S.E. Revunov	Monitoring of polar cap spatial dynamics based on the data from the Greenland chain of magnetic observatories	31
N.P. Dmitrieva	Cross-tail fast flows and their relation to the plasma sheet phenomena	31

Y.I. Feldstein, V.A. Popov, J.A. Cumnock, A. Prigancova, L.G. Blomberg, J.U. Kozyra, B. T. Tsurutani, L.I. Gromova, A.E. Levitin	Auroral electrojets and boundaries of plasma domains in the magnetosphere during magnetically disturbed intervals	32
L.I. Gromova, L.A. Dremukhina, A.E. Levitin, E.G. Avdeeva, D.I. Korzhan	SSt- analysis of hourly geomagnetic field values to determine the variations caused by the Main magnetic field of the Earth and solar activity cycle	32
L.I. Gromova, L.A. Dremukhina, A.E. Levitin, E.G. Avdeeva, D.I. Korzhan	Asymmetry of high-latitude geomagnetic variations, electric fields and currents over the northern and southern polar regions	33
V.M. Gubchenko, H.K. Biernat, M.L. Khodachenko, H.O. Rucker	Dipole and toroidal sources and kinetic description of the far regions of the 3d tails and solar streamers formed by maxwellian plasma flows	33
W. Hausleitner, P. Pesec, G. Kirchner, H. Sünkel	Satellite geodesy – made in Graz	34
G. Kirchner, W. Hausleitner, E. Cristea	AJISAI spin parameter determination using Graz kHz satellite laser ranging data	34
D.B. Korovinskiy, V.S. Semenov, N.V. Erkaev	The theoretical model of the steady-state reconnection in the electron Hall MHD approach	34
T.V. Kozelova, L.L. Lazutin, B.V. Kozelov, N. Meredith, M.A. Danielides	Substorm low-energy particle decrease near the inner edge of the plasma sheet	35
A. E. Kozlovsky	Dayside auroral oval dynamics related to a solar wind pressure pulse and associated IMF disturbances	35
L.L. Lazutin, S.N. Kuznetsov	Solar proton belts in the inner magnetosphere	35
S. I. Solovyev, A. V. Moiseyev, K. Yumoto, M. Engebretson, A. Du	Magnetospheric-ionospheric response to variations in the solar wind dynamic pressure during positive IMF Bz and a sharp change of IMF By direction	36
S. I. Solovyev, A. V. Moiseyev, M. Engebretson, K. Yumoto, A. Du	Geomagnetic sudden impulse characteristics depending on the IMF orientation	36
G.V. Starkov, V.G. Vorobjev, L.I. Gromova, O.I. Yagodkina, Ya.I. Feldstein	Mapping of auroral precipitation boundaries of various types into the magnetosphere	37
M.V. Uspensky, A.V. Koustov, S. Nozawa	Ion acoustic speed and STARE velocity at the large flow angles	37
M.A. Volkov, N.Yu. Romanova	Magnetospheric-ionospheric convection for the open magnetospheric model	38
V.G. Vorobjev, I.A. Kornilov, T.A. Kornilova, B.V. Kozelov	Nighttime subvisual aurorae in high latitudes	38
L.M. Zelenyi, H.V. Malova, I.V. Mingalev, O.V. Mingalev	Self-consistent simulation of 1D3V current sheet using macroparticle technique	38

### SESSION 3. WAVES, WAVE-PARTICLE INTERACTION

O.M. Chugunova, V.A. Pilipenko, M.J. Engebretson, A. Rodger	Seasonal and diurnal dependence of Pc3 and Pc4 geomagnetic pulsation power and background noise power at very high latitudes	41
A.G. Demekhov, V.Y. Trakhtengerts, M.J. Rycroft and D. Nunn	Cyclotron acceleration of radiation belt electrons by whistler-mode waves with varying frequency	41
I.V. Despirak, A.A. Lubchich, V.Y. Trakhtengerts	Excitation of Alfvén vortices in the ionosphere by the magnetospheric convection	41
E.N. Fedorov, V.A. Pilipenko, V.V. Vovchenko	Alfvén wave interaction with a turbulent layer	42
I. V. Golovchanskaya, O. V. Mingalev	Solution of the wave equation for the ballooning waves in the magnetotail	42
I. V. Golovchanskaya	Ballooning wave propagation in the case of finite $k_{\parallel}$ included	42
V.S. Ismagulov, Yu.A. Kopytenko, N.A. Semenov	2D distributions of amplitudes, gradients and phase velocities of geomagnetic pulsations	42
B.V. Kozelov, E.E. Titova, F. Honary, S. Marple	Principal component analysis of simultaneous IRIS and TV observations of pulsating patches	43
B.V. Kozelov, I.V. Golovchanskaya	Scaling of electric field fluctuations associated with the aurora during positive $B_z$ IMF	43
B.V. Kozelov, A.G. Demekhov, E.E. Titova, V.Y. Trakhtengerts, O. Santolik, E. Macusova, M. Parrot, N. Cornilleau-Wehrlin	Variations of chorus source location: Comparison of Cluster data and the backward-wave oscillator model	44
O. G. Onishchenko, O. A. Pokhotelov, M. A. Balikhin, R. A. Treumann	Magnetosonic solitons in high- $\beta$ non-Maxwellian space plasmas	44
O. A. Pokhotelov, O. G. Onishchenko	Shell distribution instability upstream to the terrestrial bow shock	44
O. A. Pokhotelov, O. G. Onishchenko, M. A. Balikhin, R. A. Treumann	Nonlinear ion-cyclotron waves in high pressure plasmas: Kinetic and fluid description	45
S. V. Polyakov	Global ionospheric Alfvén resonator (GIAR), a new near-Earth ULF resonance system	45
V.C. Roldugin, A.V. Roldugin, N.G. Kleimcnova, O.V. Kozyreva	Pc5 pulsations on the ground, in the magnetosphere and in electron precipitation: The event of 19 January 2005	45
V. C. Roldugin, A. N. Vasiljev and A.A. Ostapenko	Comparison of Schumann resonance parameters in horizontal magnetic and electric fields according to observations in the Kola Peninsula	45
V.Y. Trakhtengerts, A.G. Demekhov, E.E. Titova, B.V. Kozelov, O. Santolik, E. Macusova, D. Gurnett, J. Pickett and M. J. Rycroft	A mechanism of frequency spectrum formation for VLF chorus and its verification by Cluster data	46

N. Yagova, N. Romanova, V. Pilipenko, E. Fedorov, N. Crosby	Geostationary electrons and geomagnetic ULF fluctuations in the Pc5 range: Cross-correlative analysis	46
T.A. Yahnina, A.G. Yahnin, T. Bösinger, A.N. Voronin	Proton precipitation and Pc2 pulsations at the recovery phase of the magnetic storm	46
N.A. Zolotukhina, J. Cao, O.V. Chugunova	On the “convective” model of generation of IPDP pulsations	47

#### SESSION 4. THE SUN, SOLAR WIND, COSMIC RAYS

Yu.V. Balabin, E.V. Vashenyuk	The advanced technique of determination of relativistic solar proton parameters from ground based observations	51
Yu.V. Balabin, B.B. Gvozdevsky, L.I. Schur, E.V. Vashenyuk	The new data acquisition unit for neutron monitors in Apatity and Barentsburg	51
N.A. Barkhatov, S.E. Revunov	Classification of abrupt changes of the interplanetary medium parameters by a method of artificial neural networks	51
I. V. Getselev, V. P. Okhlopkov, M. V. Podzolko	Solar cosmic ray fluxes in the Earth’s orbit	52
S.N. Karpov, L.I. Miroshnichenko, E.V. Vashenyuk	The muon bursts with energy above 200 GeV recorded during GLE events	52
Z.M. Karpova, S.N. Karpov and A.B. Chernyaev	Using extensive air shower detectors for the study of solar cosmic rays	52
M.B. Krainev, A.V. Belov, R.T. Gushchina, V.G. Yanke	On the long-term variations of the medium energy galactic cosmic ray intensity according to the balloon and neutron monitor data at Kola Peninsula and Moscow region	53
M.B. Krainev	On the behavior of medium energy galactic cosmic ray intensity in the outer heliosphere ( $r=75-97$ AU)	53
M. Leitner, C. J. Farrugia, H. K. Biernat, N. V. Erkaev, F. T. Gratton	Evolution of interplanetary magnetic clouds	54
N.A. Lotova, K.V. Vladimirsky, V.N. Obridko	Structure of solar wind flows at maximum and decline of the 23d solar cycle	54
A.A. Lubchich, I.V. Despirak, V.B. Belakhovsky	Alfven wave interaction with a fast shock	54
I.N. Myagkova, M.I. Panasyuk, S.N. Kuznetsov, B.Yu. Yushkov, E.A. Muravieva, L.I. Starostin, T.A. Ivanova, I.A. Rubinshtein, N.N. Vedenkin, N.A. Vlasova	Geomagnetic cutoff variations during solar energetic particle events of May and June 2005 : “Universitetskiy-Tatyana” and CORONAS-F satellite data	55
A. I. Podgorny, I. M. Podgorny, N. S. Meshalkina	Current sheet of the solar corona as a source of solar flare radio-emission	55
I.M. Podgorny, A. I. Podgorny	Hard X-rays generation at a solar flare	56

A.B. Struminsky	Multiple proton acceleration at the Sun and their scatter-free propagation to the Earth on 20 January 2005	56
T.E. Val'chuk	Seasonal variations of geomagnetic disturbance inferred from aa-index analysis and solar activity	56
E.V. Vashenyuk, Yu.V. Balabin, L.I. Miroshnichenko	Relativistic solar cosmic rays in the GLE of 23 February 1956. New study	57
E.V. Vashenyuk	Relativistic solar cosmic rays. Review of recent results	57
V.L. Zverev, T.A. Hviuzova, S.V. Tolochkina	Some characteristics of auroras under the interaction of the Earth's magnetosphere with solar wind streams from different solar sources	57

## **SESSION 5. IONOSPHERE AND UPPER ATMOSPHERE**

A.V. Agapitov, S.I. Musatenko	Corpuscular mechanism of Es layer formation	61
M.Yu. Andreev, G.I. Mingaleva and V.S. Mingalev	Simulation of diurnal variations of the oblique HF propagation along a high-latitude meridional route	61
L. Biktash	Space weather effects in the generation of the equatorial scintillation during geomagnetic storms	61
U. Brändström, I. Sandahl, T. Sergienko, A. Pellinen-Wannberg, B. Gustavsson, M. Rietveld, T. Aso and Å. Steen	ALIS - highlights, status and future plans	62
S.A. Ishanov, V.V. Medvedev, V.A. Zaleskaya	Injection of H <sub>2</sub> O molecules into the F-region of the Earth's ionosphere	62
S.A. Ishanov, V.V. Medvedev, V.G. Tokar, Y.S. Zharkova	Possibility of applying the mathematical models to the problems of radiowave propagation	62
A.S. Kirillov	Electronically excited molecular nitrogen and molecular oxygen at high and low altitudes of the high-latitude ionosphere	63
M.A. Knyazeva, A.A. Namgaladze	A model study of seasonal and solar activity variations of the enhanced electron density regions in the night-time ionospheric F2-layer and plasmasphere	63
E.A. Kopytenko, V.S. Ismagilov, Yu.A. Kopytenko, A.B. Pashin	First measurements of the gradients of ULF magnetic field from auroral sources with a gradiometer with a small spaced units	64
A.L. Kotikov, S.A. Shibkov, V.V. Vinnikov	The possibility of small-scale field-aligned currents generation by HF-transmitter operation	64
Y.N. Kulikov, H. Lammer, H.I. M. Lichtenegger, T. Penz, and H.K. Biernat	Solar radiation and particle induced effects on the early Martian atmosphere and loss	64
O.V. Martynenko, M.M. Gladkikh, I.V. Artamonov	Application of the object-oriented approach in upper atmosphere modeling	65
V.V. Medvedev, Y.S. Zharkova	Mathematical modeling for the processes upper atmosphere and ionosphere	65

V.V. Medvedev, Y.S. Zharkova	Numerical model of the heat budget of the Earth's upper atmosphere	66
A.A. Namgaladze, E.N. Doronina, M. Förster	The role of electric fields and magnetospheric electron precipitations in the formation of the equatorial total mass density minimum	66
A. Pashin, and A. Mochalov	Influence of neutral species on artificial magnetic pulsation excitation	67
V.C. Roldugin, B.V. Kozelov	Schumann frequency decrease during PCA depending on proton flux rigidity	67
A. Schekotov, O. Molchanov, E. Fedorov, V. Chebrov, V. Sinitsin, E. Gordeev, G. Belyaev, M. Hayakawa	ULF electromagnetic emission from the atmosphere perturbed by seismicity	67
A.I. Semenov, N.N. Shefov	Re-analysis of long-term hydroxyl rotational temperature trend based on the measurements in Spitsbergen	67
A.I. Semenov and N.N. Shefov	Long-term variations of a temperature and structure of the middle atmosphere within last century	68
N.V. Semenova, A.G. Yahnin	Substorm effect on resonant structures in spectra of the background magnetic noise	69
T. Sergienko, I. Sandahl, B. Gustavsson, U. Brändström, M. Rietveld and T. Leyser	Auroral arc triggering by powerful HF ionosphere heating	69
V. V. Surkov	ULF electromagnetic noise due to random variations of background atmospheric current	69
V.D. Tereshchenko, E.B. Vasiljev, O.F. Ogioblina, V.A. Tereshchenko, A.P. Osepian, S.M. Chernyakov	Response of the lower polar ionosphere to X-class solar flares in January 2005	69
V.D. Tereshchenko, A.P. Osepian, O.F. Ogioblina, E.B. Vasiljev, V.A. Tereshchenko	Change of the polar ionosphere structure during solar flares. Experiment and model	70
V.D. Tereshchenko, E.B. Vasiljev, O.F. Ogioblina, V.A. Tereshchenko, S.M. Chernyakov	An ionospheric effect of a lunar echo from a space gamma-splash	70
Е.Н. Ермакова, Д.С. Котик, С.В. Поляков	Исследование зависимости параметров резонансной структуры спектра (РСС) фонового шума от направления на источник для плоскостной модели ионосферы с наклонным магнитным полем	71
Е.Н. Ермакова, Д.С. Котик, С.В. Поляков	Механизм формирования широкополосного максимума в спектре фонового шума на частотах 2-6 Гц	71
О. А. Молчанов, А. Ю. Щекотов	О механизмах взаимодействия литосфера-атмосфера-ионосфера	72
Н.Г. Сергеева, Е.Б. Васильев, О.Ф. Оглоблина	Исследование параметров высокоширотной ионосферы методом разнесенного приема	72

## SESSION 6. LOW ATMOSPHERE, OZONE

A.I. Akhmetov, Yu.V. Fedorenko, M.I. Beloglazov, V.A. Shishaev	Some results of atmospheric currents and acoustic-gravitational waves measurements in Apatity	75
M.I. Beloglazov, L.A. Pershakov, G.P. Beloglazova	On the influence of geomagnetic activity on atmospheric intensity at the Kola Peninsula	75
V.I. Demin, M.I. Beloglazov	On the atmosphere stratification effect in the ground-level ozone concentration in the Kola Peninsula	75
V.I. Demin, N.F. Elansky, I.A. Senik	Changes in the ozone contents at the Kislovodsk mountain observatory during the foehns caused by the air crossing of the Big Caucasian ridge	76
A.A. Krasilnikov, Y.Y. Kulikov, V.G. Ryskin	Monitoring of stratospheric ozone in Arctic from a board icebreaker «Kapitan Dranitsyn»	76
I.V. Mingalev and V.S. Mingalev	On the influence of the non-spherical form of the Earth on the global neutral wind system in the lower and middle atmosphere	76
O.A. Tarasova, G.I. Kuznetsov, N.F. Elansky	Impact of dry deposition on the surface ozone variability	77
V.Ye. Timofeev, L.I. Miroshnichenko, S.N. Samsonov, N.G. Skryabin	Synchronous manifestations of 160-min pulsations of the ground pressure in the area of Russia	77
A.M. Zvyagintsev, I.N. Kuznetsova	Regression relations of surface ozone and meteorological parameters and possibilities of surface ozone forecasting	78
Yu. L. Zyuzin 1, V.I. Demin	On climatic variations in the Khibiny mountains	78
A.B. Агапитов, А.В. Грицай, А.М. Евтушевский, Г.П. Милюневский	Планетарные волны в общем содержании озона южной полярной области	78
Б.Д. Белан	Многолетние вариации приземной концентрации озона и их возможные причины	79
Б.Д. Белан	Самолетные технологии в исследовании окружающей среды и их применение на примере Норильска	80
В.И. Демин, А.М. Звягинцев, И.Н. Кузнецова, О.А. Тарасова	О контроле содержания озона в приземном слое на территории Российской Федерации	80
Т.И. Сысоева, С.П. Черников	Решение фундаментальных и прикладных задач по изучению околоземного космического пространства с помощью воздухоплавательной техники	81

## SESSION 7. HELIOBIOSPHERE

N.K. Belisheva, H.K. Biemat, H. Lammer, C.S. Cockell	How can geomagnetic reversals be related to biological evolution?	85
---	---	----

S. Chernouss, N. Perevozchikov, V. Shishaev, O. Antonenko, A. Mikhaylov, N. Belisheva	Investigation of sensitivity and noise characteristics of the bioeffective UV radiation sensors in field conditions	85
A.G. Kanatjev, O.I. Shumilov, E.A. Kasatkina, I.Yu. Kirtsideli	A measuring complex for tree-rings analysis	86
P.A. Kashulin, N.V. Kalachveva	Some contemporary patterns in long-term global dynamics of terrestrial biota suggesting geophysical mediation	86
A.E. Levitin, L.I. Gromova, L.A. Dremukhina, E.G. Avdeeva, D.I. Korzhan	Quantitative description of geomagnetic activity for study of heliogeomagnetic factors influence on the biosphere	87
S.I. Mazukhina, D.B. Denisov	Reconstruction of natural water ionic composition, forming within Khibiny massif	87
I.N. Perminova, V.S. Krestov, A.L. Kosova, M.V. Shulina	Mortality dynamics assessment during 22 <sup>nd</sup> -23 <sup>d</sup> 11-year solar cycles in the North European region	88
I.N. Perminova, E.V. Perminova, M.N. Yakovleva	Influence of geomagnetic fields on ability of human cells to repair DNA damage	88
O.I. Shumilov, E.A. Kasatkina, N.V. Lukina, I.Yu. Kirtsideli, A.G. Kanatjev	Dendroclimatic potential of the oldest juniper trees at Kola Peninsula	88
Author index		90

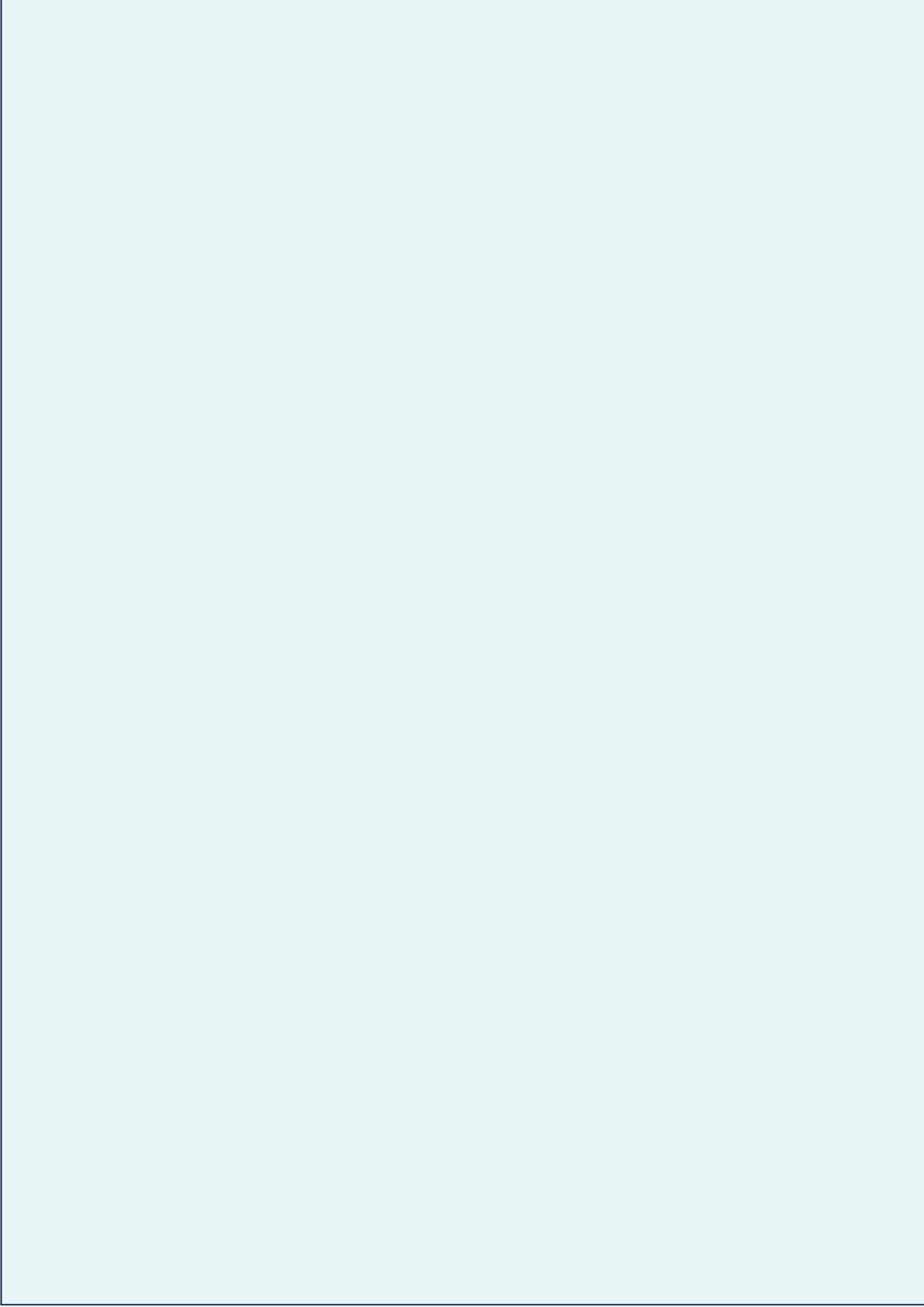


*In memory of Y. P. Maltsev*



**Yuri Pavlovich Maltsev**

**(12.10.1945 -03.06.2005)**



## **Magnetic storm as it has been seeing by Yuri Maltsev**

I.I. Alexeev (*Skobeltsyn Institute of Nuclear Physics, Lomonosov Moscow State University, Leninskie Gory, Moscow 119992, Russia*)

Magnetic storm is a most powerful active phenomenon in the magnetospheric dynamics. It is presented by a strong reconfiguration of the Earth's magnetosphere. The physical models, which described ring current particle injection and the sources of the depression of the main Earth's magnetic field on the ground had been studied by Yuri Maltsev for a long time. More than ten years ago (at 1993), he put forward a new idea about the crucial role of the magnetotail current sheet for the observed storm-time profile of the Dst-variation. The last review by Yuri Maltsev, which has been published in *Space Science Review* on February 2004, described these points in detail. Recent published results on the dynamics of severe magnetic storms are discussed.

## **On the electric potential pattern corresponding to the Maltsev and Ostapenko FAC2 model**

I.V. Artamonov<sup>1</sup>, E.V. Vasilyeva<sup>1</sup>, A.A. Namgaladze<sup>1,2</sup>, O.V. Martynenko<sup>1</sup>

<sup>1</sup>*Murmansk State Technical University*

<sup>2</sup>*Polar Geophysical Institute, Murmansk*

*e-mail: namgaladze@mstu.edu.ru*

Functioning of the magnetospheric block of the global numerical model of the Earth's upper atmosphere (UAM) has been analyzed. The hot ion concentration, velocity, pressure and Region 2 field-aligned currents (FAC2) were calculated in this block by solving the system of MHD equations for plasma sheet ions.

The input parameters of the magnetospheric block include the initial density and pressure distributions and boundary conditions for the electric potential. The FAC2 are the output of the magnetospheric block and they are used to calculate the potential. For the calculations we selected the initial pressure distribution in such a way that the simulated FAC2 were consistent with those proposed by Maltsev and Ostapenko, with FAC2 amplitude of  $1e-12$  A/cm<sup>2</sup> and FAC2 location near 61 degree magnetic latitude. The cross polar cap potential drop was taken as 60 kV. The calculated potential distribution was a classic two-vortex pattern without any distinct visible shielding effect.

Then the calculations were repeated without FAC2. The result was nearly the same. This shows that the obtained Region 2 field-aligned currents don't influence the potential distribution practically.

The third version was realized, in which the simulated FAC2 were doubled. In this case the electric field potential differed significantly from the both previous runs. The classic potential pattern became corrupt. Two large 'petals' of the opposite sign appeared around midnight from the pre-midnight and post-midnight sides. Such a pattern appears to be quite in agreement with incoherent scatter data from Millstone Hill on 15-16 April 2002. The primary electric field, corresponding to the Region 1 field-aligned currents, generates the FAC2 and corresponding secondary electric field. The doubling of these currents results in increase of the secondary field and this field becomes comparable and even larger than the primary field. As a result, the nightside zonal plasma flow becomes converging near midnight instead of being diverging, in agreement with the observations.

This work was supported by the grant N 05-05-97511 of the Russian Foundation for Basic Research.

## **Comparative modeling (by Tsyganenko 96 and 01, and Paraboloid models) of the large-scale distortions in the geomagnetic field during the 24–27 September 1998 major magnetic storm**

Y.I. Feldstein<sup>1</sup>, L.I. Gromova<sup>1</sup>, J.U. Kozyra<sup>2</sup>, B.T. Tsurutani<sup>3</sup>, A. Prigancova<sup>4</sup>, I.I. Alexeev<sup>5</sup>, A.E. Levitin<sup>1</sup>, and L.A. Dremukhina<sup>1</sup>

<sup>1</sup>*Institute of Terrestrial Magnetism, Ionosphere and Radio Wave Propagation, Troitsk, Russia.*

<sup>2</sup>*Space Physics Research Laboratory, University of Michigan, Ann Arbor, Michigan, USA.*

<sup>3</sup>*Jet Propulsion Laboratory, Pasadena, California, USA.*

<sup>4</sup>*Geophysical Institute, Slovak Academy of Sciences, Bratislava, Slovakia.*

<sup>5</sup>*Institute of Nuclear Physics, Moscow State University, Moscow, Russia.*

A new self-consistent version of a time-dependent magnetospheric paraboloid model is presented and tested on the 24–27 September 1998 magnetic storm interval. The model uses DMSP satellite data to identify the location of the inner boundary of the magnetotail current sheet and the magnetic flux in the lobes, and their variations with time.

### *In memory of Y.P. Maltsev*

These inputs along with the upstream solar wind dynamic pressure and IMF Bz values are used to iteratively model the Earth's field during the storm. The results obtained are: (1) model tail current field strength at the Earth's surface is close to that of the ring current; (2) the movement of the tail current sheet inward to  $L = 3.5-4.0$  at storm maximum is consistent with geosynchronous magnetic field data; (3) at the Earth's surface the Chapman-Ferraro magnetopause current field is almost equal at storm maximum to the field of the tail current, thus the fields from the two systems are nearly cancelled; (4) the magnetic flux in the lobes nearly doubles in the course of magnetic storm main phase, as compared to the magneto-quiet interval, just before the storm onset; (5) the large-scale internal magnetospheric currents (the ring current, field-aligned currents, and magnetotail current) have a significant influence on the shape and size of the magnetosphere.

### **Current systems of large-scale geomagnetic variations: Evolution of modeling**

A. Levitin, L. Gromova, L. Dremukhina (*Institute Terrestrial Magnetism, Ionosphere and Radio Wave Propagation, Troitsk, Moscow region, Russia*)

Magnetic field in near-Earth space is generated by the current systems, with energy supply directly from the Sun (conductivity), from the interplanetary environment (electric field, plasma), and from the surface layer (dynamo-wind). Rapid progress in modeling the electric fields and current systems responsible for the spatio-temporal distribution of large-scale geomagnetic variations has been made at different Institutes and scientific centers for the last decades. Bright ideas are used to develop new models, to advance the theoretical background, to improve the techniques of calculations. All this refers to the problem of fitting the magnetosphere-ionosphere current systems to the magnetic field observations both on the ground and aboard spacecraft as well as to the inverse problem of reconstructing magnetosphere-ionosphere current systems from geomagnetic data. The research team of the Polar Geophysical Institute of Kola Scientific Center of RAS has always been an active participant of this activity. Yu. P. Maltsev was one of the leading scientists of the research team. His ideas and proposals were original and had a strong impact on the concepts about the sources of Earth's magnetic field variations. We present a review of history and of present state of near-Earth current system modeling. At the same time, we emphasize the studies by Yu. P. Maltsev, which are the most important for modeling Sq-variation of the geomagnetic field, high-latitude variations parameterized by the solar wind and interplanetary magnetic field and Dst-variation during magnetic storms. This study is supported by INTAS grant No 03-51-5359 and RFBR grant 05-05-65196

### **On the altitude dependence of Schumann resonance frequencies**

H. Lichtenegger<sup>1</sup>, J.A. Morente<sup>2</sup> and B.P. Besser<sup>1</sup>

<sup>1</sup>Space Research Institute, Austrian Academy of Sciences, Graz, Austria

<sup>2</sup>Department of Applied Physics, University of Granada, Granada, Spain

Based on a realistic conductivity profile, the numerical modelling of the electromagnetic wave propagation in the cavity bounded by the Earth's conducting surface and the ionosphere has shown that Schumann frequencies depend on height. At altitudes above 70 km, where the conductivity becomes high, a gradual decrease in the frequency has been found. This can be attributed to the fact that although the peaks for the total electromagnetic energy stored inside the cavity define a unique value for each Schumann resonance, the experimental determination of Schumann frequencies related with the maxima in the amplitude of the electromagnetic field Fourier transform spectrum is sensitive to the conductivity profile and will thus change with altitude. We show that this frequency shift can be obtained by using a simple analytical model for the Earth-ionosphere cavity.

### **Slipping deformation of the plasma sheet magnetic structure**

A.A. Petrukovich<sup>1</sup>, T.-L.Zhang<sup>2</sup>, W. Baumjohann<sup>2</sup>, R. Nakamura<sup>2</sup>, A. Runov<sup>2</sup>, A. Balogh<sup>3</sup>

<sup>1</sup>Space Research Institute, Moscow, Russia

<sup>2</sup>Space Research Institute, Austrian Academy of Sciences, Graz, Austria,

<sup>3</sup>Imperial college, UK

Cluster observations revealed an abundance of crossings of significantly inclined current sheets in the magnetotail. We determine the magnetic configuration of some such crossings, observed during quiet conditions. These waves

appear to move azimuthally and can be interpreted as relative (almost vertical) slipping motion of the neighboring magnetic flux tubes in the inner plasma sheet, rather than the large-scale flapping. In particular, wavy sheet motions with significant inclination changes can be explained with the mechanism, proposed by Golovchanskaya & Maltsev, 2005.

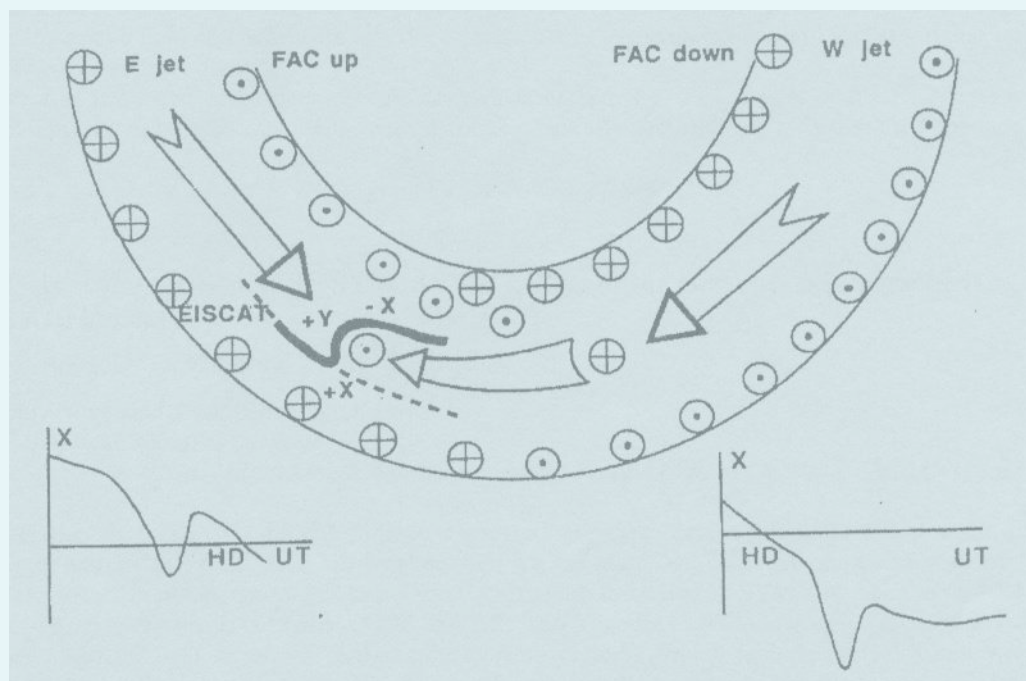
**Boundary condition for the field-aligned current on the horizontally non-uniform ionosphere with accounting for Earth's magnetic field inclination**

S.V. Polyakov (*Radiophysical research Institute, Nizhny Novgorod, Russia* )

A generalization of the well-known ionospheric boundary conditions for the Alfvén wave, for which correct formulation Yu.P. Maltsev is renowned, has been made. The importance of the works by Yu.P. Maltsev on boundary condition formulations for the study of magnetosphere-ionosphere coupling is discussed.



# Geomagnetic Storms and Substorms





## **Complex observations of ULF wave packets in the Earth's plasma sheet**

A.V. Agapitov (*Kiev national University after T. Shevchenko, Ukrainian centre of Antarctic*)

Based on the observations of the spacecraft Equator-S, Geotail, Interball-1, AMPTE C, ground-based magnetometer network CANOPUS and database INTERMAGNET, we report on the ULF wave events of Ps6 type. The perturbations propagate earthward and across the tail toward the flanks. The waves are of the Alfvén type but have a magnetosonic component. The most pronounced events are associated with the enhanced geomagnetic activity, i.e. substorms of different intensity. The time of registration and reconstruction of the dynamics indicate a temporal and spatial relation to substorm expansion. By performing coordinated magnetic measurements in the plasma sheet and at magnetically conjugated points on the ground, we have estimated the sizes and propagation velocities of the structures. The transverse to the magnetic field sizes are 5-10 Re. At distance of 15-20 Re in the magnetotail, the velocities of propagation perpendicular to the magnetic field are 6 – 12 km/s and increase toward the Earth, being consistent with the values of plasma drift velocity. Assuming a plane plasma sheet, we have found the solution of the Shredenger type equation in the form of envelope solitons. Time-and-frequency characteristics of the wave structure correspond to those of magnetosonic solitons in the plasma sheet. The perturbations, i.e. magnetic tubes with disturbed parameters, form global magnetospheric structures. Mapping on the auroral oval, they can be registered on the ground in the visual auroral emissions. For example, a passing of Ps6 packet in October 1996 was registered at Gilian station (CANOPUS) both in magnetic and proton (496 nm emission) data. It has been revealed that the most intense events occur on the flanks of the plasma sheet. Maximum occurrence rate also refers to the flanks. Thus it can be supposed that the low-frequency wave packets form in the magnetotail by sharp variations in the geomagnetic field and propagate nearly perpendicularly to the magnetic field earthward and toward the flanks in the form of envelope solitons.

Statistics of the event occurrence reveals dawn-dusk asymmetry, with a lack of the ULF events in the nighttime sector. This might be associated with ionospheric conductivity peculiarities, affecting the boundary conditions of the problem.

The work was partly supported by the grant CRDF №UKP2-2644-KV-05

## **Analysis of the relation of the SYM, ASYM indices of the ring current magnetic field to the AE (AU, AL) indices**

N.A. Barkhatov<sup>1,2</sup>, A.E. Levitin<sup>3</sup>, O.M. Tserkovniuk<sup>1</sup>

<sup>1</sup> *Nizhniy Novgorod State Pedagogical University*

<sup>2</sup> *Radiophysical Research Institute (NIRFI)*

<sup>3</sup> *Institute of Terrestrial Magnetism, Ionosphere and Propagation of Radio Waves (IZMIRAN) of RAS*

The relation of the SYM, ASYM indices, characterizing ring current magnetic field, to the indices of auroral electrojet activity AE (AU, AL) has been studied for the main and recovery phases of magnetic storms in 2000-2001. At the main phase, the largest correlation coefficients are between SYM and AU, ASYM and AU, ASYM and AL; at the recovery phase between ASYM and AE, ASYM and AL, SYM and AE. Thus, the asymmetry in the ring current magnetic field is related to particular current systems, which include eastward and westward electrojets during the whole magnetic storm. The symmetric part of the magnetic disturbance at the storm main phase is associated with the current system, which includes the eastward electrojet; at the recovery phase it is related to the integral current activity in the whole auroral oval.

The correlation, analysis that we have conducted suggests a scheme of equivalent current systems, which is consistent with the revealed peculiarities in magnetic disturbance behavior. In addition to the correlation analysis, performed without time delay between the studied quantities, the analysis with the time delay of half an hour through two hours between AE (AU, AL) and SYM, ASYM was carried out. It was shown that the development of the symmetrical part of the magnetic disturbance produced by the ring current lags behind the development of the westward electrojet, while its asymmetric part develops simultaneously with the westward and eastward electrojets.

## **Problems of Dst index simulation**

L. Biktash (*Institute of Terrestrial Magnetism, Ionosphere and Radio Wave Propagation, Troitsk, Moscow Region, Russia*)

An overview of Dst index simulation problems is presented. The results of our study of the rate of the energy input to the ring current in the main phase of magnetic storms versus the Y component of the solar wind electric field are shown for two last solar cycles. For the last solar cycle, the rate of energy input Q to the ring current is calculated for the wide range of the solar wind electric field (up to 40 mV/m}. It is shown that the relationship between Q and

## ***Geomagnetic storms and substorms***

$E_y$  remains linear for the great values of  $E_y$ . With our earlier simulation technique developed, the functions describing the rate of energy input into the ring current, the time of decay and other parameters of the ring current, as well as the Dst index, are calculated.

### **Proton precipitation during a small substorm on December 16, 2004**

L.P. Borovkov, B.V. Kozelov (*Polar Geophysical Institute, Apatity, Murmansk region, 184209 Russia*)

Hydrogen Balmer alpha emission was observed during a small substorm event on December 16, 2004 (the onset at ~ 20:35UT) with a spectrograph in Apatity (67.58 N, 33.31 E). This event was also well documented by coordinated ground-based optical and riometer observations at Lovozero observatory (67.97 N, 35.02 E). The dynamics of electron and proton precipitation during this event is discussed with taking into account the observed spatial-temporal manifestations in aurora: the breakup arc, hydrogen band, WTS, N-S forms, etc.

### **Influence of the IMF azimuthal component on the longitudinal location of westward electrojet maximum intensity during magnetic super storms in November 2004**

R.N. Boroyev, S.I. Solovyev, V.A. Velichko (*Institute of Cosmophysical Research and Aeronomy, Yakutsk, Russia*)  
A. Du (*Institute of Geology and Geophysics, Beijing, China*)

Spatial-temporal distribution of the westward electrojet in the night sector of the Northern Hemisphere versus IMF orientation has been investigated for a geomagnetic storm on 9-10 November 2004 by using ground geomagnetic observations. It is shown that during magnetic disturbances the intensity maximum of the westward electrojet is localized in the evening (morning) sector under IMF  $B_y < 0$  (IMF  $B_y > 0$ ). With positive IMF  $B_y$  increasing, the region of maximum intensity shifts toward morning hours. It is supposed that a possible reason of such a dynamics may be strengthening of the field-aligned currents at the cusp latitudes, whose direction is governed by IMF  $B_y$  orientation.

This work was supported by the Russian Foundation for Basic Research, project no. 03-05-39011-GFEN and partially by the programm of presidium of RAS no. 16 p.3

### **The relationship of dissipation energy in the magnetotail and energy of particle precipitation during substorm**

I.V. Despirak, B.V. Kozelov, A.G. Yahnin, A.A. Lubchich (*Polar Geophysical Institute, Apatity, Russia*)

The substorm explosive phase is characterized by formation of the auroral bulge in the night-side ionosphere, the area of the auroral bulge can be considered as a measure of the energy of electron precipitation. In the magnetosphere the explosive phase is associated with dissipation of the magnetic energy in the tail lobes. A measure for magnetic energy (more correctly, for the energy density) is the magnetic pressure in the tail lobe or the total pressure in the plasma sheet. To investigate the relationship between these quantities, the Polar data have been combined with the Geotail data. The energy of particle precipitation was determined by the Ultra Violet Imager onboard Polar (images obtained in the LBHL (1600-1800 Å) emission with time resolution from 0.5 min to 3 minutes). We calculated the area of the auroral bulge defining it as a region which luminosity level exceeds by 25% the luminosity of the auroral oval before the substorm onset, the integrated area being  $S = \int s(t)dt$  and integrated energy  $E = \int w(t)dt$ , where  $s(t)$  and  $w(t)$  are the auroral bulge area and the energy deposition into this area by auroral electrons at time  $t$ , the integration performed over the lifetime of auroral bulge. The total pressure  $P_{total}$  decrease was estimated from the Geotail plasma and magnetic data by  $P_{total} = P_{mag} + P_{thr}$ . It is shown that the value of the total pressure decrease in the magnetotail is proportional to the integrated area  $S$  and integrated energy  $E$ , that is, the value of dissipation energy in the magnetotail is proportional to the energy of particle precipitation in the ionosphere.

According to *Uritsky et al. (2002)*, the integrated area of a "patch" of enhanced auroral intensity is proportional to the energy of electron precipitation, but this result was obtained without specifying the nature of the "patch". We have verified this result for such a specific object as the auroral bulge by showing that the integrated auroral bulge area  $S$  is directly proportional to the integrated energy  $E$  of particle precipitation.

*Uritsky, V. M, A. J. Klimas, D. Vassiliadis, D. Chua, and G. Parks, Scale-free statistics of spatiotemporal auroral emissions as depicted by POLAR UVI images: Dynamic magnetosphere is an avalanching system, J. Geophys. Res., 107(A12), 1426, doi:10.1029/2001JA000281, 2002.*

## **Data acquisition systems at observatory Lovozero of the Polar Geophysical Institute as a distant segment of communication net**

Yu. V. Kat'kalov, Ya. A. Sakharov, Yu. V. Fedorenko ( *Polar Geophysical Institute, Apatity, Russia* )

Data acquisition systems as a distant segment of communication net of the PGI provide a communication channel between the observatory Lovozero and PGI main building. It links the local network of obs. Lovozero with the PGI local network. The following problems can be resolved with this design:

Data acquisition system operative control and near-real-time data exchange, including quick-look data representation;

Running time services (based on GPS receiver) in order to synchronize computers in the local networks of obs. Lovozero;

Remote operation and control of the data acquisition systems in Lovozero from the PGI;

Providing of e-mail and access to Internet from obs. Lovozero;

We have developed a software to establish a permanent cost effective data link between the PGI and obs. Lovozero. This software provides an easy access for any user to Lovozero, e.g., via MS Windows environment and e-mail services as well.

We used up-to-date wireless technology GSM/GPRS, which allow us to set up the communication channel which is cost-efficient compared to direct satellite telephone channels.

## **Night-time magnetic, riometer and auroral disturbances in the late recovery phase of November 2004 superstorm**

N.G. Kleimenova<sup>1</sup>, O.V. Kozyreva<sup>1</sup>, T.A. Kornilova<sup>2</sup>, I.A. Kornilov<sup>2</sup>, J. Manninen<sup>3</sup>, A. Ranta<sup>3</sup>, and K. Kauriste<sup>4</sup>

<sup>1</sup> *Institute of the Physics of the Earth RAS, Moscow, Russia, e-mail: kleimen@ifz.ru*

<sup>2</sup> *Polar Geophysical Institute RAS, Apatity, Russia,*

<sup>3</sup> *Sodankyla Geophysical Observatory, Sodankyla, Finland*

<sup>4</sup> *Finish Meteorological Institute, Helsinki, Finland*

One year after an extreme October-November 2003 superstorm events a new sequence of very intense magnetic storms occurred on 7-11 November 2004 with a Dst value as great as  $-373$  nT. This event was a double-dip storm consisted of two very strong magnetic storms: on 7-8 November and on 9-10 November 2004. The interval between 18 UT on 8 November and 06 UT on 9 November referred to the late recovery phase of the first strongest storm. At this time there were no disturbances in the solar wind and IMF. This interval separated two super storms. In the event under study the Dst-index was stable but considerably strong ( $\sim -125$  nT). Typically, a recovery phase of a storm is characterized by generation of morning geomagnetic Pc5 pulsations. However, unlike that, in the analysed period the strongest magnetic disturbances were observed in the night sector of the Earth. We present here the results of the analysis of the Scandinavian multi-point observations: (i) geomagnetic variations and pulsations (IMAGE magnetometer network, 23 stations), (ii) visible auroras (6 all-sky cameras and Lovozero TV-camera), and (iii) energetic particle precipitation (8 riometers including the imaging IRIS riometer set). The strong (down to  $\sim 1000$  nT) negative bay-like magnetic variations, accompanied by the simultaneous similar bursts of the riometer absorption (up to 6 dB), and auroral activations were observed at geomagnetic latitudes higher than  $60^\circ$ . Several examples of spatial correlation between the ASC auroral forms and particle precipitation (IRIS riometer data) were found. The latitude-time maps (keograms) of Pi2 and Pi3 pulsations and the spatial-temporal distributions of the riometer absorption indicate their simultaneous occurrence and collocation, suggesting the common source. Different types of discrete aurora activations such as polar boundary intensification (PBI) events, accompanied by Pi2 geomagnetic pulsations, streamers, black auroras and others were observed. The source of the considered disturbances was probably related to bursty bulk flows (BBFs) and dipolarization processes. The energy for these processes could be stored in the magnetotail during the preceding main phase of the magnetic super storm. This work was supported by the Grant №05-05-64495 of Russian Foundation for Basic Research and partly by the program "Solar-Terrestrial activity and physical processes in the Sun-Earth system".

## **Numerical modeling of auroral electrojet during geomagnetic disturbances with particle precipitation included**

M.V. Klimenko<sup>1</sup>, V.V. Klimenko<sup>2</sup>, and V.V. Bryukhanov<sup>1</sup>

<sup>1</sup>*Kaliningrad State Technical University, 236000, Kaliningrad, Russia*

<sup>2</sup>*West Department of IZMIRAN, Kaliningrad, Russia*

Model studies of particle precipitation effect in auroral electrojet dynamics during magnetospheric substorms have been performed. The calculations were conducted with the use of the Global Self-consistent Model of the Thermosphere, Ionosphere and Protonosphere (GSM TIP) designed in the West Department of IZMIRAN, with the calculations of electric fields in the Earth's ionosphere included.

It is shown that, taking into account particle precipitation, one can reproduce in the model such a well-known morphological feature as a much greater strengthening of the westward electrojet during substorm than of the eastward one. It is also demonstrated that substorm associated precipitation effects in the F2-layer of the ionosphere are connected with the redistribution of the electric field potential in the Earth's ionosphere.

Based on the results obtained, a conclusion is made that for the correct description of substorm-time behavior of the auroral electrojets and F2-layer of the ionosphere not only at high but also at middle and low geomagnetic latitudes, particle precipitation should be taken into account.

## **Spatial and temporal dynamic of active polar cap arcs as a special type of breakup**

I. A. Kornilov<sup>1</sup>, T. A. Kornilova<sup>1</sup>, O. I. Kornilov<sup>2</sup>

<sup>1</sup>*Polar Geophysical Institute, Apatity, Russia. kornilov@pgi.kolasc.net.ru*

<sup>2</sup>*St. Petersburg, Petrodvorets, Russia. oleg@geo.phys.spbu.ru*

Active polar cap arcs are usually very bright, and exhibit intense spatial – temporal dynamics, the energy dissipation in those arcs being well compatible with energetics of auroral breakup. We present some initial results of polar arc study, based on Barentsburg and Lovozero TV, VLF and magnetic pulsation data, satellite imaginary, and magnetic field measurements in the solar wind and magnetotail. We have found that the main active processes in the polar arcs are very similar to auroral zone breakup development. It can be preliminarily concluded that in contrast to the ordinary auroral zone breakup, when energy is stored in the compressed magnetic field in the magnetosphere, polar breakup takes energy from elastic deformations of the twisted magnetotail.

## **Searching of optical effects induced by ionospheric HF heating**

I. A. Kornilov<sup>1</sup>, O. I. Kornilov<sup>2</sup>

<sup>1</sup>*Polar Geophysical Institute, Apatity, Russia. kornilov@pgi.kolasc.net.ru*

<sup>2</sup>*St. Petersburg, Petrodvorets, Russia. oleg@geo.phys.spbu.ru*

Ionosphere optical effects induced by high frequency heating are very weak. Maximum amplitude of a signal in 6300A emission stimulated by Tromso HF heater was about 100 Raileighs, with typical artificial aurora intensity being ~1-10 R only. Especially difficult is a detection of heating effect in the presence of bright, highly dynamical in time and space natural aurora (10-50 kR). We discuss some important TV camera technical requirements, different techniques of image processing and searching for weak periodical signal with using *a priori* information. Examples of applying those methods to different model noisy TV frames with addition of a small heating signal are presented. We also demonstrate some initial results of Spitsbergen heating facility operation.

## **Distinctive features of aurora dynamics at the high latitudes during magnetic storm on January 1-7, 2005**

T.A. Kornilova<sup>1</sup>, I. A. Kornilov<sup>1</sup>, O. I. Kornilov<sup>2</sup>

<sup>1</sup>*Polar Geophysical Institute, Apatity, Russia. kornilova@pgi.kolasc.net.ru*

<sup>2</sup>*St. Petersburg, Petrodvorets, Russia. oleg@geo.phys.spbu.ru*

Features of auroral dynamics of two substorms occurred during the recovery phase of a magnetic storm on January 1-7, 2005 are compared on the basis of TV data from the high latitude observatory of Barentsburg. The position of

obs. Barentsburg permits to monitor the auroras of the main auroral oval and of the polar cap. Both substorms were triggered by Bz IMF northward turn and were associated with a solar wind velocity enhancement. The first substorm under study took place at the beginning of magnetic storm recovery phase and was stronger than the second one, which proceeded in the middle of the recovery phase. It was found that during the growth and expansive phase of both substorms the aurora developed in a similar way: Polar cap arcs were observed during the growth phase. The expansion phase was signified by the development of auroral bulge with rotating auroral spirals inside it. Some distinctions in auroral dynamics manifested in the recovery phases of the substorms. During the first substorm, a double auroral oval formed, with its poleward boundary at the northern horizon of obs. Barentsburg and equatorward edge at the southern horizon. The polar boundary intensifications (PBIs) and equatorward drifting streamers were observed. The recovery phase of the second substorm was characterized by polar arc development, which behaved like an auroral breakup in the polar cap.

### **Scaling collapse and structure functions in TV data of substorm-time aurora**

B.V. Kozelov<sup>1</sup>, K. Rypdal<sup>2</sup>

<sup>1</sup> *Polar Geophysical Institute, Apatity, Murmansk region, 184209 Russia*

<sup>2</sup> *Department of Physics, University of Tromsø, Norway*

We present a statistical study of scaling features of spatial and temporal variations in the optical auroral luminosity during substorm expansion phase. The data of all-sky TV observations at Barentsburg observatory (Svalbard) and Kola Peninsula have been used. Generalized structure functions (GSF) for luminosity fluctuations are calculated to determine the scaling properties of the higher order moments. Also we examine the shape of probability density function (PDF) of auroral fluctuations to find a scaling collapse in some range of spatial/temporal scales. We found that the observed PDFs have a non-Gaussian shape for auroral structures during expansion phase of substorm. The observed scaling features are compared with the results previously obtained for aurora by fractal, avalanche and spreading analysis. Possible consequences for SOC and turbulence models of substorm activity are discussed.

### **Dynamics of geomagnetic pulsations, riometer absorption and auroras in the main phase of the November 2004 superstorm**

O.V. Kozyreva and N.G. Kleimenova (*Institute of the Earth Physics RAS, Moscow, Russia*)

A super strong magnetic storm started on 7 November 2004. The main phase maximum (Dst~-370 nT) was observed at 06-07 UT on 8 November 2004. The storm main phase was characterised by several intense (down to  $\approx$  -2000 nT) magnetosphere substorms with the largest amplitudes at the early morning sector. The negative bay-like magnetic variations were accompanied by the bursts in riometer absorption (up to 5 dB) and auroral activations. The global-scale spatial dynamics of substorm associated Pi3 geomagnetic pulsations has been analysed on the basis of the ground magnetometer network observations. The location of active auroras was studied by using the Scandinavian all sky camera data, which were kindly provided by Dr. K. Kauristie (Finnish Meteorological Institute). At the beginning of the storm main phase the magnetic activity as well as intense auroras and Pi3 geomagnetic pulsations very quickly shifted from subauroral to polar latitudes, as is typical for the classical substorm. One hour later, an extremely strong displacement (from 72-74° to ~55-56°) of all these phenomena was observed. The latitude-UT maps (keograms) of Pi3 pulsations were computed from IMAGE magnetometer data. A similar spatial-temporal dynamics of the Pi3 pulsations, active auroras and ionospheric equivalent currents is discussed.

This work was supported by the Grant №05-05-64495 of Russian Foundation for Basic Research and partly by the program "Solar-Terrestrial activity and physical processes in the Sun-Earth system".

### **Extreme magnetic storms and storm-substorm relation problems**

L.L. Lazutin (*Space Science Division, Scobeltsyn Institute of Nuclear Physics of Moscow State University, Russia*)

The following problems will be addressed in the presentation: what differs the extreme magnetic storms from the "ordinary" ones, the relation between Dst and magnetospheric configuration during the Storm main phase, the response of magnetospheric particle population to the SC, and storm-to-substorm relations.

Solar wind is a common source of energy for magnetic storms and magnetospheric substorms, therefore both these phenomena must be related. A controversy between researchers concerns the estimation of magnitude and the features of their mutual influence. The problems of substorm activity effect in the ring current and storm-time

### ***Geomagnetic storms and substorms***

distortion of magnetospheric configuration, as well as the adverse influence of magnetic storms on substorm structure and development, will be discussed.

### **Dst-index models: Physical and mathematical aspects of modeling**

A.E. Levitin, L.I. Gromova, L.A. Dremukhina, E.G. Avdeeva, D.I. Korzhan (*Institute Terrestrial Magnetism, Ionosphere and Radio Wave Propagation, Troitsk, Moscow region, Russia*)

The procedure of Dst modeling proposed in [Burton et al., *J. Geophys. Res.*, 80, 4204, 1975] is widely employed now. It is based on the equations  $Dst = DR + DCF$  and  $d(DR)/dt = F(E) - DR/\tau$ , where the magnetic field generated by the currents on the magnetopause is calculated from the solar wind velocity and density:  $DCF \sim (NV^2)^{1/2}$ ,  $F(E)$  is the rate of ring current injection as a function of delayed and filtered solar wind electric field, and  $\tau$  is the characteristic time of ring current decay. Different scientific groups try to increase the accuracy of this method by constructing more and more complicated functions for reproducing the temporal dynamics of the physical processes described by  $F(E)$  and  $\tau$ . As it is known, the Dst-index is a measure of the amplitude of geomagnetic disturbance. We aim to find out how this method of Dst modeling evaluates the physical process of geomagnetic disturbance generation and whether this approach is not a mathematical formalism only. The variation  $Dst(t)$  has been modeled for several magnetic storms based on different Dst-index models. It has been demonstrated that in calculating  $F(E)$  and  $\tau$ , the accuracy of the most advanced models is the same as that of the models that date back to 1980s. We also argue that the physical mechanism responsible for storm-time magnetic disturbances can not be described by the above mentioned relations. In our opinion, the advantage of the up-to-date Dst models, derived from satellite measurements of space parameters, is an ability to predict mathematically the Dst-index with the accuracy that is good enough for the applied problems when preliminary information on a possible peak in cosmic weather activity is needed.

This study is supported by INTAS grant No 03-51-5359 and RFBR grant 05-05-65196

### **CORONAS-F observations of strong magnetic storm-associated electron flux variations in the outer radiation belt of the Earth**

I.N. Myagkova, S.N. Kuznetsov, E.A. Muravieva (*Skobeltsyn Institute of Nuclear Physics, Moscow State University, Moscow, Russia*)

Dynamics of the relativistic electron population in the outer radiation belt of the Earth (ERB) during magnetic storms have been observed for many years. The relativistic electron flux decreases during the main phase of the storm, and then recovers and increases from late main phase to the recovery phase. Thus the development of an empirical dynamical model based on modern experimental data is needed for quantitative understanding of the processes in the radiation belts during and after strong magnetic storms.

Data obtained onboard the CORONAS-F satellite, which operated from August, 2001 to December, 2005, enable to create an empirical model of the outer ERB. CORONAS-F had the polar orbit with the inclination of  $82.5^\circ$ , its altitude being  $\sim 500$  km in 2001 and  $\sim 300$  km in 2005. Relativistic electrons with the energy from 300 keV to 6 MeV in four energy ranges were detected by MKL instrument onboard CORONAS-F satellite. Several strong magnetic storms occurred in the time period from 2001 to 2005, including those in November, 2001, April 2002, October-November 2003, November, 2004, January and May 2005. The relation of ERB variations to solar wind and interplanetary medium parameters, as well as to geomagnetic cutoff variations during solar energetic particles events, was also investigated.

### Wave structures excited in compressible Petschek-type magnetic reconnection

Thomas Penz<sup>1,2</sup>, V.S. Semenov<sup>3</sup>, M.F. Heyn<sup>4</sup>, V.V. Ivanova<sup>3</sup>, I.B. Ivanov<sup>5</sup>, H.K. Biernat<sup>1,2</sup>, C.J. Farrugia<sup>6</sup>, F. T. Gratton<sup>7</sup>

<sup>1</sup>Space Research Institute, Austrian Academy of Sciences, Schmiedlstrasse 6, A-8042 Graz, Austria

<sup>2</sup>Institute of Physics, University of Graz, Universitätsplatz 5, A-8010 Graz, Austria

<sup>3</sup>Institute of Physics, State University St. Petersburg, St. Petersburg, 198504, Russia

<sup>4</sup>Institute for Theoretical Physics, Technical University Graz, Petersgasse 15, A-8010 Graz, Austria

<sup>5</sup>Petersburg Nuclear Physics Institute, Gatchina, 188300, Russia

<sup>6</sup>Institute for the Study of Earth, Oceans, and Planets, University of New Hampshire, Durham, NH 03824, USA

<sup>7</sup>Institute of Plasma Physics, University of Buenos Aires, 1114 Buenos Aires, Argentina

We present a method to analyze the wave and shock structures arising from Petschek-type magnetic reconnection. Based on a time-dependent analytical approach developed by Heyn and Semenov (1996) and Semenov et al. (2004), we calculate the perturbations caused by a delta function-shaped reconnection magnetic field, which allows us to achieve a representation of the plasma variables in the form of Green's functions. Different configurations for the initial conditions are considered. In the case of symmetric, antiparallel magnetic fields and symmetric plasma density, the well-known structure of an Alfvén discontinuity, a fast volume wave, a slow shock, a slow wave, and a tube wave occurs. In the case of asymmetric, antiparallel magnetic fields, the surface waves are additionally found. We also discuss the case of symmetric, antiparallel magnetic fields and asymmetric densities, which leads to a faster propagation in the lower half plane, causing side waves forming a Mach cone in the upper half plane. Complex effects like anisotropic propagation characteristics, intrinsic wave coupling, and the generation of different non-linear and linear wave modes in a finite beta plasma are retained. The temporal evolution of these wave and shock structures is shown.

### Storm-time occurrence of TEC fluctuations associated with polar patches as evidenced from GPS observations

I.I. Shagimuratov, I.I. Efshov, Yu.Ya. Ruzhin, N.Yu. Tepenitsyna (*West Department of IZMIRAN, Kaliningrad, Russia*)

We have studied the occurrence of strong phase fluctuations of GPS signals based on the observations at Antarctic stations. The fluctuations were caused by large-scale ionospheric irregularities associated with the occurrence of polar patches in TEC variations. A new technique was developed for estimating TEC absolute value in patch-type structures. The technique was applied to obtain the characteristics of patch structures in TEC during storms. We present a storm-time development of TEC fluctuations for geomagnetically active period of 6-12 November 2004. The data on temporal variations in TEC along individual satellite passes were analyzed. Strong TEC fluctuations with TEC enhancements of 2-5 times relative to the background level were revealed in the polar ionosphere. The duration of such events was 10 - 20 min. In the time interval of 4-5 hours, 3 to 5 strong and several weak patches were detected. The activity of the patches slightly depends on the Kp index only, with the intensity of patches increasing during substorm activity.

### Quantitative geomagnetic field characteristics at geosynchronous orbit during substorm growth phase

M.A. Shukhtina (*Institute of Physics, University of St-Petersburg, St-Petersburg, Russia*)

Geomagnetic field evolution during the substorm growth phase depending on external parameters (solar wind dynamic pressure  $P_d$ , averaged for the preceding hour dayside 'merging electric field'  $E_m$  and corrected for the dynamic pressure  $Dst^*$  index) has been studied based on geostationary GOES-8, GOES-9 and solar wind Wind spacecraft data for the period 1996-1998 using 105 events.

The analysis has been performed in the coordinate system of the model magnetotail neutral sheet from Tsyganenko and Fairfield (2004) separately for the magnetic field components normal ( $B_n$ ) and tangential ( $B_t$ ) to the model neutral sheet. The 'tail magnetic field'  $B_e = B - B_{Dip} - B_{DCF}$  ( $B_{Dip}$  and  $B_{DCF}$  are the dipole and DCF field according to the Tsyganenko (2002) T01 model) and its components  $B_{e_n}$  and  $B_{e_t}$  were also considered.

The results can be formulated as follows:

1. The  $B_n / B_{e_n}$  values at substorm onset strongly depend on  $P_d$  ( $cc=0.65/0.72$ ) and  $E_m$  ( $cc=0.59/0.74$ ) values and somewhat weaker ( $cc=0.52/0.55$ ) on the  $Dst^*$  value. These dependences differ from those given by the standard T01 model.

### **Geomagnetic storms and substorms**

2. The vertical profile of the total tangential component  $B_t$  is nearly unchanged during the growth phase (considered to be 54 min) and well coincides with the T01 model profile. The parameter of adiabaticity  $k=R_c/\rho$  ( $R_c$  for the curvature radius,  $\rho$  for the particle Larmor radius) for protons with energy  $>30$  keV decreases during the growth phase from 2.7 to 1.8 (from 2.3 to 1.0) for  $E_m=1$  mV/m ( $E_m=2$  mV/m) completely due to the normal component decrease.
3. The tangential tail magnetic field  $B_{et}$  vertical profile within  $1.5-2 R_E$  seems to indicate current sheet splitting (current density growth away from the neutral sheet), especially near substorm onset.
4. The  $B_{et}$  value at  $dZ=1.5 R_E$  on average grows during the growth phase from 11 to 16 nT, i.e. the average current density increases  $\sim 1.5$  fold within  $dZ=1.5 R_E$ . So for the given data set no large current density increase in this  $dZ$  range is observed at the geostationary orbit during the growth phase.

*N. A. Tsyganenko, and D.H. Fairfield, Global shape of the magnetotail current sheet derived from Geotail and Polar data, J. Geophys. Res., 109, A03218, doi:10.1029/2003JA01000662, 2004.*

*Tsyganenko, N. A. : A model of the near magnetosphere with a dawn-dusk asymmetry. 1. Mathematical structure, J. Geophys. Res., 107, 10.1029/2001JA000219, 2002.*

### **Geomagnetic "crochet" as a predictor of an intense storm in November 2004**

V.A. Velichko, I.Ya. Plotnikov, D.G. Baishev, N.G. Skryabin, R.N. Boroyev, A.V. Moiseyev (*Yu.G. Shafer Institute of Cosmophysical Research and Aeronomy, Yakutsk, Russia*)

An intense magnetic storm on November 7, 2004 with  $Dst = -373$  nT (at 07 UT on November, 8) was observed after geomagnetic "crochet" (on November 6). A characteristic series of X-ray splashes are registered during an optical flash. In the daytime MLT sector the magnetic H, D and Z components on the ground were changing synchronously with the X-ray splashes in the range of 1-8 Å, detected onboard Geos-12 satellite. Probably, the X-radiation causes an additional ionization in the D and E layers of the illuminated ionosphere, which also affects the current system of geomagnetic Sq-variation. The duration of geomagnetic field response amounts to several hours and corresponds to the duration of X-ray flash. A possibility to use the data of subsolar magnetometer stations for detecting magnetic "crochet" as a predictor of a flare associated geomagnetic storm is discussed.

This work was supported by the Russian Foundation for Basic Research, project no. 03-05-39011-GFEN and partially by the programm of presidium of RAS no. 16 p.3

### **Auroral precipitation dynamics during magnetic storms**

O.I. Yagodkina, V.G. Vorobjev (*Polar Geophysical Institute, RAS, Apatity, Murmansk region, 184200, Russia*)

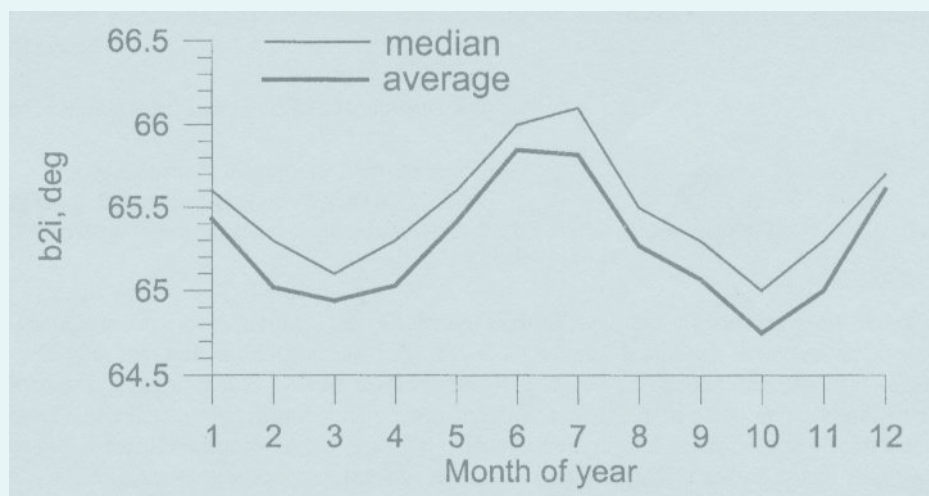
Auroral precipitation boundaries during giant magnetic storms on February 06-16, 1986 and March 11-21, 1989 with intensity of about 300 nT and 600 nT, respectively, were investigated from DMSP spacecraft observations. It is shown that the significant displacement of the equatorward boundaries of electron precipitation in both midday and midnight sectors were observed along with the magnetic activity growth. Visually, the dynamics of precipitation boundaries correlated with the magnetic activity level in the auroral zone (AE index) rather than with the variations of the Dst index. There was no equatorward displacement of the polar cap boundary in the nighttime throughout magnetic storms. Moreover, a noticeable poleward displacement of the polar cap boundary could be seen here during the magnetic storm main phase. The polar cap expansion occurred only due to the equatorward displacement of the poleward precipitation boundary in the daytime which was as large as  $16^\circ-18^\circ$  of geomagnetic latitudes. Comparisons between the precipitation boundary position observed by the spacecraft and the one calculated from empirical equations were carried out for magnetic storms of different intensity.

### **Short-term variations of the intensity of H-alpha hydrogen emission of auroras in the initial period of auroral substorm**

L. S. Yevlashin (*Polar Geophysical Institute, Apatity, Murmansk region*)

Spectral data of auroras obtained by using a C-180-S camera with CCD (the exposure time is 2 min, the resolution 2 nm) at the Loparskaya observatory during IMS have been studied. For the 8 events that were analyzed no systematic short-term decrease or enhancement of  $H_\alpha$  line intensity in the initial period of auroral substorm were found. Nor these changes were revealed at the moment of breakup. In the future a more profound statistical study should be performed in order to find any significant effect in this phenomenon.

## *Fields, Currents, Particles in the magnetosphere*





## **Compressed solar wind control of the auroral oval expansion**

I.I. Alexeev (*Skobeltsyn Institute of Nuclear Physics, Lomonosov Moscow State University, Leninskie Gory, Moscow 119992, Russia*)

A dependence of the magnetic flux in the polar cap on the interplanetary magnetic field and solar wind dynamic pressure is studied. The model calculations of polar cap and auroral oval magnetic fluxes at the ionospheric level are presented within the paraboloid model of the magnetosphere. The scaling law for polar cap diameter changing for different subsolar distances is demonstrated. Quiet conditions are used to compare the theoretical results with the UV images of the Earth's polar region obtained by the Polar and IMAGE spacecraft. The model calculations enable finding not only the average polar cap magnetic flux but also the extreme values of the polar cap and auroral oval magnetic fluxes. These quantities can be reached in the course of severe magnetic storms. Spectacular aurora can often be seen at mid-latitudes during such disturbances. In particular, the Bastille Day storm of 15-16 July 2000 was a severe magnetic storm when auroral displays at mid-latitudes were reported. The enhancement of global magnetospheric current systems (the ring current and tail current) and corresponding reconstruction of the magnetosphere is a reason for the equatorward displacement of the auroral zone. But at the beginning of the event under study, the contracted polar cap and auroral oval were observed. In this case a sudden solar wind pressure pulse was associated with a simultaneous northward IMF turning. Such IMF and solar wind pressure behavior is a cause of the observed aurora dynamics.

## **Monitoring of polar cap spatial dynamics based on the data from the Greenland chain of magnetic observatories**

N.A. Barkhatov<sup>1,2</sup>, A.E. Levitin<sup>3</sup>, S.E. Revunov<sup>1</sup>

<sup>1</sup>*Nizhniy Novgorod State Pedagogical University*

<sup>2</sup>*Radiophysical Research Institute (NIRFI)*

<sup>3</sup>*Institute Terrestrial Magnetism, Ionosphere and Radio Wave Propagation (IZMIRAN), Troitsk, Moscow region, Russia*

Three high latitude regions, namely, the polar cap, auroral oval and subauroral zone are characterized by different structure of geomagnetic activity caused by different spatial-temporal structure of magnetospheric-ionospheric current systems. Location and spatial dimensions of each of the above regions may change with changing the interplanetary conditions. Monitoring of spatial dynamics of the polar cap and auroral oval is very important for analyzing geophysical events with the use of specific models parameterized by the scales of these regions. Besides, it can help solving some applied problems related to a negative influence of space weather on the biosphere. We present a technique of calculation of polar cap, auroral oval and subauroral zone locations based on the method of artificial neural networks (ANN). The ANN input parameters are the gain-frequency spectrums and matrix of wavelet coefficients obtained from the data of Greenland chain magnetic observatories. This study was supported by INTAS grant N 03-51-5359 and RFBR grant 05-05-6519.

## **Cross-tail fast flows and their relation to the plasma sheet phenomena**

N.P. Dmitrieva (*Institute of Physics, University of St-Petersburg, St-Petersburg, Russia*)

Recent results concerning the average pattern of the plasma velocity in the middle magnetotail indicate a significant cross-tail component ( $V_y$ ), comparable with the plasma velocity along the tail axis ( $V_x$ ). However, it is known that up to 80% of the transfer of mass and magnetic field fluxes in the plasma sheet is provided by the Bursty Bulk Flows (BBFs), which are collimated along the X-axis. This contradiction is the main motivation for the present experimental study.

We have analyzed the statistics of spatial and temporal characteristics of fast flows and plasma parameters in the middle tail using Geotail data for 1995-1999. A number of velocity magnitudes ( $V_{th}$ ), equal to 200, 300, 400 and 600 km/s, were taken as thresholds for the data selection criteria. It is shown that:

- Occurrence of large  $|V_y|$  samples depends on the X coordinate, similarly to that of large  $|V_x|$ , but the probability values are 3-10 times less for  $V_y$  component than for  $V_x$  one.
- The majority of the large  $V_y$  events correspond to fast  $V_x$  flows.
- Observed plasma density and temperature variations during large  $V_y$  events are typical for BBFs.

## ***Fields, currents, particles in the magnetosphere***

- In many cases quasi-periodic variations of the transverse and parallel to the magnetic field velocity components are observed. Their characteristic time scales are about 1-3 minutes. Possible interrelations of the fast flow features described above and plasma sheet flapping motions are discussed.

## **Auroral electrojets and boundaries of plasma domains in the magnetosphere during magnetically disturbed intervals**

Y.I. Feldstein<sup>1</sup>, V.A. Popov<sup>1</sup>, J.A. Cumnock<sup>2</sup>, A. Prigancova<sup>3</sup>, L.G. Blomberg<sup>2</sup>, J.U. Kozyra<sup>4</sup>, B.T. Tsurutani<sup>5</sup>, L.I. Gromova<sup>1</sup>, A.E. Levitin<sup>1</sup>

<sup>1</sup>*Institute of Terrestrial Magnetism, Ionosphere and Radio Wave Propagation, Troitsk, Moscow Region, Russia*

<sup>2</sup>*Alfvén Laboratory, Royal Institute of Technology, Stockholm, Sweden*

<sup>3</sup>*Geophysical Institute, Slovak Academy of Sciences, Bratislava, Slovakia*

<sup>4</sup>*Space Physics Research Laboratory, University of Michigan, Ann Arbor, MI, USA*

<sup>5</sup>*Jet Propulsion Laboratory, Pasadena, CA, USA*

We investigate variations in the location and intensity of the auroral electrojets during magnetic storms and substorms using a numerical method for estimating the equivalent ionospheric currents based on data from meridian chains of magnetic observatories. Special attention was paid to the complex structure of the electrojets and their interrelationship with diffuse and discrete particle precipitation and field-aligned currents in the dusk sector. During magnetospheric substorms the eastward electrojet (EE) location in the evening sector changes with local time from cusp latitudes ( $\Phi \sim 77^\circ$ ) during early afternoon to latitudes of diffuse auroral precipitation ( $\Phi \sim 65^\circ$ ) equatorward of the auroral oval before midnight. During the main phase of an intense magnetic storm, the eastward currents in the noon-early evening sector adjoin to the cusp at  $\Phi \sim 65^\circ$  and in the pre-midnight sector are located at subauroral latitude  $\Phi \sim 57^\circ$ . The westward electrojet (WE) is located along the auroral oval from evening through night to morning sector and adjoins to the polar electrojet (PE) located at cusp latitudes in the dayside sector. The integrated values of the eastward (westward) equivalent ionospheric current during the intense substorm are  $\sim 0.5$  MA ( $\sim 1.5$  MA), whereas they are 0.7 MA (3.0 MA) during the storm main phase maximum. The latitudes of auroral particle precipitation in the dusk sector are identical to those of both electrojets. The EE in the evening sector is accompanied by particle precipitation mainly from the Alfvén layer but also from the near-Earth part of the central plasma sheet. In the lower-latitude part of the EE the field-aligned currents (FACs) flow into the ionosphere (Region 2 FAC), at its higher-latitude part the FACs flow out of the ionosphere (Region 1 FAC). During intense disturbances, in addition to the Region 2 FAC and the Region 1 FAC, a Region 3 FAC with the downward current was identified. This FAC is accompanied by diffuse electron precipitation from the plasma sheet boundary layer. Actually, the triple system of FAC is observed in the evening sector and as a consequence the WE and the EE overlap. The WE in the evening sector comprises only the high-latitude periphery of the plasma precipitation region and corresponds to the Hall current between the Region 1 FAC and Region 3 FAC. During the September 1998 magnetic storm two velocity bursts ( $\sim 2$ -4 km/s) in the magnetospheric convection were observed at the latitudes of particle precipitation from the central plasma sheet and at subauroral latitudes near the ionospheric trough. This kind of bursts is known as subauroral polarization streams (SAPS). In the evening sector the Alfvén layer equatorial boundary for precipitating ions is located more equatorward than that for electrons. This may favour northward electric field generation between these boundaries and may cause high speed westward ions drift visualized as SAPS. Meanwhile, high speed ion drifts cover a wider range of latitudes than the distance between the equatorward boundaries of ions and electrons precipitation. To summarize the results obtained a new scheme of 3D currents in the magnetosphere-ionosphere system and a clarified view of interrelated 3D currents and magnetospheric plasma domains are proposed.

## **SSt- analysis of hourly geomagnetic field values to determine the variations caused by the Main magnetic field of the Earth and solar activity cycle**

L.I. Gromova, L.A. Dremukhina, A.E. Levitin, E.G. Avdeeva, D.I. Korzhan (*Institute Terrestrial Magnetism, Ionosphere and Radio Wave Propagation, Troitsk, Moscow region, Russia*)

In our idea, the large-scale magnetospheric current system, persisting for many years, has a most steady state. The STEADY STATE (SSt) of the variable magnetic field of the Earth conforms to the steady state of the magnetosphere. We suppose that the SSt can be determined from processing the hourly averaged values of geomagnetic field components measured at magnetic observatories. The SSt can become a reference level for

geomagnetic activity and an indicator of reasonableness and availability of classical indices of geomagnetic activity that were introduced at the initial stage of the study of magnetospheric current generation mechanisms. By using the SSt, we can classify space weather states for scientific and applied problems more reliably. Hourly averaged amplitudes of the horizontal vector of geomagnetic field measured at *aa*-index observatories for the period of 1981-2003 have been studied based on the method of separation of the most frequently occurring values for every UT hour during each season of the year. This method enables to find the most steady state of the geomagnetic field  $(X_0, Y_0)$  for every UT hour during each season of the year at any observatory and to study the annual  $(X_0, Y_0)$  variation and  $(X_0, Y_0)$  variation for 1981-2003. These variations are caused by seasonal and annual variation of the ionospheric conductivity, dynamics of Earth's location in space, secular variation of the Main magnetic field of the Earth and 11-year cycle of solar activity.

This study is supported by INTAS grant No 03-51-5359 and RFFI grant 05-05-65196

### **Asymmetry of high-latitude geomagnetic variations, electric fields and currents over the northern and southern polar regions**

L.I. Gromova, L.A. Dremukhina, A.E. Levitin, E.G. Avdeeva, D.I. Korzhan (*Institute Terrestrial Magnetism, Ionosphere and Radio Wave Propagation, Troitsk, Moscow region, Russia*)

Geomagnetic variations at high latitudes are controlled by Interplanetary Magnetic Field (IMF) and Solar Wind (SW). Statistical correlative relations between geomagnetic variations and IMF/SW parameters are rather reliable, and models derived from linear regression analysis are the basis for reconstruction of magnetosphere-ionosphere current systems in the polar regions and auroral zone. Asymmetry in spatial-temporal distribution of the electric field and currents over the polar regions can be explained by either northern ionosphere conductivity model applied to the southern polar region, or some natural phenomena, such as due to seasonal effect. This asymmetry should be included in estimating Joule heating  $U_j$  of the high-latitude ionosphere as well as the polar cap potential drop  $\Delta\phi$ . IZMIRAN Electrodynamics Model (IZMEM) parameterized by IMF components, SW velocity and plasma density indicates the seasonal asymmetry mentioned above for the northern and southern polar regions. The differences in the amplitudes of  $U_j$  and  $\Delta\phi$  calculated with the IZMEM for both hemispheres have been estimated for summer, winter and equinox conditions and compared with the results of other models derived from the data of the Northern Hemisphere only.

This study is supported by INTAS grant No 03-51-5359 and RFFI grant 05-05-65196

### **Dipole and toroidal sources and kinetic description of the far regions of the 3d tails and solar streamers formed by maxwellian plasma flows**

V.M. Cubchenko<sup>1</sup>, H.R. Biernat<sup>2</sup>, M.L. Khodachenko<sup>2</sup>, H.O. Rucker<sup>2</sup>

<sup>1</sup>*Institute of Applied Physics, Russian Academy of Science, Nizhny Novgorod, Russia*

<sup>2</sup>*Space Research Institute, Austrian Academy of Sciences, Graz, Austria*

*e-mail: ua3thw@appl.sci-nnov.ru*

We consider a classical problem of inductive generation by the solar wind of 3D magnetospheric tail/solar streamer structures originating by magnetic flux sources. The problem is treated within the Vlasov-Maxwell kinetic approach. The flowing plasma is assumed to be hot, collisionless and having maxwellian distribution at infinity. The interacting particles are divided in trapped and untrapped ("fly by") ones. The trapped particles are partly parameterised by magnetic flux source. The source is described by the densities of magnetic dipole  $\vec{\mu}$  and magnetic toroid  $\vec{\tau}$  currents distributed over the characteristic scale  $r_0$  and characterised by the ratio of the integral currents  $\Gamma_{\tau\mu} = I_{\tau}/I_{\mu}$ . The motion of the "fly by" particles is treated via the perturbations resulting from the linear analytical approach. The plasma is considered to be conductive and diamagnetic medium. The resistive currents are characterized by anomalous skin  $r_G$ , while the diamagnetic currents by magnetic Debye scale  $r_{DM}$ . The ratio of diamagnetic currents to resistive ones is a quality of magnetospheres and is characterised by the ratio  $G = r_G / r_{DM}$ . We get an integral representation of a self-consistent global 3D magnetic configuration, which is defined via two different kinds of cylindrical harmonics. For incoming maxwellian plasma flow we have a low quality regime  $G \ll 1$  when 3D structure is with the resistive currents and the governing parameter is magnetic

## **Fields, currents, particles in the magnetosphere**

Reynolds number  $Re_m = r_0 / r_G$ . A dipole generates 3D “two wire” multi magnetic ropes current configuration (cylindrical dipole harmonics) which is observed in the far downtail regions of the magnetosphere. A toroid generates classical 3D “theta type” current configuration (cylindrical toroid harmonics) with a modulated neutral sheet inside, which is observed near the sources. We associate the separation of the two configurations in the tail/streamer with the difference in the internal structure, mutually perpendicular orientation of the vectors  $\vec{\mu}, \vec{\tau}$  and the value of  $\Gamma_{\tau\mu}$ . Toroid is a spatially more complicated current system and its current is defined by higher order derivatives of Green like characteristic function of the problem  $\Pi(\vec{X})$ , which has power law decay in asymptotic with fine spatial modulations of the scale  $L(X, r_G)$ . We have faster decay of the “theta type configuration” in comparison with the “two wire configuration” downward of the sources. Our kinetic approach, via the introduction of new plasma spatial dispersion parameters and new dimensionless values, gives us a possibility to get analytically a selfconsistent 3D fine structure of magnetic configuration for the far regions of the tail/streamer.

## **Satellite geodesy – made in Graz**

W. Hausleitner, P. Pesec, G. Kirchner, H. Sünkel (*Space Research Institute, Austrian Academy of Sciences, Schmiedlstrasse 6, A-8042 Graz, Austria*)

Permanent monitoring of the Earth’s actual status and its temporal variation is vital for understanding the dynamics of the solid Earth and the investigation of the global change. Experiments conducted over the past decade have shown that it is possible to study the dynamic behavior of the Earth by means of space techniques getting a clear picture at a global scale. The discipline of satellite geodesy offers a wide range of practical and cost-effective techniques for producing systematic data sets over a wide range of spatial and temporal scales.

The Department of Satellite Geodesy of the Austrian Academy of Sciences is engaged in the application of satellite laser ranging (SLR), GPS/Geodynamics, satellite altimetry and satellite gravity gradiometry (SGG) with the aim to determine satellite orbits, the Earth’s gravity field, movements of the Earth’s crust, the orientation of the Earth in the interplanetary space, the sea surface topography as well as the mass distribution in the Earth’s interior.

## **AJISAI spin parameter determination using Graz kHz satellite laser ranging data**

G. Kirchner, W. Hausleitner, E. Cristea (*Space Research Institute, Austrian Academy of Sciences, Schmiedlstrasse 6, A-8042 Graz, Austria*)

We determine the spin rate and direction of the spherical satellite AJISAI as well as its slow down between 2003/10 and 2005/06 using Graz full rate kHz satellite laser ranging (SLR) data.

Since October 2003, the Graz/Lustbuehel SLR station is capable of laser ranging to Earth satellites with a repetition rate of 2 kHz as the first and only station worldwide. The high density of the kHz data - compared to the regular 10 Hz systems - results in a precise scanning of the satellite’s retro-reflector panel orientation during the spin motion. Applying spectral analysis methods, the resulting frequencies allow to identify the arrangement of the involved laser retro reflector panels at any instant in time during the pass. Using this method, we calculated the spin rate with very high accuracy (RMS of  $4.6 \times 10^{-4}$  Hz), and determined a slow down of the spin rate during the investigated period of 0.0081 Hz/year.

The main reason of this long term slow down is presumably due to the interaction between the satellite’s metallic parts and the Earth’s magnetic field causing eddy currents. However, these mechanisms have not yet been modeled precisely.

## **The theoretical model of the steady-state reconnection in the electron Hall MHD approach**

D.B. Korovin<sup>1</sup>, V.S. Semenov<sup>1</sup>, N.V. Erkaev<sup>2</sup>

<sup>1</sup>*Institute of Physics, University of St-Petersburg, St-Petersburg, Russia*

<sup>2</sup>*Institute of Computational Modeling, Russian Academy of Sciences, Krasnoyarsk, Russia*

The theoretical model of the steady-state magnetic reconnection in the infinite current layer in the incompressible non-resistive (except for the electron diffusion region) collisionless plasma using electron Hall MHD approach has

been developed. The analytical solution in the vicinity of separatrix lines is obtained by using the border layer approximation. It is shown that the solution structure is fixing by the solution of the Grad-Shafranov equation for the

magnetic field potential. The model developed reproduces all essential Hall reconnection features, namely, proton acceleration up to the Alfvén velocities, and the formation of the Hall current system and magnetic field structure. The reconnection rate, as well as other reconnection characteristics, depends solely on the size of the electron diffusion region, not on the internal processes in it. The reconnection is not possible in the absence of the electron diffusion region. The obtained solution implies that the necessary condition for the steady-state reconnection to proceed is a jump of electric field potential across the electron diffusion region and the presence of separatrix lines. The value of the jump in the density of electron fluid potential energy should be of the order of external magnetic pressure. Another necessary condition is that the electron velocity should increase up to the electron Alfvén velocity in the diffusion region and along the separatrix lines.

### **Substorm low-energy particle decrease near the inner edge of the plasma sheet**

T. V. Kozelova<sup>1</sup>, L.L. Lazutin<sup>2</sup>, B.V. Kozelov<sup>1</sup>, N. Meredith<sup>3</sup>, M.A. Danielides<sup>4</sup>

<sup>1</sup>*Polar Geophysical Institute, Apatity, Russia*

<sup>2</sup>*Scobeltsyn Institute for Nuclear Physics of Moscow State University, Russia*

<sup>3</sup>*Mullard Space Science Laboratory, University College, London, Britain*

<sup>4</sup>*Space Physics Group, University of Oulu, Finland*

The injections of energetic particles and dipolarization of the magnetic field are well-known signatures of magnetospheric substorm in the near-Earth region of the plasma sheet. However, the contribution of low-energy particles to these phenomena is not sufficiently examined. Here we consider the behavior of the low-energy (30 eV – 28.5 keV) electrons and ions near the earthward edge of the plasma sheet as observed by CRRES satellite during several substorms. We have found that the low-energy ion flux and particle energy density at distance  $r \sim 6 R_E$  decrease suddenly during the local dipolarization. The data support the idea that the auroral bulge may be a region of decreased pressure of the particles.

### **Dayside auroral oval dynamics related to a solar wind pressure pulse and associated IMF disturbances**

A. E. Kozlovsky (*Sodankylä Geophysical Observatory/Oulu unit, University of Oulu, Oulu, Finland*)

Global auroral images of the IMAGE satellite were used to study the motion of the dayside auroral oval and its poleward boundary (POB) following within 20 min after abrupt increases of solar wind ram pressure (Sudden Impulse, SI). Contributions from the IMF changes associated with the SI have also been investigated. The effects of the IMF and pressure changes were separated with using the multi-factor correlation analysis. The most prominent effect of solar wind pressure increase is the equatorward shift of the dayside oval within 6 min after SI that is consistent with the midday sub-auroral patches above 65° MLAT. The second effect of solar wind pressure increase is a poleward shift of the POB, caused by auroral intensification at high latitudes in a vicinity of the polar cap boundary. The most obvious effect of IMF changes associated with SI is the IMF By effect in the positions of dayside POB and oval at 6-20 min after SI. This is interpreted as an intensification of the most poleward auroras due to IMF By turning to negative (when the oval and POB are moving toward the pole). The IMF By turning to positive leads to fading of the most poleward auroras (that is observed as a shift of the POB toward the equator). Such an effect is consistent with the IMF By-related system of field-aligned currents. No significant motion of the dayside auroral oval was observed in association with IMF Bz changes that can be explained by a larger than 20 min response time to IMF Bz changes.

### **Solar proton belts in the inner magnetosphere**

L.L. Lazutin, S.N. Kuznetsov (*Scobeltsyn Institute for Nuclear Physics of Moscow State University, Russia*)

At the time of magnetic storms, solar cosmic rays with the energies of 1-100 MeV penetrate into the magnetotail/polar cap and quasi-trapping region/auroral zone down to  $L=2$ . During magnetospheric reconfiguration and penetration boundary retreat, a part of the solar particles remain trapped, forming solar proton and alpha particle temporary belts in addition to the stable inner radiation belt.

## ***Fields, currents, particles in the magnetosphere***

Our study presents experimental description of the dynamics of solar proton belts in the inner magnetosphere, based on the solar proton and ion measurements by the low-altitude polar orbiting spacecraft Coronas-F.

### **Magnetospheric-ionospheric response to variations in the solar wind dynamic pressure during positive IMF Bz and a sharp change of IMF By direction**

S.I. Solovyev<sup>1</sup>, A.V. Moiseyev<sup>1</sup>, K. Yumoto<sup>2</sup>, M. Engebretson<sup>3</sup>, A. Du<sup>4</sup>

<sup>1</sup>*Yu. G. Shafer Institute of Cosmophysical Research and Aeronomy, Siberian Division, Russian Academy of Sciences, Yakutsk, Russia*

<sup>2</sup>*Space Environment Research Center, Kyushu University, Fukuoka, Japan*

<sup>3</sup>*Augsburg College, Minneapolis, USA*

<sup>4</sup>*Institute of Geology and Geophysics, Beijing, China*

Magnetospheric-ionospheric response to the variations of solar wind dynamic pressure (Pd) in the periods of positive IMF Bz has been studied based on the data of global geomagnetic observations and auroral observations of Polar satellite. The following results are obtained:

(1) An increase (a drop) in the Pd leads to an enhancement (weakening) of luminosity intensity in both the dayside and nightside parts of the auroral oval, being accompanied by an enhancement in the DP2-type two-vortex current system.

(2) An increase in the Pd also results in a poleward expansion of the poleward boundary of luminosity (PBL) of the nightside auroral oval. The displacement is up to 7° in latitude with the velocity of 0.5 km/s. At the same time, the dayside boundary of the auroral oval, which is located at the latitudes of  $\Phi'=77-78^\circ$ , does not change its position in response to Pd variations.

(3) An abrupt change of IMF By polarity from positive to negative during decreased Pd can lead to further poleward expansion of the PBL. This also leads to an enhancement of the westward electrojet in the nightside and morning sectors, with the current center moving poleward to  $\Phi'=75^\circ$  with the same velocity as that of PBL expansion. Simultaneously, the eastward electrojet intensifies in the premidnight-to-evening sector at  $\Phi'=65-66^\circ$ . We relate the enhancement of the electrojets to a decrease in the level of magnetospheric convection.

(4) There are at least three types of auroral responses to Pd variations manifesting in the azimuthal velocities of the luminosity region or particle precipitation along the auroral oval. The velocities of  $V1=30-40$  km/s,  $V2=10$  km/s, and  $V3=1.0$  km/s are suggested to indicate the interaction of the magnetosonic and/or Alfvén waves, surface waves on the magnetopause, and electromagnetic waves, respectively, with the trapped magnetospheric particles as well as their pitch-angle diffusion.

This work was supported by the Russian Foundation for Basic Research, project no. 03-05-39011-GFEN and partially by the program of presidium of RAS no. 16 p.3

### **Geomagnetic sudden impulse characteristics depending on the IMF orientation**

S.I. Solovyev<sup>1</sup>, A.V. Moiseyev<sup>1</sup>, M. Engebretson<sup>2</sup>, K. Yumoto<sup>3</sup>, A. Du<sup>4</sup>

<sup>1</sup>*Yu. G. Shafer Institute of Cosmophysical Research and Aeronomy, Siberian Division, Russian Academy of Sciences, Yakutsk, Russia*

<sup>2</sup>*Space Environment Research Center, Kyushu University, Fukuoka, Japan*

<sup>3</sup>*Augsburg College, Minneapolis, USA*

<sup>4</sup>*Institute of Geology and Geophysics, Beijing, China*

Formation and propagation of geomagnetic sudden impulses (SIs) depending on the sign of the IMF Bz and By components are investigated in the periods of  $|By/Bz| \leq 1$  and  $|By/Bz| > 1$ . The results can be formulated as follows:

(1) In the periods of  $|By/Bz| \leq 1$ , regardless of the sign of the IMF Bz and By, SI generation is mainly accompanied by the enhancement of the eastward (westward) current at latitudes of  $\Phi'=70-75^\circ$  in the prenoon–morning (afternoon–evening) sector. The currents may extend both to lower latitudes and into the polar cap. At the times of SI generation at lower latitudes in the daytime ionosphere, the eastward currents appear in both sectors. In the  $|By/Bz| > 1$  periods, during the SI generation in the daytime (0900-1600) MLT sector, the eastward (westward) currents are also increased at latitudes of  $\Phi'=75^\circ$  at  $By > 0$  ( $By < 0$ ).

(2) SI appeared to propagate poleward, which is most pronounced in the afternoon–evening sector at IMF Bz > 0, and in the azimuthal direction from the noon meridian both eastward and westward at  $|By/Bz| \leq 1$ . In the periods of

large IMF  $B_y$  at  $B_y > 0$  ( $B_y < 0$ ), SI propagates westward (eastward) in the daytime (~1600-0900) MLT sector at latitudes of  $\Phi' \approx 75^\circ$ .

(3) Generation of a geomagnetic disturbance under a sharp compression of the magnetosphere by the solar wind seems to be mainly caused by the enhancement of the region 0 and region 1 field-aligned currents. During some SI events, this can be associated with the intensification of the region 2 field-aligned currents and of the currents related to the IMF  $B_y$ . A disturbance caused by magnetospheric compression propagates from the nose part of the magnetosphere to its tail in the form of a surface wave and is accompanied precipitation of previously trapped particles. Temporal and spatial variations in the ionospheric conductivity lead to redistribution of the ionospheric current systems responsible for SI. A sharp compression of the magnetosphere also results in generation of MHD waves propagating in the inhomogeneous magnetospheric waveguide.

This work was supported by the Russian Foundation for Basic Research, project no. 03-05-39011-GFEN and partially by the programm of presidium of RAS no. 16 p.3

## **Mapping of auroral precipitation boundaries of various types into the magnetosphere**

G.V. Starkov<sup>1</sup>, V.G. Vorobjev<sup>1</sup>, L.I. Gromova<sup>2</sup>, O.I. Yagodkina<sup>1</sup>, Ya.I. Feldstein<sup>2</sup>

<sup>1</sup>*Polar Geophysical Institute, Academy of Sciences, Apatity, Russia*

<sup>2</sup>*IZMIRAN Academy of Sciences, Troitsk, Russia*

The position of auroral precipitation boundaries of various types obtained from observations onboard DMSP spacecraft under different levels of magnetic activity are mapped onto the equatorial plane of the Earth's magnetosphere. The mapping is performed with the parabolic model of the magnetic field using the input parameters separately for nighttime and daytime MLT hours. In the nightside under quite conditions, the poleward boundary of auroral oval structured precipitation (AOP) maps to the distances of 15-18 Re, whereas the equatorward boundary to the distances of 6-8 Re. The projection of the b2i boundary, corresponding to the boundary of isotropy and nearly coincident with the boundary of stable trapping, is close to the projection of the equatorward boundary of AOP. Magnetic activity enhancement results in the displacement of the equatorward boundary of AOP towards the Earth, whereas the poleward boundary is displaced away from the Earth. In the dayside, under quite conditions, the diffuse precipitation region (DAZ) represents a band ~ 4 Re wide, while the region of AOP ~ 1 Re wide with some extension at the evening and morning hours. With magnetic activity intensifying, the dimensions of magnetospheric formations, connected with AOP and DAZ, practically do not change. One can observe their movement towards the Earth, with keeping the dimensions and shape. The total shift in the magnetosphere for AL changing from 140 nT to 540 nT is about 2 Re.

## **Ion acoustic speed and STARE velocity at the large flow angles**

M.V. Uspensky<sup>1</sup>, A.V. Koustov<sup>2</sup>, S. Nozawa<sup>3</sup>

<sup>1</sup>*Finnish Meteorological Institute, Finland*

<sup>2</sup>*University of Saskatchewan, Saskatoon, Canada*

<sup>3</sup>*Solar-Terrestrial Environment Laboratory, Nagoya University*

The electron drift and ion-acoustic speeds in the E region inferred from EISCAT measurements are compared with concurrent STARE radar velocity data. This is done in order to test a recent hypothesis by Bahcivan et al. (2005) that the electrojet irregularity velocity at large flow angles is simply a product of the ion-acoustic speed and the cosine of an angle between the electron flow and irregularity propagation direction. About 3,000 measurements for the flow angles of  $50^\circ$ - $70^\circ$  and electron drifts of 400-1500 m/s are considered. It is shown that the correlation coefficient and the slope of the best linear fit line between the predicted STARE velocity (based solely on EISCAT data and the Bahcivan et al.'s (2005) hypothesis) and the measured one are both of the order of ~0.4. Velocity predictions are somewhat better if one assumes that the irregularity phase velocity is the line-of-sight component of the  $E \times B$  drift scaled down by a factor ~0.6 due to off-orthogonality of irregularity propagation (non-zero effective aspect angles of STARE observations).

## **Magnetospheric-ionospheric convection for the open magnetospheric model**

M. A. Volkov<sup>1,2</sup>, N. Yu. Romanova<sup>2</sup>

<sup>1</sup> *Murmansk State Technical University, Murmansk, Russia, e-mail: mavol@mstu.edu.ru*

<sup>2</sup> *Polar Geophysical Institute, Murmansk, Russia, e-mail: romanova@pgi.ru*

Calculations of the magnetospheric-ionospheric convection for the open magnetosphere with ellipsoidal magnetopause have been made under the assumption that only 0.1 fraction of the interplanetary magnetic field (IMF) penetrates into the magnetosphere. We performed calculations for the southward IMF  $B_z$  and IMF  $B_y > 0$ , IMF  $B_y < 0$ . The results of calculations were compared with the observations of the ion drifts. Some inconsistency between simulation results and observations in case of IMF  $B_y > 0$  is revealed. The location of the convection throat and sizes of morning and evening convection vortices are distinct from experimental data. It is shown that accounting for the reduced Pedersen conductivity in the noon ionospheric sector and finite field-aligned conductivity results in better agreement between the calculation results and experimental data.

## **Nighttime subvisual aurorae in high latitudes**

V.G. Vorobjev, I.A. Kornilov, T.A. Kornilova, B.V. Kozelov (*Polar Geophysical Institute, RAS, Apatity, Murmansk region, 184200, Russia*)

Special methods of TV images processing, which enable recognizing rather weak signals confidently, were used to examine polar aurorae at high-latitude observatory Barentsburg (Spitsbergen). Faint subvisual aurorae (SVA) appearing  $3^\circ$ - $4^\circ$  of latitude poleward of brighter auroral forms of the ordinary auroral oval were found in the nighttime sector from 19 to 04 MLT. The SVA events were observed during rather quiet periods, generally for the northward direction of the IMF  $B_z$  component. However, the SVAs are not the sun-aligned polar cap aurorae, for they are more extended in the east-west direction. The SVA forms were observed moving to the equator with the velocity changing from 0.1 up to 1.4 km/s with the average of about 0.6 km/s. The average living time of a single SVA form was approximately 7 min. According to DMSP spacecraft observations, the latitude of the SVA coincides well with the  $b_{3b}$  boundary, which is the polewardmost boundary of electron acceleration events. The spectrum of SVA electrons has a maximum within the range of 0.4-0.8 keV. It testifies that the SVA height makes about 150-200 km. At these altitudes the auroral brightness in the 630.0 nm emission is normally more than in the 557.7 nm. For the SVA arcs the 630.0 nm intensity was about 0.3-0.5 kR. The SVA events have not been detected by the IMAGE spacecraft UVI imagery.

The SVA events were registered when the interplanetary magnetic field was commonly northward and antisunward ( $B_z > 0$  and  $B_x < 0$ ) and generally during intervals of low solar wind density,  $N \sim 3$ - $5 \text{ cm}^{-3}$ . It is suggested that energetic coronal electrons, which are associated with the central region of solar coronal holes can play an essential role in the SVA generation. We believe that SVA could be considered as a plausible candidate for the ionospheric counterpart of BBFs during prolonged intervals of the northward IMF.

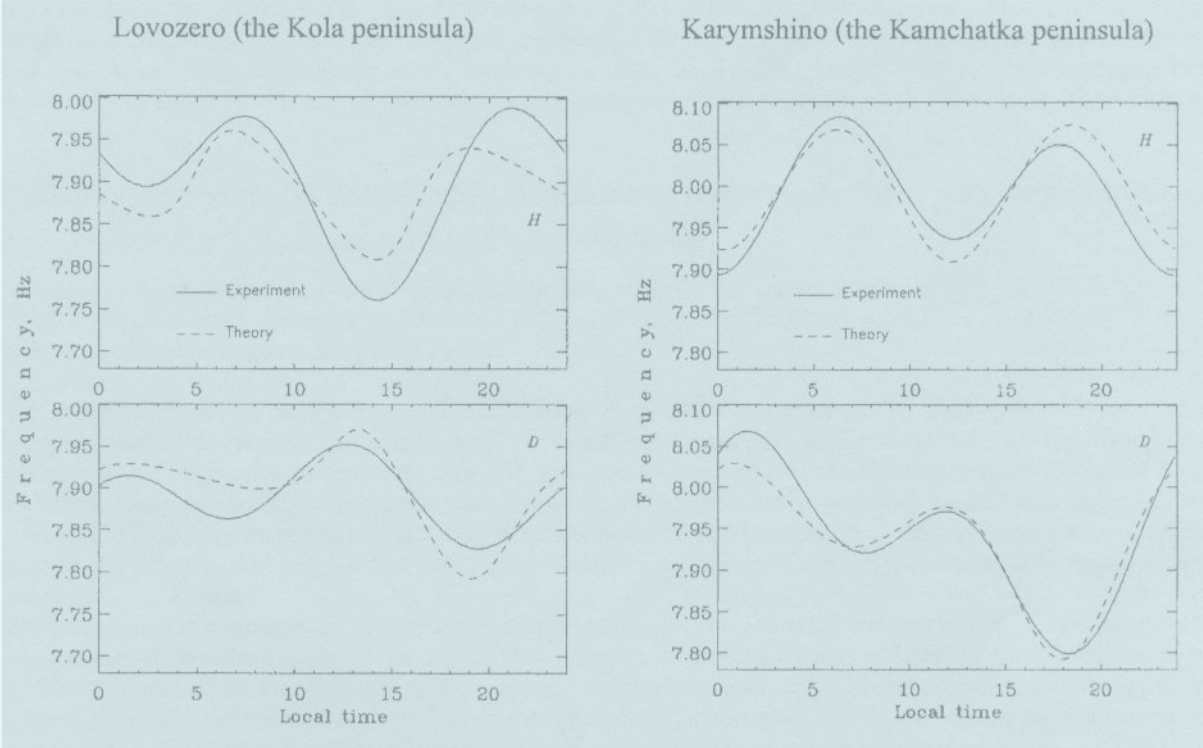
## **Self-consistent simulation of 1D3V current sheet using macroparticle technique**

L.M. Zelenyi, H.V. Malova (*Space Research Institute, Moscow*),

I.V. Mingalev, O.V. Mingalev (*Polar Geophysical Institute, Apatity*)

Numerical self-consistent 1D3V model of the current sheet based on the macroparticle technique has been elaborated. Compared to the previous treatments, this model is more realistic. In particular, it accounts for the real ratio of charge to mass for electrons. With using this model, some configurations of a thin current sheet for different conditions in the lobes have been simulated.

# Waves, Wave-Particle Interaction





## Seasonal and diurnal dependence of Pc3 and Pc4 geomagnetic pulsation power and background noise power at very high latitudes

O.M. Chugunova<sup>1</sup>, V.A. Pilipenko<sup>1</sup>, and M.J. Engebretson<sup>2</sup>, and A. Rodger<sup>3</sup>

<sup>1</sup>*Institute of the Physics of the Earth, Moscow*

<sup>2</sup>*Augsburg College, Minneapolis, MN*

<sup>3</sup>*British Antarctic Survey, Cambridge, UK*

Seasonal and diurnal variations of Pc3 and Pc4 geomagnetic pulsation powers and background noise in Pc3-4 frequency range have been examined using 5 years of search-coil magnetometer data from Antarctic station P5 well in the polar cap ( $-87^\circ$  CGM). Discrimination of signals and noise and calculation of wave power have been made using an approach based on the determination of the wave packet parameters from dynamic spectra of the recordings. Diurnal variations of the hourly power are different for Pc3 and Pc4 pulsations in the polar cap. Two maxima of Pc4 pulsations and background noise in Pc3-4 frequency range have been revealed: in near-noon hours, corresponding to the cusp activities, and early morning hours. For Pc3 pulsations only one (early morning) maximum has been detected. This morning maximum, possibly, corresponds to the geomagnetic projection of the mantle or lobe flanks. The Pc3 pulsation powers have been found to be strongly dependent on season: the power ratio between summer and winter seasons is about 6. For Pc4 pulsations and background noise in Pc3-4 frequency range this ratio is about 3. The 5 year averaged spectrum of the time series of hourly background noise power during one year period shows the occurrence of periodicity about 90, 28, 18 and 13 days. The Pc3 pulsation power exhibits the periods of about 90, 18, and 13 days, whereas the Pc4 power indicates the periods of about 90, 28, and 18 days.

## Cyclotron acceleration of radiation belt electrons by whistler-mode waves with varying frequency

A.G. Demekhov<sup>1</sup>, V.Y. Trakhtengerts<sup>1</sup>, M.J. Rycroft<sup>2</sup> and D. Nunn<sup>3</sup>

<sup>1</sup>*Institute of Applied Physics, Nizhny Novgorod, Russia (andrei@appl.sci-nnov.ru)*

<sup>2</sup>*CAESAR Consultancy, Cambridge, UK*

<sup>3</sup>*University of Southampton, Southampton, UK*

We present a model of the gyroresonant acceleration of radiation-belt electrons by quasimonochromatic whistler-mode waves with varying frequency, such as chorus emissions and natural whistlers arising from lightning discharges in the Earth's atmosphere. Specific attention is paid to the acceleration regime in which energetic electrons, being in cyclotron resonance with the wave, are trapped in the potential well of this wave. For such a regime, the time-varying frequency of wave packets is essential and can lead to much higher acceleration efficiency than in the conventional acceleration regime due to stochastic energy diffusion. Formulas valid in the relativistic case have been obtained.

Estimates show that an increase in the energy of a resonant electron can reach several to tens of keV during a single interaction with a wave packet. It was shown that for chorus wave amplitudes estimated from the backward-wave-oscillator model of chorus generation, the trapping condition is well satisfied for perpendicular energies several times higher than the energy of electrons generating chorus. This implies that in the case of chorus emissions, the acceleration in the nonlinear-trapping regime can operate for higher-energy tail of the distribution, and this process can lead to the formation of highly anisotropic energetic-electron distributions.

## Excitation of Alfvén vortices in the ionosphere by the magnetospheric convection

I.V. Despirak<sup>1</sup>, A.A. Lubchich<sup>1</sup>, V.Y. Trakhtengerts<sup>2</sup>

<sup>1</sup>*Polar Geophysical Institute, Apatity, Russia,*

<sup>2</sup>*Institute of Applied Physics, Nizhny Novgorod, Russia*

Excitation of the ULF waves in the Ionospheric Alfvén Resonator (IAR) is considered, with taking into account an inhomogeneous profile of magnetospheric convection velocity. This profile is formed by interaction of the convective flow with the neutral atmosphere at heights 90 -150 km. The ULF waves include the oblique Alfvén waves trapped in the IAR and drift ionospheric waves, which are in resonance with each other. These waves form strongly anisotropic closed current loops with the scale along the magnetic field much larger than the transverse scale ( $l_z \gg l_\perp$ ) and can be considered as Alfvén vortices. The instability threshold and growth rate are investigated as functions of different parameters (the wave vector  $k_\perp$ ,  $\phi = \frac{k_\perp v}{\omega}$ , ratio of Alfvén wave and Pedersen conductivities) in a model of the ionosphere close to the real one. Some estimates are given in application to observed short-scale field-aligned currents in the auroral ionosphere.

### **Alfven wave interaction with a turbulent layer**

E.N. Fedorov<sup>1</sup>, V.A. Pilipenko<sup>2</sup>, V.V. Vovchenko<sup>2</sup>

<sup>1</sup>*Institute of physics of the Earth, RAS, Moscow, Russia*

<sup>2</sup>*Institute of space research, RAS, Moscow, Russia*

The problem of Alfven wave interaction with a turbulent conductive layer is considered. High-frequency turbulence results in both field-aligned and transverse conductivity of plasma. The Alfven waves can partly reflect from, pass through or be absorbed in the layer. If the field-aligned conductivity is dominated, the relative efficiency of the reflection, absorption or passing through the layer is strongly dependent on the perpendicular wavelength. In case the width of a turbulent layer is small compared to the wavelength, the governing parameter of the problem is the resistive Alfven length  $\lambda_A$ , which is determined by the field-aligned resistivity and Alfven velocity above the layer. The values of decrement obtained from the analytical solutions for a thin layer are consistent with those calculated numerically with using rigorous formulas for a layer of finite width, thus proving that a thin-layer approximation is reasonable for all wavelengths, except for very small ones. The developed model is applied for interpretation of the early results on the damping of Alfven oscillations excited by a pulse source during substorm expansion phase (Pi2 pulsations) in the Earth's magnetosphere. The results suggested stronger decrement for more intense geomagnetic disturbances. Our consideration proves that this effect is associated with a set up of the field-aligned resistivity when the field-aligned currents exceed the threshold values needed for high frequency turbulence to develop.

### **Solution of the wave equation for the ballooning waves in the magnetotail**

I.V. Golovchanskaya, O. V. Mingalev (*Polar Geophysical Institute, Apatity, Russia*)

In the accompanying paper of Golovchanskaya [2006] it is shown that the terms containing  $k_{\parallel}$  in the dispersion relation for the ballooning waves in the limit  $\beta \gg 1$  have little effect in their propagation perpendicularly to the magnetic field. In such a case case, the transverse propagation of the ballooning waves is described by 2D partial derivative linear equation of the 4<sup>th</sup> order. Formulation of the Cauchy problem for this equation is similar to that for the classical linear wave equation. Representation of the solution in terms of the initial conditions can be found by using the Fourier transform. Some aspects of solution behavior are discussed.

### **Ballooning wave propagation in the case of finite $k_{\parallel}$ included**

I.V. Golovchanskaya (*Polar Geophysical Institute, Apatity, Russia*)

In the paper [Golovchanskaya and Maltsev, GRL, 2005] the group velocity of the ballooning waves in the Earth's magnetotail was found with neglecting the term  $\sim 4 \cdot k_{\parallel} (k_n^2 + k_y^2) / k_y^2$  in the wave dispersion relation,  $k_{\parallel}$ ,  $k_n$ , and  $k_y$  being the components of the wave vector along the magnetic field, in the direction of magnetic tension and in the azimuthal direction, respectively. In such a case, the similarity of the ballooning waves to the internal gravitational waves in the upper atmosphere is especially evident. In this study the requirement of the above term smallness is relaxed, and more rigorous formulas for the ballooning propagation velocities are derived. The distinctions between the approximate and more accurate expressions are estimated for the T96 equilibrium magnetotail configurations corresponding to the quiet and moderately disturbed conditions. It is shown that the corrections do not typically exceed a few per cent. That is, the approximate expressions for ballooning wave propagation velocities can be used in most of the problems of magnetospheric physics.

### **2D distributions of amplitudes, gradients and phase velocities of geomagnetic pulsations**

V.S. Ismaguiov, Yu.A. Kopytenko, N.A. Semenov (*Saint Petersburg Branch of IZMIRAN, Russia*)

During June-July, 1998 more than 50 three-component magnetic stations were working in Europe at a square 1500 X 2500 km (experiment BEAR). Data of the stations were used for constructing of 2D momentary distributions of amplitudes and gradient and phase velocity vectors of the geomagnetic pulsations. We can calculate the vectors using any three magnetic stations situated at the Earth's surface in tops of a triangle.

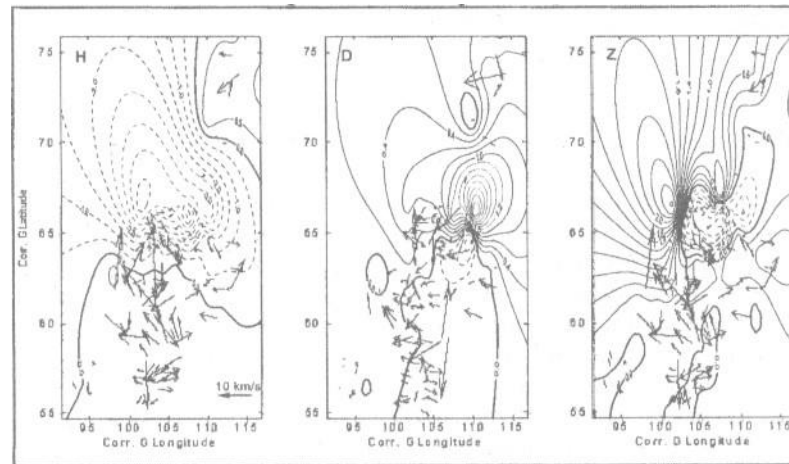
Results of the work are next:

- Directions of the gradients of the geomagnetic pulsations in horizontal components depend on a position of ionosphere sources and from geoelectric properties of the Earth's crust. Directions of the gradients in the vertical component mostly depend on geoelectric properties of the Earth's crust.

- Highest values of the gradients are observed in a region of the ionosphere source and near anomalies of conductivity of the Earth's crust.
- Directions and values of the phase velocities of the geomagnetic pulsations in a region of observations depend only on geoelectric properties of the Earth's crust.

An example of distributions of the phase velocity vectors for H, D and Z magnetic field components is presented at the figure for pulsation periods  $T = 50 - 150$  s.

Momentary 2D distributions of amplitudes (isolines) and phase velocity vectors (arrows) for H, D and Z magnetic field components  $T = 50 - 150$  s)



### **Principal component analysis of simultaneous IRIS and TV observations of pulsating patches**

B.V. Kozelov<sup>1</sup>, E.E. Titova<sup>1</sup>, F. Honary<sup>2</sup>, S. Marple<sup>2</sup>

<sup>1</sup>*Polar Geophysical Institute, Apatity, Murmansk region, 184209 Russia*

<sup>2</sup>*Dept. Communication Systems, Lancaster University, United Kingdom*

Observations of aurora by highly sensitive television (TV) cameras and of riometric absorption by IRIS imaging riometer allows one to study spatio-temporal dynamics of precipitated particles. The dissipation of energetic particles in the atmosphere is accompanied by excitation of auroral emissions at altitudes of 100-200 km, which is observed by optical instruments. If the precipitated particles are sufficiently energetic to penetrate to altitudes below 90 km, then the ionization of atmospheric gases that they produce leads to effective absorption of radiowaves, which is registered by riometers. Pulsating electron precipitations are commonly believed to be a consequence of wave-particle interactions in the magnetosphere. Such pulsating forms in the morning sector are usual for recovery phase of a substorm. However, one-to-one correspondence between the optical and riometric variations is usually not obvious. Here we apply the principal component analysis (also known as proper orthogonal decomposition) to find the correlated spatial structures in simultaneous two-dimensional observations by IRIS (Kilpisjärvi, 69.05° N, 20.79° E) and TV all-sky camera (Porojarvi, 69.17° N, 21.47° E). Results of several case studies are discussed.

### **Scaling of electric field fluctuations associated with the aurora during positive Bz IMF**

B. V. Kozelov and I.V. Golovchanskaya (*Polar Geophysical Institute, Apatity, Murmansk region, 184209 Russia*)

Intermittent fluctuations of the electric and magnetic fields across the polar caps are often observed by low-altitude satellites during positive Bz IMF. They are typically associated with so-called ‘theta’-aurora and transpolar arcs. Here, we present a statistical study of scaling features of the field fluctuations during several events when the theta-aurora was observed by DE-1 satellite. The generalized structure functions (GSF) for the electric field fluctuations have been calculated to determine the scaling properties of the higher order moments. It was found that the GSF usually has the power-law region corresponding to spatial scales from a limit of resolution (~4 km) up to 150-200 km. Also we found a scaling collapse of the probability density function (PDF) of the electric field fluctuations in the same range of spatial scales. The observed PDFs have a non-Gaussian form with long tails. Some dependencies of the PDF form on the solar wind characteristics are discussed. The observed scaling of the field fluctuations has been compared with the results of the same analysis applied to the TV observations of the theta-aurora. The turbulent nature of the fields that we have revealed is interpreted within velocity shear driven turbulization mechanisms.

## **Variations of chorus source location: comparison of Cluster data and the backward-wave oscillator model**

B. V. Kozelov<sup>1</sup>, A. G. Demekhov<sup>2</sup>, E. E. Titova<sup>1</sup>, V. Y. Trakhtengerts<sup>2</sup>, O. Santolik<sup>3</sup>, E. Macusova<sup>3</sup>, M. Parrot<sup>4</sup> and N. Cornilleau-Wehrlin<sup>5</sup>

<sup>1</sup>*Polar Geophysical Institute, Apatity, Russia*

<sup>2</sup>*Institute of Applied Physics, 46 Ulyanov st., 603950 Nizhny Novgorod, Russia*

<sup>3</sup>*Charles University, Prague, Czech Republic,*

<sup>4</sup>*CNRS/LPCE, Orleans, France, (5) CETP/UVSQ, Velizy, France.*

*andrei@appl.sci-nnov.ru/Fax: +7 8312 16 0616*

We study the motion of the source region of magnetospheric chorus emissions using multipoint measurements of VLF wave emissions and geomagnetic field onboard Cluster spacecraft. The wave data from STAFF instrument are used to obtain the energy flux in chorus waves, and the chorus-source region is found as the region where the energy flux is bi-directional. The geomagnetic-field data are matched to a parameterized model of local magnetic field, and the spatio-temporal dynamics of the magnetic field is obtained on this basis. Comparison of these data shows that the chorus-source location remains related to the magnetic-field minimum, while the position of this minimum can vary rather strongly during periods of enhanced geomagnetic activity. These results support the backward-wave oscillator (BWO) model of chorus emissions, which attributes chorus generation to an absolute instability of whistler-mode waves in the presence of a step-like velocity distribution of energetic electrons. Such an instability takes place in a small vicinity of the local “magnetic equator” of a magnetic flux tube. Quantitative agreement between the data and the model is demonstrated by the results of numerical simulations of self-consistent equations of magnetospheric BWO in which the experimentally obtained time-varying profile of the geomagnetic field is used.

## **Magnetosonic solitons in high- $\beta$ non-Maxwellian space plasmas**

O. G. Onishchenko, O. A. Pokhotelov (*Institute of Physics of the Earth, Moscow, Russia*)

M. A. Balikhin (*Automatic Control and Systems Engineering, University of Sheffield, Sheffield, UK*)

R. A. Treumann (*Centre for Interdisciplinary Plasma Science, Max-Planck-Institute for Extraterrestrial Physics, P.O.Box 1312, D-85741 Garching, Germany*)

A nonlinear theory of large-amplitude magnetosonic waves in high- $\beta$  space plasma is developed. It is shown that depending on the form of the equilibrium ion distribution function these waves can exist in the form of magnetic hump or well. The basic parameter that controls the form of the nonlinear structure is the wave dispersion which can be either positive or negative. In Maxwellian plasma the dispersion is negative, i.e. the phase velocity decreases with increase in the wave number and thus the solitary solution has the form of the magnetic hump. On the contrary, in non-Maxwellian plasma such as the Lorentzian plasma this solution may have the form of the magnetic drop-out, or magnetic hole. The relevance of our theoretical results to the existing satellite wave observations is outlined.

## **Shell distribution instability upstream to the terrestrial bow shock**

O.A. Pokhotelov, O.G. Onishchenko (*Institute of Physics of the Earth, 123995, 10 B. Gruzinskaya, Moscow, Russian Federation*)

It is shown that the stability of isotropic ion shell distribution upstream the terrestrial bow shock, previously stated within MHD approximation, is violated at finite ion Larmor radius (FLR) wavelengths. A new instability that results in the growth of compressional mode in the upstream region due to FLR is found. A general dispersion relation as well as a growth rate for the least stable perturbations are derived. The results obtained are applied for the interpretation of satellite observations.

### **Nonlinear ion-cyclotron waves in high pressure plasmas: Kinetic and fluid description**

O.A. Pokhotelov, O.G. Onishchenko (*Institute of Physics of the Earth, Moscow, Russia*)

M.A. Balikhin (*Automatic Control and Systems Engineering, University of Sheffield, Sheffield, UK*)

R.A. Treumann (*Centre for Interdisciplinary Plasma Science, Max-Planck-Institute for Extraterrestrial Physics, P. O.Box 1312, D-85741 Garching, Germany*)

A fully kinetic theory of ion-cyclotron type modes accounting for the collisionless magnetic viscosity in high pressure Maxwellian space plasmas is developed. A comparison of the kinetic results with those obtained in Hall-MHD is provided. It is shown that in order to coincide with the fully kinetic treatment, the Hall-MHD equations should be supplemented by terms describing the effect due to collisionless magnetic viscosity, not included in the previous analysis. This, in turn, leads to the modification of the corresponding nonlinear equation, which describes nonlinear dynamics of ion-cyclotron waves. Results of the theory are applied to existing satellite observations.

### **Global ionospheric Alfvén resonator (GIAR), a new near-Earth ULF resonance system**

S.V. Polyakov (*Institute of radiophysical researches, Nizhny Novgorod, Russia*)

It is shown that different and located apart from each other ionospheric Alfvén resonators (IAR) can interact via the ionospheric current layer, thus behaving self-consistently and forming a new near-Earth ULF resonance system – a global ionospheric Alfvén resonator (GIAR). For the interaction to be efficient, strong horizontal ionospheric inhomogeneities should be present. The following systems are considered: nightside IAR – terminator IAR, polar cap IAR – auroral oval IAR. The theory is applied to explain the observed peculiarities in the spectrum of the background noise at the frequencies lower than that of the first Schumann resonance.

The work is supported by the RFFR (grant N 04-02-17333)

### **Pc5 pulsations on the ground, in the magnetosphere and in electron precipitation: The event of 19 January 2005**

V.C. Roldugin<sup>1</sup>, A.V. Roldugin<sup>1</sup>, N.G. Kleimenova<sup>2</sup> and O.V. Kozyreva<sup>2</sup>

<sup>1</sup>*Polar Geophysical Institute, Apatity*

<sup>2</sup>*Institute of the Earth Physics RAS, Moscow*

At the recovery phase of intense geomagnetic disturbance of 19 January 2005, the Pc5 regular magnetic pulsations with a period of about 5 min and amplitude up to 400 nT were observed in Lovozero. At the same time the TV camera displayed bright aurora near the zenith. The periodicity of the geomagnetic pulsations correlated well with the periodicity of auroral intensifications and motions. The auroral enhancements corresponded to a positive increase in the *H*-component and to a decrease in the *D*-component, in the *Z*-component they fell on a negative semiperiod. The regular pulsations with the same period were observed at wide network of ground observatories up to Japan, but with small amplitude of several nT. Similar pulsations in the magnetic field were registered by the satellites GOES10 and GOES12. In spite of the same period and amplitude of the waves, the polarization was different: at GOES10 the oscillations were toroidal, while at GOES12 they were poloidal. At these satellites the pulsations of relativistic electron fluxes were seen; the maxima of the fluxes were coincident with the minima in electron precipitation over Lovozero.

From Lovozero magnetic data, the directions and distances to the sources have been calculated, using the model of a circular Hall current around a point source. The directions appeared to be rather closely coincident with the aurora position. Thus, it can be concluded that the field of geomagnetic pulsation, observed on the earth's surface, is determined by the 3D current system, its field-aligned part being associated with the flux of auroral electrons. In the magnetosphere the pulsation wave is a traveling wave. In the absence of auroral electron precipitation, the amplitude of magnetic pulsations is not large.

### **Comparison of Schumann resonance parameters in horizontal magnetic and electric fields according to observations in the Kola Peninsula**

V.C. Roldugin, A.N. Vasiljev and A.A. Ostapenko (*Polar Geophysical Institute, Apatity*)

The measurements of horizontal electric components at extremely low frequencies 0.1 – 20 Hz have been started in the high-latitude observatory Lovozero in the Kola Peninsula. It is found that the electric components are not less informative for Schumann resonance study than the horizontal magnetic ones. Diurnal variations of amplitude, frequency and bandwidth of the first Schumann resonance mode in the electric W-E and N-S components are similar

to the variations in the H- and D-components, respectively. The correspondence of the components also takes place for the Q-bursts. The frequencies of the electric and magnetic components are not always equal: in summer, the frequency of the electric N-S component in diurnal variation exceeds the frequency of the magnetic D-component by 0.1 Hz. The parameters of both magnetic and electric components have seasonal variations. Three maxima of thunderstorm activity are observed in daily variations of the amplitude of the electric components. The width of the resonance bands in the electric components is somewhat larger than in the magnetic ones. The calculations of ELF wave components near poorly conducting medium have been performed, the results appear to be consistent with the experimental data.

### **A mechanism of frequency spectrum formation for VLF chorus and its verification by Cluster data**

V. Y. Trakhtengerts<sup>1</sup>, A.G. Demekhov<sup>1</sup>, E.E. Titova<sup>2</sup>, B.V. Kozelov<sup>2</sup>, O. Santolik<sup>3</sup>, E. Macusova<sup>3</sup>, D. Gurnett<sup>4</sup>, J. Pickett<sup>4</sup> and M. J. Rycroft<sup>5</sup>

<sup>1</sup>*Institute of Applied Physics, Nizhny Novgorod, Russia,*

<sup>2</sup>*Polar Geophysical Institute, Apatity, Russia,*

<sup>3</sup>*Charles University, Prague, Czech Republic,*

<sup>4</sup>*University of Iowa, Iowa City, IA, USA,*

<sup>5</sup>*CAESAR Consultancy, Cambridge, UK.*

*vyt@appl.sci-nnov.ru/Fax: +7 8312 16 0616*

Formation of VLF chorus spectrum is considered on the basis of a Backward Wave Oscillator model of chorus generation. Within the framework of this model, chorus elements are generated by a step-like velocity distribution of energetic electrons at the small region of a magnetic flux tube near its equatorial cross-section. The chorus frequency is determined by the local cyclotron resonance of a whistler wave with electrons whose velocity equals the step velocity. The wave frequency spectrum is formed in the process of a nonlinear deformation of the step under the action of chorus emission. The theory yields the spectral form dependence of a separate chorus element on the wave energy flux direction and on the position of observation point inside the generation region. These parameters are verified on the basis of multi-satellite Cluster data. The chorus source is localized using multicomponent measurements of the electric and magnetic fields. Inside the source region, we analyze high-resolution frequency spectra of chorus wave packets based on the data of the WBD instrument. The analysis confirms that spectrum of detected chorus indeed varies depending on the satellite position with respect to the source region. These variations are in qualitative agreement with the theoretical model.

### **Geostationary electrons and geomagnetic ULF fluctuations in the Pc5 range: Cross-correlative analysis**

N. Yagova<sup>1</sup>, N. Romanova<sup>1</sup>, V. Pilipenko<sup>1</sup>, E. Fedorov<sup>1</sup>, and N. Crosby<sup>2</sup>

<sup>1</sup>*Institute of the Physics of the Earth, Moscow*

<sup>2</sup>*Belgian Institute for Space Aeronomy, Brussel*

The correlation of the 50-15000 keV electron fluxes measured by the LANL geostationary satellites with the parameters of spatio-temporal distribution of geomagnetic field variations in the Pcs frequency range is studied. A significant correlation between the ULF spectral power and electron flux is found at time shifts of about  $10^3$ - $10^5$  s. Time shifts and absolute values of correlation coefficients depend on electron energy, geomagnetic latitude of an observational point, and magnetic local time. Possible acceleration mechanisms of magnetospheric electrons by Pc5 wave field are discussed.

### **Proton precipitation and Pc2 pulsations at the recovery phase of the magnetic storm**

T.A. Yahnina<sup>1</sup>, A.G. Yahnin<sup>1</sup>, T. Bösinger<sup>2</sup>, A.N. Voronin<sup>1</sup>

<sup>1</sup>*Polar Geophysical Institute, Apatity, Russia*

<sup>2</sup>*Department of Physical Sciences, University of Oulu, Oulu, Finland*

Localized energetic proton precipitation well inside the region of anisotropic fluxes has been recently found to be closely related to Pc 1-2 pulsations. Another type of proton precipitation adjacent to the isotropy boundary from the equatorial side can be observed at the same time. This proton precipitation can also be considered as a signature of the EMIC wave activity. We examined several Pc2 events ( $f=0.1$ - $0.2$  Hz) observed during the recovery phase of the

magnetic storm when both of the above types of the proton precipitation were registered by low-orbiting NOAA satellites. Our analysis proves that the considered Pc2 are related to the proton bursts within the anisotropic flux region rather than to the precipitation adjacent to the isotropy boundary. This conclusion was confirmed using the data from the Finnish meridional network of search-coil magnetometers. It has been found that the amplitude of the Pc2 signal on the ground has its maximum at the latitude of the localized proton burst.

### **On the “convective” model of generation of IPDP pulsations**

N.A. Zolotukhina<sup>1</sup>, J. Cao<sup>2</sup>, O.V. Chugunova<sup>3</sup>

<sup>1</sup>*Institute of Solar-Terrestrial Physics, Irkutsk, Russia*

<sup>2</sup>*Center for Space Science and Applied Research, Peking, China*

<sup>3</sup>*Institute of the Physics of the Earth, Moscow, Russia*

We present a Pc1-IPDP succession of geomagnetic pulsations generated on April 7, 2000 during the early recovery phase of a great magnetic storm. The wave phenomenon started as Pc1 forty minutes after the first enhancement of the magnetospheric convection and merged continuously into IPDP twenty minutes after the next convection enhancement. A comparative analysis of the ground-based and satellite data indicates Pc1 and IPDP generation in association with convective disturbances. The bay-like disturbances of the horizontal component H of the geomagnetic field (positive in the evening sector and negative in the morning sector) started to develop simultaneously with Pc1 onset. The maxima of H disturbances moved gradually to the equator as the wave phenomenon evolved. The inner edge of the plasma sheet moved to the Earth and overlapped the geosynchronous orbit. All positive bay-like H disturbances, which were registered at this time at low-latitude, were not substorm manifestations but variations of the solar wind dynamic pressure. Then, the phenomena similar to that registered on April 7, 2000 may be a result of magnetospheric convection enhancement.

We have shown that the frequency of Pc1-IPDP is changing with time in a similar way as the displacement of the inner edge of the plasma sheet. Hence, the IPDP geomagnetic pulsations can be generated without any substorm injection, and the “convective” model of IPDP generation (Zolotukhina, 1982; Kangas et al., 1998) gives a good prediction for the evolution of IPDP frequency in such events.

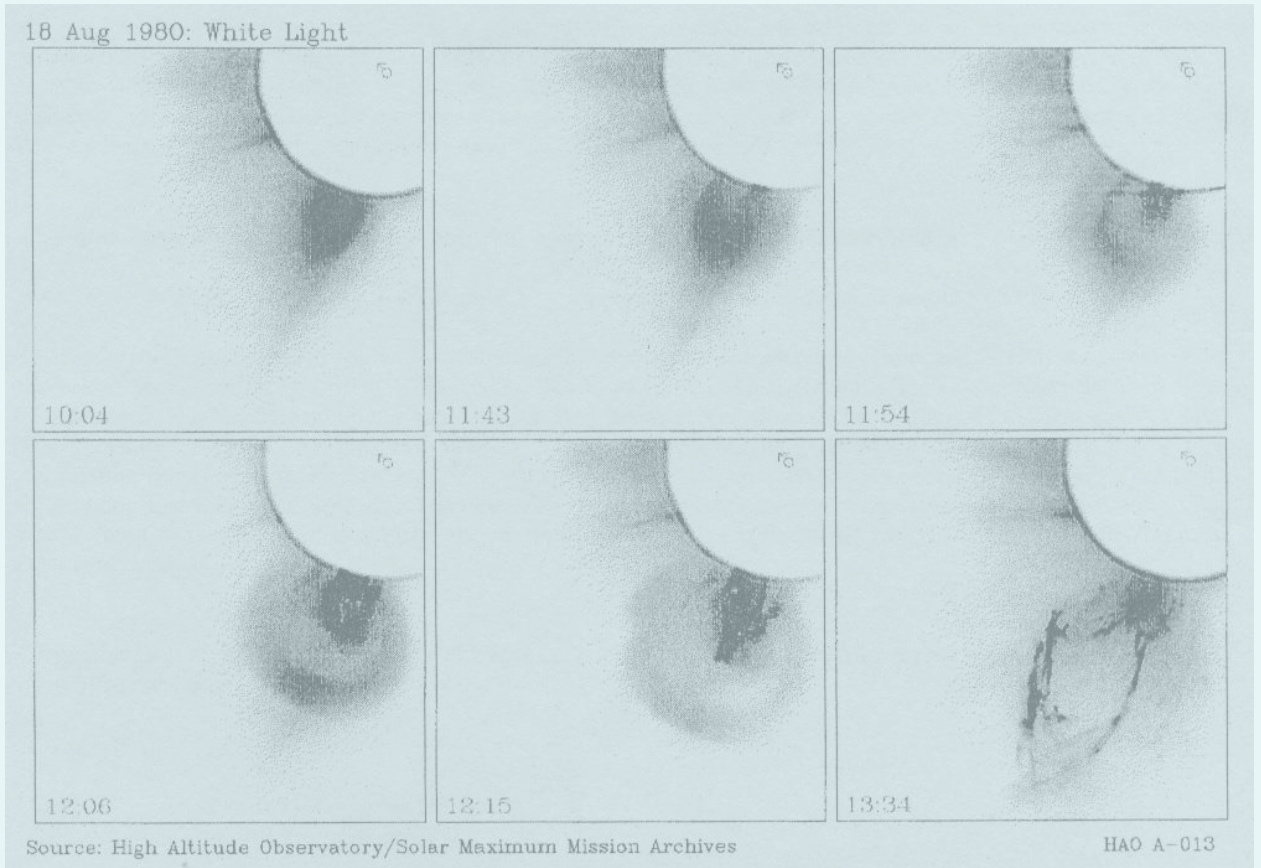
This study is supported by the INTAS grant 03-51-5359.

*Zolotukhina N.A. On the interpretation of geomagnetic IPDP pulsations in the context of kinetic instability of ring current protons. Issled. Geomagn. Aeron. Fiz Solnisa (in Russian). 58. 41-47. 1982.*

*Kangas J., Guglielmi A., Pokhotelov O. Morphology and physics of short-period magnetic pulsations (a review) // Space Sci. Rev. V.83. № 4. P.435-512. 1998.*



# *The Sun, Solar Wind, Cosmic Rays*





## **The advanced technique of determination of relativistic solar proton parameters from ground based observations**

Yu.V. Balabin, E.V. Vashenyuk (*Polar Geophysical Institute, Apatity, Russia*)

The worldwide neutron monitor network can be considered as a united multidirectional solar proton spectrometer in the relativistic energy range. From modeling neutron monitor (NM) responses to anisotropic solar proton flux and comparing them with observations, the parameters of primary relativistic solar protons outside the magnetosphere can be obtained. The data of not less than 25-30 neutron monitor (NM) stations are needed for such kind of analysis which consists of a few steps: a) definition of asymptotic viewing cones of neutron monitor stations by particle trajectory computations in the model magnetosphere (with the step in rigidity of 0.001 GV): The magnetosphere model T01 is employed; b) calculation of neutron monitor responses at variable parameters of solar proton flux; c) determination by the least square technique (optimization) of primary solar proton parameters outside the magnetosphere by comparison of computed responses with observations. Previously, we utilized a simplified technique, only accounting for the particles falling vertically on the neutron monitor. At the same time, an essential contribution to the counting rate of a neutron monitor is due to the particles with oblique incidence. It is especially important for low- and mid-latitude stations. We have developed a technique of modeling of responses of ground based cosmic ray detectors with taking into account oblique incidence primaries. This complicated the calculations considerably but the convergence of the solution of the inverse problem of obtaining RSP parameters from NM data improved noticeably. With a new technique applied, a revision of a number of previously studied events has been made. A good consistence of derived RSP parameters with direct solar proton data in adjacent energy ranges is shown.

## **The new data acquisition unit for neutron monitors in Apatity and Barentsburg**

Yu.V. Balabin, B.B. Gvozdevsky, L.I. Schur, E.V. Vashenyuk (*Polar Geophysical Institute, Apatity, Russia*)

The new data acquisition unit for neutron monitors in Apatity and Barentsburg is proposed. The system is based on the use of special PCI cards of PCI-7233H and PCI-8554 (ADLINK Technology Inc.) type. With the digital 32-channel card PCI-7233H a computer can read out the information on each of 18 counters of neutron monitor data. The 8-channel counter/timer card PCI-8554 is used to perform auxiliary functions such as reading out service information (pressure, temperature, etc.). The card PCI-8554 also generates clocks necessary for reading out basic information that facilitates work of a computer. The proposed system provides not only direct data collecting, but also permits to use software to register the multiplicities. It will enable to determine not only intensity but also cosmic ray spectra.

## **Classification of abrupt changes of the interplanetary medium parameters by a method of artificial neural networks**

N.A. Barkhatov <sup>1,2</sup>, S.E. Revunov

<sup>1</sup>*Nizhniy Novgorod State Pedagogical University*

<sup>2</sup>*Radiophysical Research Institute (NIRFI)*

The technique of classification of abrupt changes or discontinuities in registered parameters of space plasma and magnetic field into groups corresponding to the known types of MHD gaps is developed with using artificial neural networks (ANN). For this purpose, the ANN of Kohonen layer type is created, permitting to perform automatic classification of discontinuities. The classification and its interpretation require a development of numerical experiment techniques. Two algorithms have been tested. In one of them the classification starts with the division of discontinuities by the sum of pressures, in the other - with the division by the magnetic field. The designed technique is applied for the classification of parameters of the discontinuities registered by WIND spacecraft in 1996-1999. The network performance is tested and confirmed by comparison of automatic classification results obtained with the both algorithms and the results of the classification performed "manually" with the same algorithms. It is established that the percentage of discrepancies for different versions of classification is within 12-25 %.

The method alternative to the known one [Sonnerup, et.al., 2005] is proposed to determine the orientation of discontinuities fronts. Its application is possible after discontinuity classification is accomplished. The method is based on the set of conditions for particular types of gaps in interplanetary medium parameters. The main data source for solution of this problem is information on behavior of magnetic field and flow velocity components. As a

### ***The sun, solar wind, cosmic rays***

result, for the gaps of established classes, the orientation of their surface planes in 3D space is determined on the basis of 1D observations. A special research on evolution of established shock waves testifies to instability of all considered events.

*Sonnerup B.U.O, H. Hasegawa Orientation and motion of two-dimensional structures in a space plasma, J. Geophys. Res., 2005, Vol. 110, N A06208, doi:10.1029/2004JA010853.*

### **Solar cosmic ray fluxes in the Earth's orbit**

I. V. Getslev, V. P. Okhlopkov, M. V. Podzolko (*Skobeltsyn Institute of Nuclear Physics, Moscow State University, Moscow, Russia*)

We have reviewed the data on solar cosmic ray proton fluxes in the Earth's orbit outside the magnetosphere from 1956 to 2005. 338 solar proton events, with the fluence of protons with energies  $> 30$  MeV exceeding  $10^3$  cm<sup>-2</sup>, were considered. The results of the analysis of proton frequency and amplitude distribution and their energy spectra are presented. An essential irregularity in the distribution of proton sources on the Sun in Carrington longitudes, as well as in longitudes from the central meridian, is shown. The peculiarities and reliability of the results obtained are being discussed. From comparing the proton fluences in different time periods, the distribution of their values is examined, with finding out strong and weak solar cycles from this viewpoint. The correlation between 3-month, half-year and one-year proton fluence time series and corresponding data on sunspot numbers and radio emission at the frequency of 10.6 MHz is studied. The data on a decrease of solar proton event number and total fluences of protons of various energies and changing their spectra during the period of solar magnetic field sign change are presented.

The necessity of permanent monitoring of various parameters of solar proton events and accompanying physical phenomena is emphasized.

### **The muon bursts with energy above 200 GeV recorded during GLE events**

S.N. Karpov<sup>1</sup>, L.I. Miroshnichenko<sup>2</sup> and E.V. Vashenyuk<sup>3</sup>

<sup>1</sup>*Institute for Nuclear Research of RAS, Baksan Neutrino Observatory, Neutrino, KBR, 361609, Russia*

<sup>2</sup>*N.V. Pushkov Institute of Terrestrial Magnetism, Ionosphere and Radio Waves Propagation (IZMIRAN), Troitsk, Moscow Region, 142190, Russia*

<sup>3</sup>*Polar Geophysical Institute, Kola Science Center of RAS, Apatity, Murmansk Region, 184209, Russia*  
*karpovsn@yandex.ru*

Statistical analysis of the muon bursts with energy  $\geq 200$  GeV recorded at the Baksan Underground Scintillation Telescope (BUST) during GLE events is extended on the current 23rd cycle of solar activity. The observed surplus of bursts with large amplitude possibly indicates a presence of an additional muon flux. The muon bursts of significant amplitude were registered during four GLEs: on 29 September 1989, 28 October 2003, 15 June 1991 and 12 October 1981. The temporal distribution of the newly occurred bursts shows the asymmetry found earlier: the delay of the bursts relative to the maximum of corresponding X-ray flare is equal to 1-2 hours. The ecliptic longitude distribution of the bursts shows a surplus in the range of angles from 0° to 60° to the West from the Sun-Earth direction, which may infer a link with the IMF.

### **Using extensive air shower detectors for the study of solar cosmic rays**

Z.M. Karpova, S.N. Karpov and A.B. Chernyaev (*Institute for Nuclear Research of RAS, Baksan Neutrino Observatory, Neutrino, KBR, 361609, Russia, zkarпова@yandex.ru*)

Extensive Air Shower (EAS) Detectors which use one-particle mode of registration should be more sensitive to Solar Cosmic Rays (SCR) with energies above 5 GeV due to their larger effective area compared to the standard Neutron Monitors (NMs). The analysis of Ground Level Enhancements (GLE) occurred in 21-23 cycles of solar activity has been performed based on the data of three Baksan EAS detectors. The intensity increases related to SCR were registered in 15 of 30 GLE events studied, which corresponds to 50 per cent of the specified events, the accuracy being a tenth of per cent. Therefore, the increases cannot be registered by neutron monitors with the same geomagnetic cutoff. Combining all data of three Baksan EAS detectors and worldwide network of NMs allows us to

extend the spectrum of SCR into the energy range up to 5-10 GeV, where the data of NMs are often absent. The yield and response functions of Baksan detectors are needed to derive the primary SCR intensity by recorded count rate of secondary particles. The results of calculation of these functions for all three Baksan detectors are presented.

### **On the long-term variations of the medium energy galactic cosmic ray intensity according to the balloon and neutron monitor data at Kola peninsula and Moscow region**

M.B. Krainev<sup>1</sup>, A.V. Belov<sup>2</sup>, R.T. Gushchina<sup>2</sup>, V.G. Yanke<sup>2</sup>

<sup>1</sup> *Lebedev Physical Institute, Moscow, Russia*

<sup>2</sup> *IZMIRAN, Troitsk, Moscow region*

The long-term behavior of galactic cosmic ray (GCR) intensity of medium energy nuclei (100-500 MeV/n) is of special interest. It is only for these particles that 1) the intensity, and hence the statistical accuracy of intensity measurements, is high; 2) the solar modulation is significant during all phases of the solar cycle and everywhere in the heliosphere; 3) the contribution of anomalous cosmic rays to the intensity is small; 4) there have been long-term experiments that provided a lot of data on the GCR intensity in this range measured aboard spacecraft both in the inner heliosphere (the IMPs at  $r=1$  AU since the end of 1960s) and in the intermediate and outer heliosphere (the Pioneer-10, 11 since 1972, 1973, and Voyager-1, 2 since 1977, respectively). Unfortunately, detailed direct measurements near the Earth had been carrying out only till October 2001.

It was shown earlier that one of the effective indirect methods of the study of medium energy GCR intensity at 1 AU is the investigation of the difference between atmospheric ionizing particle fluxes measured at high altitudes above the Kola Peninsula (the cutoff rigidity  $R_c \approx 0.6$  GV, corresponding to  $T_c^P \approx 180$  MeV for protons) and Moscow region ( $R_c=2.3$  GV,  $T_c^P \approx 1500$  MeV for protons) in the course of frequent balloon monitoring of cosmic rays. The investigation of the medium energy GCRs by this method has been conducting since 1957 up to now.

In this talk we try to estimate to what extent one can approach the GCR medium energy range using the neutron monitor data (both the global survey and difference in the count rates of high and middle latitude neutron monitors). Besides, the results on the difference between the atmospheric particle fluxes measured at high and middle latitude points may strongly depend on some factors, only insignificantly influencing the fluxes measured at each point. From the results of simultaneous balloon and neutron monitoring of cosmic rays at approximately the same locations (Apatity at Kola Peninsula and Dolgoprudny and Troitsk in the Moscow region) we estimate the influence of small duration of each balloon flight and variable number of flights per month. In addition, the influence of change with time of the location of the balloon monitoring at Kola Peninsula (Loparskaya, Olenya, Apatity) is estimated.

### **On the behavior of medium energy galactic cosmic ray intensity in the outer heliosphere ( $r=75-97$ AU)**

M.B. Krainev (*Lebedev Physical Institute, Russian Academy of Sciences, Moscow, Russia*)

The development of the minimum phase between the 23 and 24 solar cycles is considered in the solar and inner heliospheric characteristics and in the galactic cosmic ray (GCR) intensity both near the Earth and in the outer heliosphere (at heliocentric distances  $r = 75 - 97$  AU, using the Voyager 1, 2 data). Because of contribution of the anomalous component at energies  $E < 100$  MeV, the best energy region to study the behavior of the GCR intensity in the outer heliosphere is a so-called medium energy range (100-500 MeV/n). As we mentioned in the accompanying talk, one of the effective indirect methods of the study of medium energy GCR intensity at 1 AU is the investigation of the difference between the atmospheric ionizing particle fluxes measured at high altitudes at Kola peninsula and in Moscow region in the course of the frequent balloon monitoring of cosmic rays (FBMCR), allowing the investigation of the medium energy GCRs since 1957 up to now.

In this talk our attention is focused on the following problems:

- 1) The present day phase of the solar cycle in the characteristics considered;
- 2) The observed behavior of medium energy GCR intensity in the inner heliosphere according to the FBMCR experiment and its expected behavior in the outer heliosphere with normalization by the radial profiles of the intensity in the extreme phases of solar cycle;
- 3) The main features in the GCR intensity modulation in the outer heliosphere:

## ***The sun, solar wind, cosmic rays***

- the relationship between the quiet development of the solar cycle minimum phase corresponding to the ( $A < 0$ ) phase of the 22-year (or magnetic) solar cycle and the active phenomena;
- the expected vs observed manifestations of the Strong negative latitude gradient in the IGR intensity with respect to the global heliospheric current sheet;
- the expected vs observed manifestations of the reported crossing of the termination shock front by the Voyager-1 spacecraft at the end of 2005 in the medium energy GCR and anomalous component.

## **Evolution of interplanetary magnetic clouds**

M. Leitner<sup>1,2</sup>, C. J. Farrugia<sup>3,4</sup>, H. K. Biernat<sup>1,2</sup>, N. V. Erkaev<sup>5</sup>, F. T. Gratton<sup>6</sup>

<sup>1</sup>*Space Research Institute, Austrian Academy of Sciences, A-8042 Graz, Austria,*

<sup>2</sup>*Institute for Geophysics, Astrophysics, and Meteorology, University of Graz, A-8010 Graz, Austria,*

<sup>3</sup>*Institute of the Study of Earth, Oceans and Space, University of New Hampshire, Durham, NH 03824, USA,*

<sup>4</sup>*Physics Department, University of New Hampshire, Durham, NH 03824, USA,*

<sup>5</sup>*Institute of Computational Modelling, Russian Academy of Sciences, 660036 Krasnoyarsk, Russia*

<sup>6</sup>*Institute of Plasma Physics, Univ. of Buenos Aires, 1114 Buenos Aires, Argentina*

*e-mail: martin.leitner@oeaw.ac.at / phone: +43 316 4120 633*

Interplanetary magnetic cloud parameters change while these structures propagate into the heliosphere. By fitting the data to a force-free field model (Lundquist, 1950; Burlaga, 1988), we obtain results which are statistically analyzed in reference to the change with heliospheric distance,  $r_h$ . We work with ensemble averages, binning the results in radial intervals of width 0.1 AU for the range  $0.3 < r_h < 1$  AU.

Doing this we obtain the change with heliospheric distance for the fitted magnetic field strength, the size of the structure, and the mean proton density and temperature within magnetic clouds. The orientation of the axis of the underlying magnetic flux tube is generally found to lie along the east-west direction and in the ecliptic plane.

For this study we employ primarily events observed by Helios 1 and 2 and Wind, which are extended by observations from spacecraft operating during the Helios mission (e.g. Voyager 1 and 2, Pioneer 10 and 11, and others). This gives us the possibility to monitor the evolution of magnetic cloud parameters for a given event as a function of  $r_h$  directly by line-up observations. (Several events were found). From these line-ups, we find further that the values obtained by magnetic clouds beyond 1AU differ from the results above.

## **Structure of solar wind flows at maximum and decline of the 23d solar cycle**

N. A. Lotova<sup>1</sup>, K. V. Vladimirovsky<sup>2</sup>, V. N. Obridko<sup>1</sup>

<sup>1</sup>*IZMIRAN, Troitsk, Moscow region, Russia*

<sup>2</sup>*Lebedev Physical Institute of the RAS, Moscow, Russia*

The structure of solar wind flows is studied based on complex analysis of the location of the inner boundary of the transition transonic region  $R_{in}$  of the solar wind, calculations of the magnetic field in the solar corona, and white coronal images obtained by the coronagraph LASCO C2 KA SOHO.

Regular experiments on sounding of the near-Sun plasma by the radiation from natural sources enable to build radio maps, positioning the transition region versus radial distance and helio latitude, which visualize the large-scale helio-latitudinal structure of plasma flows. From the results of the complex analysis of data, an increase in the velocity of solar wind flows in 2003-2004, as compared to the solar maximum of 2000-2002, has been revealed. It was also established that the year of the change of activity maximum epoch for activity decline epoch is not coincident with its definition from the Wolf numbers,  $R_z$  and green coronal emission data.

## **Alfven wave interaction with a fast shock**

A.A. Lubchich, I.V. Despirak, V.B. Belakhovsky (*Polar Geophysical Institute, Apatity, Russia*)

In the approximation of ideal one-fluid MHD, an interaction of an incident plane Alfven wave of small amplitude with a plane fast shock of arbitrary intensity is analyzed. In a general case, beyond the shock front six outgoing MHD waves arise, namely, direct and reverse Alfven and slow magnetosonic waves, a direct fast magnetosonic wave and an entropy wave. Besides, the shock surface itself suffers small perturbations. Typically, in describing the

latters, two well-known kinematic effects are taken into account. These are associated with shock velocity perturbations and the oscillations of the normal to the shock surface. In our consideration, we account for a less known dynamical effect proceeding from a non-inertial character of the local framework of the perturbed shock surface. In this framework, an additional pressure, arising due to inertial forces, is acting on the perturbed discontinuity surface. The physical reason of the inertial force arising is non-ideality of the medium inside the front of a real shock wave.

It has been previously shown by Lubchich and Pudovkin (Phys. Fluids, 2004) that this additional dynamical effect essentially changes the solution of the problem of incident wave interaction with a shock. In the present study we analyze the amplitudes and propagation angles of all outgoing waves depending on the direction of the wave vector of the incident Alfvén wave, intensity of the shock, value and orientation of the background magnetic field. The results obtained can be applied for the problem of wave perturbation passing from the solar wind into the magnetosheath.

### **Geomagnetic cutoff variations during solar energetic particle events of May and June 2005 : “Universitetskiy-Tatyana” and CORONAS-F satellite data**

I.N. Myagkova, M.I. Panasyuk, S.N. Kuznetsov, B.Yu. Yushkov, E.A. Muravieva, L.I. Starostin, T.A. Ivanova, I.A. Rubinshtein, N.N. Vedenkin, N.A. Vlasova (*Skobel'syn Institute of Nuclear Physics, Moscow State University, Moscow, Russia*)

2005 year is far enough from the solar activity maximum of the current cycle, but several rather powerful flares of M class, e.g., on May, 13 (M8.0/2B, N12E11) and June, 16 (M4.0/SF, N08W90), occurred and became a source of solar energetic particle (SEP) events in near-Earth space. These events were detected by instruments on board two satellites: CORONAS-F (started on 30 July, 2001 into a circular polar orbit, in 2005 the height was significantly lower, about 350 km, an inclination of 82.5 degrees) and “Universitetskiy-Tatyana” – the first Space Scientific and Education mikrosatellite of the Lomonosov Moscow State University (started on 20 January, 2005 into a circular polar orbit - 950 km, an inclination of 83 degrees). Solar electrons (0.3-12 MeV) and protons (1-90 MeV) were detected on board CORONAS-F satellite and 0.07-0.9 KeV (electrons) and 2-100 MeV (protons) - on board “Universitetskiy-Tatyana”. We have investigated and compared the time and spectral characteristics of these SEP increases, as well as geomagnetic cutoff variations during these events, obtained in the two experiments. The events occurred near solar activity minimum are of significant interest, and any experimental data on them are valuable from the point of view of forecasting space weather during the periods of minimum and decay of solar activity.

### **Current sheet of the solar corona as a source of solar flare radio-emission**

A. I. Podgorny<sup>1</sup>, I. M. Podgomy<sup>2</sup>, N. S. Meshalkina<sup>3</sup>

<sup>1</sup>*Lebedev Physical Institute RAS, Moscow, Russia, podgorny@fian.fiandns.mitp.ru*

<sup>2</sup>*Institute for Astronomy RAS, Moscow, Russia, podgorny@inasan.ru*

<sup>3</sup>*Institute for Solar-Terrestrial Physics SO RAS, Irkutsk, Russia, nata@iszf.irk.ru*

It was previously reported at Apatity seminars that the current sheet is formed in the pre-flare state. The energy, sufficient for a solar flare, is accumulated in current sheet magnetic field. Still, up to now, there have not been published evidence that flare-time energy release in the corona takes place in the current sheet. 3D MHD calculations allowed us to obtain the current sheet configuration and its position above the active region AR 0365 prior to the May 27, 2003 flare. The initial potential field was found by numerical solution of the Laplace equation with oblique derivative as a boundary condition. To suppress the numerical instabilities, which arise in case of a real active region, special techniques were developed. The finite-difference scheme, which is realized in the PERESVET code, is absolutely implicit and conservative relative to the magnetic flux. The current sheet is formed in the vicinity of the magnetic field singular line due to disturbance focusing, which propagates from the photosphere. For the first time in setting the boundary conditions the distribution of line-of-sight magnetic component observed on the photosphere is used directly. The current sheet position is compared with the distribution of radio-emission brightness temperature observed by the radio-telescope SSRT (Irkutsk). The position of brightness temperature maximum at the wavelength of 5.2 cm coincides with the location of current density maximum in the current sheet with the accuracy of  $\sim 1^\circ$  in heliocentric coordinates. It means that the energy release occurs in the current sheet. The possible calculation errors are  $\sim 1^\circ$ . This result should be considered as a direct evidence of the flare mechanism, which is based on energy release in the current sheet.

## **Hard X-rays generation at a solar flare**

I.M. Podgorny<sup>1</sup>, A. I. Podgorny<sup>2</sup>

<sup>1</sup>*Institute for Astronomy RAS, Moscow, Russia, podgorny@inasan.ru*

<sup>2</sup>*Lebedev Physical Institute RAS, Moscow, Russia, podgorny@fian.fian.dns.mitp.ru*

The main part of solar flare energy is expended for X-ray generation. The observations near the solar limb (Yohkoh and RHESSI spacecraft) demonstrated that three powerful hard X-rays sources usually appear. One source is located in the corona above the loop. The feet of the loop are coincident with two other sources that are observed on the solar surface in the northern and southern spots of an active region. The X-ray energy distribution of the coronal source is well fitted by a thermal spectrum with the electron temperature of 20 keV. The two surface sources exhibit a power spectrum typical for the X-rays produced by electron beams with energy up to 200 keV in a thick target. These results show that a fast energy release occurs in the corona, with heating coronal plasma and creation of electron beams precipitating along the magnetic field lines into the chromosphere. According to the electrodynamic model of the solar flare, the electron beams are accelerated in the field-aligned currents produced by the Hall electric field in the current sheet. The data on the hard X-rays and solar cosmic rays discussed at the Apatity seminar last year are in agreement with the scenario inferred from the electrodynamic solar flare model. The general magnetic field configuration and geometry of electron precipitation pattern during a solar flare lead to a conclusion about analogy with electron precipitation in aurora.

## **Multiple proton acceleration at the Sun and their scatter-free propagation to the Earth on 20 January 2005**

A.B. Struminsky<sup>1,2</sup>

<sup>1</sup>*Space Research Institute, Moscow, Russia*

<sup>2</sup>*IZMIRAN, Troitsk, Moscow region, Russia*

Observations of solar protons near the Earth and of the solar flare in different electromagnetic wavelengths on 20 January 2005 have been analyzed. Solar protons with energies >80 MeV propagated scatter-free to the Earth for the first ~ 30 minutes after their release into interplanetary space, so that their intensity time profiles were determined solely by the temporal and energetic characteristics of the solar injection function. The injection of 80-165 MeV protons started at 06:43:80 UT. Their injection function can be expressed as a product of the ACS SPI count rate (temporal dependence) and the proton spectrum  $\sim E^{-4.7 \pm 0.1}$  (energy dependence). The protons of higher energies were injected 4 min later (the relativistic electrons 9 min later) than that time. A close connection between high energetic solar electromagnetic emission and solar proton fluxes near the Earth is a strong argument in favor of the prolonged and multiple acceleration of protons in solar flares. Possibly, a formation of the system of post-eruption flare loops was accompanied by subsequent episodes of energy release and particle acceleration. The obtained results contradict to the concept of solar energetic particle acceleration by the CME driven shock wave during gradual events.

## **Seasonal variations of geomagnetic disturbance inferred from aa-index analysis and solar activity**

T.E. Val'chuk (*Pushkov Institute of Terrestrial Magnetism, Ionosphere and Radio Wave Propagation (IZMIRAN) RAS, Troitsk of Moscow region, e-mail: val@izmiran.troitsk.ru*)

The Wolf numbers (11-year cycles from 14 to 23) and global aa-index of geomagnetic activity have been used for investigation of the semiannual variation of geomagnetic activity depending on solar cycle phase in even and odd solar cycles. Statistically meaningful geomagnetic activity maxima near the times of spring and autumn equinox motivate a search for underlying physical mechanisms. The origin of the semiannual variation is being widely discussed by the researchers. At present, there is no unambiguous explanation for this effect, but statistical reliability of the semiannual maxima near equinoxes rises interest to this problem. The calculations of the semiannual variation for diurnal and monthly values of the aa-index have been performed. There were considered 4 phases of the solar cycle - those of minimum, maximum growth and decline. The results are interpreted within heliomagnetic action on the Earth's magnetosphere and may be useful in the forecast of geomagnetic disturbances.

This work was supported by the Russian Foundation of Basic Research, grant № 040216374a.

## **Relativistic solar cosmic rays in the GLE of 23 February 1956. New study**

E.V. Vashenyuk<sup>2</sup>, Yu.V. Balabin<sup>2</sup>, L.I. Miroshnichenko<sup>1</sup>

<sup>1</sup> *N.V. Pushkov Institute of Terrestrial Magnetism, Ionosphere and Radio Waves Propagation (IZMIRAN), Troitsk, Moscow Region, 142190, Russia*

<sup>2</sup> *Polar Geophysical Institute, Kola Science Center of RAS, Apatity, Murmansk Region, 184209, Russia*

Characteristics of relativistic solar protons (RSP) are obtained and their dynamics studied in the event of 23 February, 1956, the largest in history GLE. The data of the neutron monitors available at that time and muon telescopes are used. The analysis includes: a) calculation of asymptotic cones of ground based detectors, b) modeling of cosmic ray detector responses at variable parameters of solar proton flux; c) determination of primary solar proton parameters outside the magnetosphere from comparison of the computed responses with the observations by the least square technique.

It is shown that the RSP flux consisted of two components: prompt and delayed ones. The prompt component with exponential energetic spectrum caused a giant pulse-like increase at a number of European cosmic ray stations. The delayed component had a power law spectrum and was a cause of gradual increase at CR stations in the North America region.

## **Relativistic solar cosmic rays. Review of recent results**

E.V. Vashenyuk (*Polar Geophysical Institute, Apatity, Russia*)

Relativistic solar cosmic rays consist mostly of protons with the energy higher than  $\sim 1$  GeV. They transfer information about physical processes on the Sun, interplanetary magnetic field (IMF), Earth's magnetosphere and atmosphere. So far, the ground-based detectors of cosmic rays provide most of data on relativistic solar protons (RSP). In this review the up-to-date methods of obtaining RSP characteristics from ground-based observations are considered: the use of the worldwide network of neutron monitors as a multidirectional spectrometer of cosmic rays; observations of solar cosmic rays of extremely high energy by using the instruments with great registration area. Some recent scientific results of RSP exploration are discussed, including possible mechanisms of particle acceleration in active processes on the Sun, propagation of the particles in the interplanetary magnetic fields and its large-scale structures, as well as some magnetospheric effects related to the RSP.

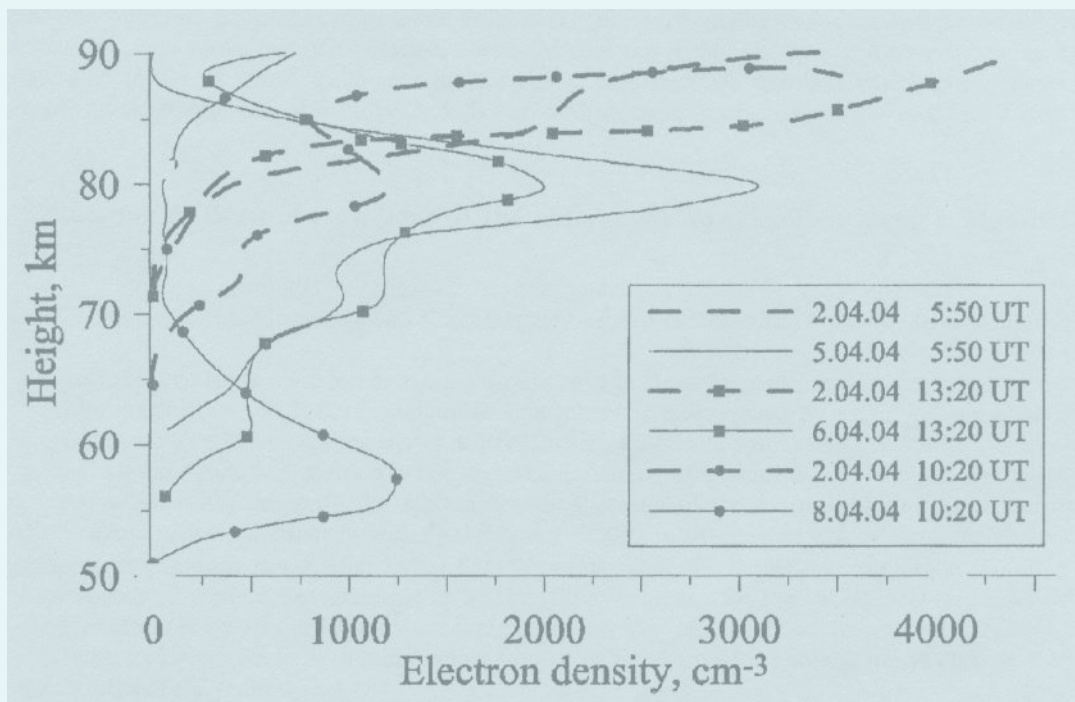
## **Some characteristics of auroras under the interaction of the Earth's magnetosphere with solar wind streams from different solar sources**

V.L. Zverev, T.A. Hviuzova, S.V. Tolochkina (*Polar Geophysical Institute, Russia*)

We have studied the behavior of spectral characteristics and latitudinal variations of the equatorward boundary of auroral luminosity in the periods of interaction of separated and compound streams of the solar wind with the Earth's magnetosphere using the auroral observations of a patrol spectrograph at the Loparskaya observatory for 1970-1983 and DMSP spacecraft data for 1972-1977. There have been considered the following spectral characteristics: the 557.7 green line intensity, the 630.0 nm red line intensity at the zenith of Loparskaya observatory, the ratio of 630.0 nm to 557.7 nm emission intensities, characterizing the hardness of precipitated electrons. Of all separated streams, the greatest ratios of emission intensities  $I_{630.0}/I_{557.7}$  (0.5-1.5) and the lowest latitudes of the equatorward boundary of the luminosity ( $54^\circ$ - $56^\circ$ ) were observed during the Earth passing through the flare and filament streams. Of all compound streams that we considered, the greatest values of auroral emission ratios (0.8-2) and the lowest latitudes of the equatorward boundary of the luminosity ( $50^\circ$ - $54^\circ$ ) were observed during the Earth passing through the streams of the type "flare+HCS+the edge of HSS from CH".



## *Ionosphere and Upper Atmosphere*





## **Corpuscular mechanism of Es layer formation**

A.V. Agapitov, S.I. Musatenko (*Kiev National University named after T. Shevchenko*)

One of the mechanisms of Es layer formation can be corpuscular ionization. This is suggested by the dependence of Es occurrence rate on geomagnetic latitude and geomagnetic activity.

The observations of radio bursts with fast shifting frequencies by RT-10 in Troitsk and BSA in Pushchino have been interpreted as cyclotron radiation of monoenergetic particle beams of magnetospheric origin penetrating to the heights of the ionospheric E-region, which is confirmed by simulation. With increasing the concentration of neutrals and decreasing the field-aligned component of particle velocity, the rate of ion production grows. A rapid growth of ion production rate is observed with height decreasing from 115 km to 95 km, a height range coincident with the region of Es occurrence. The ion production rate is maximum at the point of beam reflection, the height of reflection determining the width of the layer. The smaller is the width of the layer, the larger is the density gradient, which is consistent with the rocket observations. If the reflection point is lower than 100 km, the layer width is 3-8 km, and the concentration gradients can be by an order of magnitude smaller than for the layers with the width 1-2 km.

Thus, monoenergetic beams of electrons with the energies of  $10^2$  -  $10^3$  keV can be responsible for the formation of sporadic layers of small width and large electron concentration gradient which are observed by rockets. This confirms the hypothesis of Ivanov-Kholodny on a corpuscular mechanism of Es-layer formation.

## **Simulation of diurnal variations of the oblique HF propagation along a high-latitude meridional route**

M.Yu. Andreev, G.I. Mingaleva and V.S. Mingalev (*Polar Geophysical Institute, Apatity, Russia*)

The influence of large-scale inhomogeneous structures in electron concentration distribution on meridional HF radio wave propagation through the high-latitude ionosphere is investigated by numerical simulation. A 3D ray-tracing computer program developed earlier is utilized, which enables to synthesize the ionograms of oblique sounding by means of the "shooting method". For the simulation of HF propagation, we use the distribution of electron concentration calculated with the 3D mathematical model of the ionosphere developed earlier in the PGI. This distribution is well consistent with the electron density plot constructed by satellite radio tomography in the geomagnetic latitude range from  $53^\circ$  to  $65^\circ$ . We synthesized the ionograms of oblique sounding and calculated the dependence of vertical elevation angles on the wave frequency for the sub-auroral route Moscow-to- Barentsburg for the certain times of one whole day. It turns out that the large-scale inhomogeneous features of the high-latitude ionosphere affect essentially the diurnal variations of the form of the ionogram of oblique sounding and ray-path trajectories of HF radio waves.

## **Space weather effects in the generation of the equatorial scintillation during geomagnetic storms**

Lilia Biktash (IZMIRAN, 142190 Moscow Region, Troitsk, e-mail: [lsizova@izmiran.rssi.ru](mailto:lsizova@izmiran.rssi.ru))

Solar wind and equatorial ionosphere parameters, as well as Kp, Dst, AU, AL indices, which characterize the contributions of different magnetospheric and ionospheric currents to the H-component of the geomagnetic field are examined to test the space weather effect in the generation of ionospheric irregularities producing VLF scintillation. According to the present statistical studies, one can predict scintillation from Aarons' criteria using the Dst index, which mainly indicates magnetospheric ring current field. With considering a rapid progress in observational abilities, the point is whether one should amplify Aarons' criteria or propose new criteria for predicting scintillation characteristics. According to the present views, the intensity of the electric fields and currents in the polar regions, as well as magnetospheric ring current intensity, are strongly dependent on the variations in the interplanetary magnetic field (IMF). There are difficulties in explaining ring current relation to scintillation activity. It is known that the equatorial scintillation can be observed in the absence of the magnetospheric ring current. We show that the factor fully inhibiting the scintillation, is positive IMF Bz. During positive IMF Bz, the ionospheric F-layer cannot rise to the altitude where scintillations are formed. The auroral indices and the Kp index are more appropriate for the prediction of ionospheric scintillations at the equator. The IMF data and models can be used to explain the relation of the equatorial ionosphere parameters, h'F, foF2, and the equatorial geomagnetic variations to the solar wind and polar ionosphere currents. Taking into account the time delay between solar wind and ionospheric phenomena, the relationship between solar wind and ionosphere parameters can be used for predicting the scintillation.

## **ALIS - highlights, status and future plans**

U. Brändström<sup>1</sup>, I. Sandahl<sup>1</sup>, T. Sergienko<sup>1</sup>, A. Pellinen-Wannberg<sup>1</sup>, B. Gustavsson<sup>2</sup>, M. Rietveld<sup>3</sup>, T. Aso<sup>4</sup> and Å. Steen<sup>5</sup>

<sup>1</sup>*Swedish Institute of Space Physics, Kiruna, Sweden*

<sup>2</sup>*Institute of Physics University of Tromsø, Norway*

<sup>3</sup>*EISCAT, Ramfjordmoen, Norway*

<sup>4</sup>*National Institute of Polar Research, Tokyo, Japan*

<sup>5</sup>*RemSpace group, Övlandehult, Kvillsfors, Sweden*

In this paper, scientific achievements, present status and future plans will be presented. ALIS has been used to study a number of optical phenomena in the atmosphere, including aurora, meteors and polar stratospheric clouds. ALIS made the first unambiguous observations of Radio-induced optical emissions at high latitudes and the first detection of water in a Leonid meteor trail. The fine structure of diffuse aurora has been studied using simultaneous data from ALIS and FAST.

The present (2006) incarnation of ALIS consists of six stations, spaced about 50 km. Each station has a CCD imager with a six-position filter wheel equipped with narrow-band interference filters. The field-of-view is roughly half all-sky. A positioning system enables imaging from several sites with overlapping fields-of-view for any desired part of the sky thus making triangulation and tomography possible. The whole system can be remote controlled.

Raw data from ALIS is freely available at <http://alis.irf.se>. Present work and future plans include studies in collaboration with the Japanese satellite Reimei for studies of auroral fine structures, collaboration with EISCAT and other ground-based instruments, and activities during the International Polar Year, IPY. The ALIS group coordinates the International Network for Auroral Optical Studies of the Polar Ionosphere, which is a part of the IPY project ICESTAR.

## **Injection of H<sub>2</sub>O molecules into the F-region of the Earth's ionosphere**

S.A. Ishanov, V.V. Medvedev, V.A. Zaleskaya (*I. Kant State University of Russia, Kaliningrad, Russia*)

Injection of H<sub>2</sub>O molecules into the F-region leads to the formation of the regions with decreased plasma density, so-called ionospheric “holes”. We aim to describe the formation and filling process of the ionospheric “holes”. In the paper, the photodissociation of H<sub>2</sub>O molecules is considered as an additional source of hydrogen atom production. This process is explored via a computational experiment with the mathematical ionosphere - plasmasphere model. The model is based on numerical solutions of continuity equation for partially ionized plasma, accounting for H<sup>+</sup>, O<sup>+</sup>, N<sub>2</sub><sup>+</sup>, NO<sup>+</sup>, O<sub>2</sub><sup>+</sup>, H<sub>2</sub>O<sup>+</sup>, H<sub>3</sub>O<sup>+</sup>, OH<sup>+</sup> ions and H<sub>2</sub>O molecules, photoelectron equation, ions and electron temperature equations, and wind velocity equation. The computations show that the injection leads to a decrease in N<sub>e</sub>, an increase in V<sub>nx</sub>, T<sub>e</sub>, reduction of h<sub>m</sub>F<sub>2</sub> and, as a result, to the formation of plasma flow from the magnetosphere into the ionosphere.

## **Possibility of applying the mathematical models to the problems of radiowave propagation**

S.A. Ishanov, V.V. Medvedev, V.G. Tokar, Y.S. Zharkova (*I. Kant State University of Russia, Kaliningrad, Russia*)

One of the main purposes of developing theoretical models of ionospheric plasma is a possibility to use them in the problems of propagation of radio signals. In paper [1] it is shown that the nodal distances  $\Delta h$  and  $\Delta \varphi$  of definition of the electron concentration should satisfy the conditions  $\Delta h \leq L_h$ ,  $\Delta \varphi \leq L_\varphi$ , where  $L_h$ ,  $L_\varphi$  are the typical sizes of ionospheric irregularities in altitude and longitude. The approximations for electron concentration and the steps for integration of the characteristic system of ray optics equations are selected to account for the variations of ionospheric plasma in altitude and longitude. The approximation of ionospheric data is performed by cubic splines, which improves the calculations of trajectory parameters and enables to calculate the polarization structure of the signal, when the continuity of the second derivative of concentration is required [2].

In this work, the results of computing experiment for propagation of radio signals are presented with the use of theoretical models of the ionosphere [3; 4] and experimental model. It is shown that for the oblique trajectories it is necessary to take into account the ionospheric low layers, that is, D-layer [4].

1. Nadezhnikov Yu.I., Nikitin M.A., Tokar V.G. Examination of the requirements to the three-dimensional tabular models of the ionosphere in problems of propagation of radio shot waves // *Geomagnetism and Aeronomy*, 1982, V. 22. N.3, P. 422-426 (in Russian).
2. Tokar V.G., Rubinstain L.I., Nikitin M.A. The research of short radio wave depolarization in the ionosphere in quasi-isotropic approximation // *Izvest. Vnuzov. Radiophysicis*, 1987, V.30, N. 1, P. 36.
3. Medvedev V.V., Ishanov S.A., Zenkin V.I. Self-coordinate model of the low ionosphere // *Geomagnetism and Aeronomy*, 2002, V.42, N.6, P. 780-789 (in Russian).
4. Ishanov S.A., Latyshev S.K., Medvedev V.V. Simulation of F2-layer perturbation of ionosphere under anthropogenous actions. Kaliningrad, the interuniversity collection of the proceedings, 1989, P. 136.
5. Evans J.V. Ionospheric backscatter observation at Millstone Hill. Massachusetts, Technical report, 1974, P. 513.

### **Electronically excited molecular nitrogen and molecular oxygen at high and low altitudes of the high-latitude ionosphere**

A.S. Kirillov (*Polar Geophysical Institute of the Kola Science Centre RAS, Apatity, 184209, Russia, kirillov@pgi.kolasc.net.ru/Fax: + 7-81555-74339*)

By using the Landau-Zener and Rosen-Zener approximations for the two-state model (Kirillov, 2004, *Adv. Space Res.*, 33, 993-997), we have calculated quenching rate coefficients of some singlet and triplet states of molecular nitrogen and molecular oxygen. With the above approximations, the calculations of quantum exit efficiency values for collisional molecules can be accomplished. A very good agreement of our previous (Kirillov, 2004, *Adv. Space Res.*, 33, 998-1004) and new results with laboratory experimental data (see, e.g., Slanger and Copeland, 2003, *Chem. Rev.*, 103, 4731-4766) allows us to follow the transformation of energy of electronical excitation of the main atmospheric components in molecular collisions at low altitudes of the high-latitude ionosphere.

The application of the calculated quantum exit efficiencies is the main distinction from similar studies in (Cartwright, 1978, *J. Geophys. Res.*, A83, 517-531; Morrill and Benesch, 1996, *J. Geophys. Res.*, A101, 261-274). The vibrational distributions of triplet states of N<sub>2</sub> and 5 states of O<sub>2</sub> have been calculated for high and low altitudes.

The distributions are conditioned by spontaneous radiational transitions and intramolecular and intermolecular electron energy transfers. It is shown that collisional processes cause a redistribution of vibrational population of some states of N<sub>2</sub> and O<sub>2</sub>. This redistribution can be a reason of a change in "usual" relation (Vallance Jones, Aurora, 1974) of intensities for 1PG and other bands in the type B aurora. Auroral vibrational population of electronically excited O<sub>2</sub> reported in (Henriksen and Sivjee, 1990, *Planet. Space Sci.*, 38, 835-840) is discussed in terms of collisional molecular processes. It is pointed out on possible intramolecular and intermolecular energy transfer processes causing the vibrational population of electronic states of O<sub>2</sub>.

### **A model study of seasonal and solar activity variations of the enhanced electron density regions in the night-time ionospheric F2-layer and plasmasphere**

M.A. Knyazeva<sup>1</sup>, A.A. Namgaladze<sup>1,2</sup>

<sup>1</sup>*Murmansk State Technical University*

<sup>2</sup>*Polar Geophysical Institute, Murmansk, e-mail: namgaladze@mstu.edu.ru*

Enhanced electron density regions in the nighttime ionospheric F2-layer and plasmasphere have been modeled with using the global Upper Atmosphere Model (UAM) for eight selected days, representing four seasons and two levels of solar activity. The model calculations were performed in two manners: 1) by using the empirical thermospheric NRLMSISE-00 model for neutral component calculations and 2) by using theoretically calculated thermosphere parameters. The results were compared with the predictions of the empirical model IRI-2001. All model calculations show noticeable MLT, UT, seasonal and solar activity effects. Nighttime enhanced electron density regions are located in the 19-05 MLT sector at 30-60° magnetic latitudes. They are better pronounced in equinoxes under low solar activity. A strong UT dependence is present in all model runs, being maximum at 12-24 UT.

Enhanced electron density regions in the nighttime ionospheric F2-layer extend to the plasmasphere along geomagnetic field lines, forming the tubes of enhanced electron density. The electromagnetic drift affects the latitudinal locations of the high-latitude sides of these tubes, displacing them to lower latitudes. The main cause of the occurrence of the night increases in the electron density is the equatorward thermospheric wind, driving F2-layer plasma to higher altitudes, thus decreasing the ion loss rate. Seasonal and solar activity effects in nighttime enhanced electron density regions are related to the corresponding variations in thermospheric wind velocity.

This work was supported by the Grant No. 05-05-97511 of Russian Foundation for Basic Research.

### **First measurements of the gradients of ULF magnetic field from auroral sources with a gradiometer with a small spaced units**

E.A. Kopytenko<sup>1</sup>, V.S. Ismagilov<sup>1</sup>, Yu.A. Kopytenko<sup>1</sup>, A.B. Pashin<sup>2</sup>

<sup>1</sup>*IZMIRAN, St.-Petersburg, Russia*

<sup>2</sup>*Polar Geophysical Institute, Apatity, Russia*

High-sensitive 3-component magnetic sensors arranged in the apices of a triangle with the sides of 4-5 km form a magnetic gradiometer. With using such a system, sited in the auroral zone, we have succeeded in detection and monitoring the gradients of natural and stimulated ULF magnetic fields from auroral sources. Identification of the source was performed with all-sky TV camera. We have obtained both the gradients of ULF magnetic fields in individual short-term events and the average pattern of substorm development as it is displayed in magnetometer observations.

### **The possibility of small-scale field-aligned currents generation by HF-transmitter operation**

A.L. Kotikov, S.A. Shibkov, V.V. Vinnikov (*Institute of Physics, University of St-Petersburg, St-Petersburg, Russia*)

The experimental data of four heating campaigns are considered. The field-aligned currents were registered in the ionosphere heating volume. A preliminary experimental revision of the suggested method is represented based on comparing with independent kinds of observations. The physical interpretation of experimental results is proposed.

### **Solar radiation and particle induced effects on the early Martian atmosphere and loss**

Yuri N. Kulikov<sup>1</sup>, Helmut Lammer<sup>2</sup>, Herbert I. M. Lichtenegger<sup>2</sup>, Thomas Penz<sup>2</sup>, and Helfried K. Biernat<sup>2</sup>

<sup>1</sup>*Polar Geophysical Institute (PGI), Russian Academy of Sciences, Khalturina Str. 15, Murmansk, 183010, Russian Federation*

<sup>2</sup>*Space Research Institute, Austrian Academy of Sciences, Schmiedlstr. 6, A-8042 Graz, Austria*

The evolution of the Martian atmosphere with regard to its H<sub>2</sub>O inventory is influenced by thermal loss and non-thermal atmospheric loss processes of H, H<sub>2</sub>, O, N, C, CO, CO<sub>2</sub>, H<sup>+</sup>, O<sup>+</sup>, H<sub>2</sub><sup>+</sup>, N<sub>2</sub><sup>+</sup>, CO<sup>+</sup>, CO<sub>2</sub><sup>+</sup>, and O<sub>2</sub><sup>+</sup> into space, as well as by chemical weathering of the surface soil. The epochs related to escape of the atmosphere and water from Mars over long-term periods can be divided into 3 epochs, the present Mars, the period between the present and 3.5 Gyr ago and the first billion years. The evolution of all escape processes depend on the history of the intensity of the solar X-ray and EUV (XUV) radiation and the solar wind density. Thus, we use actual data from the observation of solar proxies with different ages from the Sun in Time program for reconstructing the Sun's radiation and particle environment from the present to 4.6 Gyr ago. We compare different model investigations for the non-thermal escape processes (ion pick up, sputtering, ionospheric clouds triggered by the Kelvin Helmholtz plasma instability) of the Martian atmosphere over long-time periods and discuss the effect on the total loss to the Martian CO<sub>2</sub> and/or H<sub>2</sub>O inventory. We apply a thermospheric model to the CO<sub>2</sub>-rich atmosphere of Mars that have been modified to high XUV flux values expected during the Sun's evolution. During the first Gyr after the Sun arrived at the Zero-Age-Main-Sequence high XUV fluxes between 10 - 100 times that of the present Sun were responsible for much higher temperatures in the thermosphere-exosphere environments on both planets. By applying a diffusive-gravitational equilibrium and thermal balance model for investigating radiation impact on the early thermospheres by photodissociation and ionization processes, due to exothermic chemical reactions and cooling by CO<sub>2</sub> IR emission in the 15 μm band we found expanded thermospheres with exobase levels between about 200 (present) to 2000 km (4.5 Gyr ago). Our model results indicate that the high temperature in the thermosphere-exosphere environment on early Mars could reach "blow-off" conditions for H atoms even at high CO<sub>2</sub> mixing ratios of 96 %. Furthermore, we show that lower CO<sub>2</sub> / N<sub>2</sub> or CO<sub>2</sub> mixing ratios in general, or higher contents of H<sub>2</sub>O-vapor in the early Martian atmosphere could have had a dramatic impact on the loss of atmosphere and water on early Mars. The duration of this phase of high thermal loss rates essentially depended on the mixing ratios of CO<sub>2</sub>, N<sub>2</sub> and H<sub>2</sub>O in the early atmosphere. Lower CO<sub>2</sub> mixing ratios on early Mars shortly after its volatile out-gassing could have had a major impact on the thermal loss of the main atomic atmospheric species (O, N, C) combined with impact erosion and loss of O due to dissociative recombination in the dense solar XUV-produced early Martian ionosphere. One should note that thermal and photochemical loss process are independent from an early Martian magnetosphere because these

atomic species escape as neutrals. Furthermore, a combination between an expanded thermosphere-exosphere region and a stronger early solar wind could have also enhanced ion pick up loss during the period where the Martian magnetic dynamo decreased.

### **Application of the object-oriented approach in upper atmosphere modeling**

O.V. Martynenko, M.M. Gladkikh, I.V. Artamonov (*Murmansk State Technical University, Murmansk, Russia, e-mail: mart@mstu.edu.ru*)

The universal modeling tool is being developed on the basis of the global Upper Atmosphere Model (UAM) for the research of interrelation of the broad range of various processes and the phenomena in the upper atmosphere. For this purpose, the UAM structure has been reorganized into the open framework of several subordinate models of separate atmospheric regions and processes. Each included model is independent from the others and calculates certain physical parameters of the modeling object. These sub-models exchange data using the unified interface. Such an approach enables easy integration of wide range of different data sources both experimental and modeled.

The framework is being created on the basis of object-oriented approach. At the present stage the objects hierarchy and obligatory functional and interface specifications are developed for each object. The observance of these specifications will allow the object to be connected to framework model.

At the top level of hierarchy there is a METAMODEL – actual frame structure, whose functions are to organize the interaction of connected objects and to provide the user with a comprehensive control facility.

The objects that are connected to the metamodel are MODELS. Functionally each model represents a method of obtaining the values of some set of physical parameters in some spatial grid points, (experimental data sources fall into this formal definition as well). The set of parameters and grid position are obligatory properties of the model, and they are described by formal specification rules.

Each model, in turn, includes objects of a following level – a spatial GRID, the DATA DESCRIPTION (what these parameters are), and DATA itself – parameter values in the grid points. For each of these objects formal specifications also are being developed.

Another object connected to a metamodel, is the DATA REPOSITORY. It "is able" to save necessary data to the disk file and to load data from there, and also the full information about parameters, the grid, and which model provided them.

Such system organization allows using of the same software for data access and processing and in particular, to provide data, obtained by various methods, in a uniform way that simplifies their comparison and analysis.

Attached models use metamodel interface to exchange data in order to use them as input parameters for other models. This permits to study interference of various processes and the phenomena, distributing self-consistence property of global theoretical models on the wide range of other models if they meet the framework requirements.

This work was supported by the grant N 05-05-97511 of the Russian Foundation for Basic Research.

### **Mathematical modeling for the processes upper atmosphere and ionosphere**

V.V. Medvedev, Y.S. Zharkova (*I. Kant State University of Russia, Kaliningrad, Russia*)

One-dimensional non-stationary model for the heights of 50–500 km is constructed. The model accounts for the molecular and eddy diffusion and more than 200 photochemical reactions. It is based on the numerical solution of the continuity, temperature and macroscopic average wind velocity equations for the partially ionized plasma, including the neutrals, ions and electrons. It enables to consistently calculate the height–time distributions of the following components:  $O(^3P)$ ,  $O(^1D)$ ,  $O(^1S)$ ,  $O_2$ ,  $O_2(^1\Delta_g)$ ,  $N(^4S)$ ,  $N(^2D)$ ,  $NO$ ,  $NO_2$ ,  $N_2O$ ,  $H$ ,  $H_2$ ,  $OH$ ,  $H_2O$ ,  $HO_2$ ,  $H_2O_2$ ,  $CO$ ,  $CO_2$ ,  $H^+$ ,  $O^+$ ,  $O_2^+$ ,  $NO^+$ ,  $N^+$ ,  $N_2^+$ ,  $Y^+$ ,  $Y^-$ ,  $Ne$ . The input parameters of the model are the coefficients of chemical reactions, vertical distribution of the temperature, coefficient of eddy diffusion, absorption and ionization cross-sections and solar EUV flux. The reaction of "hot" atoms  $O(^1D)$  with molecules  $N_2$  for the basic source of  $NO$  in the mesosphere is included. The results of numerical calculations and their comparison with the experimental data for different helio-geophysical conditions are given.

## **Numerical model of the heat budget of the Earth's upper atmosphere**

V.V. Medvedev, Y.S. Zharkova (*I. Kant State University of Russia, Kaliningrad, Russia*)

In the present work thermal sources and sinks in the upper atmosphere are studied by numerical experiments. To determine temperature altitude distributions, one-dimensional non-stationary thermal balance equations are solved along with the continuity equations for the ions and atmospheric constituents. The models of the mesosphere and lower thermosphere are considered in detail in [1].

In the heat balance equations the following heating sources and sinks are taken into account:

- 1 heating arising from absorptions of solar radiation in the Shuman-Runge continuum  $135 \leq \lambda < 175$  nm
- 2 heating by photoionization
- 3 chemical heating
- 4 cooling by the vibrational-rotational bands CO<sub>2</sub>, NO, O<sub>3</sub>, OH, CO in the 1,27  $\mu$ m O<sub>2</sub> and the 63  $\mu$ m O(<sup>1</sup>D)
- 5 molecular heat conduction
- 6 heating and cooling produced by diurnal contraction and expansion of the atmosphere.

For the function  $K_h(z)$ , which is the eddy thermal conductivity (assumed to be equal to the eddy diffusion coefficient), the analytical approximation is used. The height  $z_m$  of  $K_h$  maximum ( $K_h^{\max}$ ) has been varied within the range 90-110 km, with the value of  $K_h^{\max}$  varying from  $10^6$  to  $2.0 \cdot 10^7$   $\text{sm}^2/\text{s}$ .

The upper boundary condition of zero temperature gradient is imposed at the height of 500 km.

The lower boundary condition of zero heating flux is imposed at the height of 50 km.

We have performed a number of computational runs using various altitude profiles of the eddy thermal conductivity.

*Medvedev V.V., Ishanov S.A., Zenkin V.I., Self-consistent model of the lower ionosphere// Geomagnetism and aeronomy. V. 42. N. 6. P. 780-789. 2002.*

## **The role of electric fields and magnetospheric electron precipitations in the formation of the equatorial total mass density minimum**

A.A. Namgaladze<sup>1,2</sup>, E.N. Doronina<sup>1</sup>, M. Förster<sup>3</sup>

<sup>1</sup>*Murmansk State Technical University, Murmansk, Russia;*

<sup>2</sup>*Polar Geophysical Institute, Murmansk, Russia;*

<sup>3</sup>*GeoForschungsZentrum, Potsdam, Germany*

*namgaladze@mstu.edu.ru*

Numerical experiments have been performed using the theoretical global numerical Upper Atmosphere Model (UAM) and empirical thermospheric model NRLMSISE-00. The calculation results are presented as global maps of the latitude-longitudinal distribution of the total mass density and neutral temperature and their latitudinal variations along the 14 MLT meridian at the height of 400 km. The results of calculations with the UAM show minimum of the total mass density and neutral temperature near geomagnetic equator in agreement with global thermospheric total mass density pattern obtained by CHAMP satellite. The calculations with NRLMSISE-00 did not show this minimum. The global distribution of thermospheric total mass density from the CHAMP at 400 km altitude shows maxima at about 20-25 deg geomagnetic latitude from both sides of the equator between 10 and 20 MLT. In the UAM the density peaks are located at middle latitudes being larger in the Northern hemisphere under geomagnetically quiet conditions and in the Southern hemisphere under geomagnetically disturbed conditions. We investigated the role of the low and high latitude electric fields and magnetospheric electron precipitation in the formation of the equatorial density minimum by successive switching off the low- and high-latitude electric fields and the magnetospheric electron precipitation within the UAM calculations. We found that the neutral density distribution does not change principally after switching off the electric fields at magnetic latitudes below 30 degrees, whereas the equatorial anomaly of the electron density disappears. Therefore, the equatorial neutral density minimum is apparently not related to the ionospheric F2 layer equatorial anomaly. Another pattern takes place after switching off the high latitude electric fields and magnetospheric electron precipitation: the equatorial neutral mass density minimum disappears and only one daytime density maximum persists, being displaced into the Northern hemisphere. We conclude that the high latitude magnetospheric heating is a likely reason for the daytime thermospheric density minimum near the equator.

This work was supported by the Grant No. 05-05-97511 of Russian Foundation for Basic Research.

### **Influence of neutral species on artificial magnetic pulsation excitation**

A. Pashin, and A. Mochalov (*Polar Geophysical Institute, Apatity, Russia*)

For the last decade, series with the EISCAT Heating Facility have been carried out with the purpose to produce artificial magnetic pulsations in the 0.1 – 3 Hz frequency range. In several experiments the EISCAT radar provided measurements of ionospheric electric field and electron density. Numerical model of artificial pulsation excitation was verified. The predicted amplitude of the pulsations is in accordance with the measured values, however the model can not explain sporadic nature of the artificial signals.

Allowing for the variations in neutral species density is a possible way to explain this feature. Numerical modelling shows strong dependence of the conductivity modification on neutral density. Experiment on generation of artificial magnetic pulsations in Pc1 frequency range on November 19, 1998 is discussed in frame of numerical simulation. Clear ionospheric response was observed in the first hour of heating at 120-km distance by induction magnetometer but the artificial signal at the modulation frequencies disappeared in the next hour of heating. The main ionosphere parameters do not show significant variations during this experimental run. Disappearance of the artificial pulsations may be related to density variations of neutral components of the ionosphere.

This work in part has been supported by INTAS (grant 01-614).

### **Schumann frequency decrease during PCA depending on proton flux rigidity**

V.C. Roldugin, B.V. Kozelov (*Polar Geophysical Institute, Apatity*)

The electron density profiles are calculated for several proton events when the changes in the 1<sup>st</sup> mode Schumann resonance frequency are observed. It is found that the protons with the energy from 40 to 100 MeV are mostly responsible for the frequency decrease. The value of the decrease is strongly dependent on whether X-ray burst is superimposed or not on proton precipitation.

### **ULF electromagnetic emission from the atmosphere perturbed by seismicity**

A. Schekotov<sup>1</sup>, O. Molchanov<sup>1</sup>, E. Fedorov<sup>1</sup>, Chebrov<sup>2</sup>, V. Sinitsin<sup>2</sup>, E. Gordeev<sup>3</sup>, G. Belyaev<sup>1</sup> and M. Hayakawa<sup>4</sup>

<sup>1</sup>*Institute of Physics of the Earth, Russian Academy of Sciences, 10, Bolshaya Gruzinskaya, 124995, Moscow, Russia Phone: +7-095-254-89-085, Oleg@ifz.ru*

<sup>2</sup>*Institute of Geophysical Survey, Russian Academy of Sciences, Far-East Branch, Petropavlovsk-Kamchatski, Kamchatka, Russia*

<sup>3</sup>*Institute of Volcanology, Petropavlovsk-Kamchatski, Kamchatka, Russia*

<sup>4</sup>*The University of Electro-Communications, 1-5-1, Chofu Tokyo, 182-8585, Japan*

We have found ULF magnetic field spectrum anomalies in the frequency range 2-24 Hz observed occasionally during the period of more than 3 years in Karymshino station (Kamchatka, Russia) and demonstrate their association with several seismic activation periods. The interval from February 24, 2003 to April 6, 2003 has been analyzed in detail in order to choose optimal parameters for revelation of the correlation. Seismic influence leads to increase of ULF emission determinancy (preferential azimuths and decrease of dispersion in the values of polarization or angle of orientation ellipse). A possible mechanism can be triggering of nearby cloud-air discharges by seismo-induced Atmospheric Gravity Waves (AGW)

### **Re-analysis of long-term hydroxyl rotational temperature trend based on the measurements in Spitsbergen**

A.I. Semenov, N.N. Shefov (*Obukhov Institute of Atmospheric Physics of the Russian Academy of Science, Moscow. e-mail: meso@ifaran.ru*)

We have performed a re-analysis of long-term measurements of rotational temperature of hydroxyl emission band (6–2) made at the auroral station Adventdalen (78°N), Spitsbergen (Svalbard) for the period 1980 – 2001 and published in [1]. This was inspired by the discussion of this problem in Sozopol, Bulgaria, in 2004, In the published

## ***Ionosphere and upper atmosphere***

discussions on the problem of quantitative characteristics of temperature trends, it is concluded that the observations in Spitsbergen testify that the value of the trend is close to zero for winter conditions. To verify this conclusion, first, all of the mean seasonal variations of temperature for four winter months (November-February) were obtained. They appeared to be very similar to the published data for four winter months (May-August) of the southern hemisphere [2]. Then, it was found that the linear trend in the period near winter solstice at latitude 78°N is actually  $-(1.0 \pm 0.2)$  K·year<sup>-1</sup>. From the published data [3], a similar value of  $-(0.5 \div 1.5)$  K·year<sup>-1</sup> was obtained from winter measurements in the southern hemisphere at Davis, Antarctica (68.6°S). It is well-known that the trend is close to zero in summer period at high latitudes. Such latitudinal behavior of the long-term trend at heights ~ 87 km of the hydroxyl emission is in agreement with the latitudinal variations of the trend in the stratosphere and mesosphere according to the rocket measurements.

1. Sigernes F., Nielsen K.P., Deehr C.S., Svenoe T., Shumilov N., Ilavnes O. *The hydroxyl rotational temperature record from the auroral station in Adventdalen, Svalbard (78°N, 15°E): preliminary results* // *Sodankylä Geophys. Observ. Publ. (ed. J. Kultima). Oulu: Oulu Univ. Press. V. 92. P. 61-67. 2003.*
2. Burns G.B., French W.J.R., Greet P.A., Williams P.F.B., Finlayson K., Lowe R.P. *The mesopause region above Davis, Antarctica (68.6°S, 78.0°E) // Long term changes and trends in the atmosphere (ed. G Beig). New Delhi: New Age International Limited Publ.V. 2. P. 43-52. 2001.*
3. French W.J.R., Burns G.B. *The influence of large-scale oscillations on long-term trend assessment in hydroxyl temperatures over Davis, Antarctica* // *J. Atmos. Solar-Terr. Phys. V. 66. N 6-9. P. 493-506. 2004.*

## **Long-term variations of a temperature and structure of the middle atmosphere within last century**

A.I. Semenov and N.N. Shefov (*Obukhov Institute of Atmospheric Physics of RAS, Moscow, Russia, e-mail: meso@ifaran.ru*)

From the long-term data on mesopause temperature (1955–2005) obtained by photometry of hydroxyl and atomic oxygen emissions and analysis of the rocket and ionospheric temperature measurements, the height distributions of the temperature have been constructed. The cooling of the middle and upper atmosphere has been revealed. For the mesopause region (~87 km), the long-term variation in temperature has a non-linear character. The values of temperature long-term trend for the time intervals from 1955 to 1990 and from 1990 up to now are  $-(0.7)$  K·yr<sup>-1</sup> and  $-(0.1-0.3)$  K yr<sup>-1</sup>, respectively. The influence of solar activity has also been revealed. Another important result is that the obtained temperature profiles indicate a decrease in the heights of constant temperature and concentration. It signifies a gradual subsidence of the middle and upper atmosphere during the considered period. The calculations of height distributions of subsidence rate evidence that for the period of the 20th century the atmosphere subsidence rate at 70 and 100 km has made  $-60$  m·yr<sup>-1</sup> and  $-100$  m·yr<sup>-1</sup>, respectively. This is also confirmed by the data of ionospheric sounding from 1948 to 1990, which indicate that the height of the maximum of ionospheric F2-layer (~270 km) was subsiding with the rate of  $-250$  m·yr<sup>-1</sup>. Owing to the change in temperature (from 1955 to 2005), the concentration of the atmosphere at heights of the lower thermosphere decreased 2–2.5 times. Thus at the level of ~100 km, the concentration, which is adopted to be constant in the present models of the upper atmosphere, actually decreased 2.5 times for the second half of the century. The long-term measurements of mesopause temperature also reveal its changes for winter and summer seasons. For winter conditions in the considered period, there was a cooling of the mesopause with a trend of about  $-0.9$  K·yr<sup>-1</sup>. This refers not only to middle latitudes but also to high latitudes where the values of the temperature trend are  $-1$  K·yr<sup>-1</sup> both for the North and South hemispheres. For summer conditions, the value of long-term trend in temperature on the middle and high latitudes is close to zero. These results are in a good agreement with the long-term radiometer measurements of wind velocity at heights of the lower thermosphere (~90 km). From temperature distributions at the heights of 30–100 km, observed by rockets and with the use of spectrophotometric methods during last three solar cycles, the coefficients of temperature increment at different heights are determined versus the level of solar activity. Their seasonal behavior is studied. The greatest seasonal variations are found to be at heights ~ 80–95 km, while the weakest are observed at heights ~ 55–70 km. The height of minimal response of middle atmosphere temperature to solar activity is in the range of 55–70 km and has a distinct annual variation. The seasonal dependence of the latitudinal behaviour of temperature trend is found. It is revealed that in the mesosphere under winter conditions, the greatest absolute value of the negative trends corresponds to high latitudes. For summer periods, the absolute value of the negative trend has the smallest magnitude.

## **Substorm effect on resonant structures in spectra of the background magnetic noise**

N.V. Semenova, A.G. Yahnin (*Polar Geophysical Institute, Apatity*)

The spectral resonant structures (SRS) of the magnetic noise in the frequency range of 0.1-10 Hz are known as a phenomenon that anti-correlates with geomagnetic activity. In this report we discuss how SRS relate to substorms. It has been noted that in the auroral zone SRS disappear when such a signature of the substorm as PiB pulsations are observed. This is explained by the fact of close relationship between PiBs and active, substorm auroras. The electron precipitation produces modification of the ionosphere that leads to violation of conditions for ionospheric Alfvén resonator responsible for SRS. But, recent observations in Barentsburg, Svalbard, that is, poleward from the auroral zone, showed that SRS are rather often seen during PiBs. The interpretation of this fact is that SRS are due to IAR overhead, while PiBs observed at high latitudes are due to the ionospheric waveguide propagation from the remote source. This remote source co-locates with substorm auroras, which are situated well equatorward from Barentsburg. The interpretation is confirmed by the substorm-related aurora and electrojet observations.

## **Auroral arc triggering by powerful HF ionosphere heating**

T. Sergienko<sup>1</sup>, I. Sandahl<sup>1</sup>, B. Gustavsson<sup>1</sup>, U. Brändström<sup>1</sup>, M. Rietveld<sup>2</sup> and T. Leyser<sup>3</sup>

<sup>1</sup>*Swedish Institute of Space Physics, Kiruna, Sweden,*

<sup>2</sup>*European Incoherent Scatter Association, Ramfjordmoen, Norway,*

<sup>3</sup>*Swedish Institute of Space Physics, Uppsala, Sweden*

On November 21, 2003 an ionosphere heating experiment was conducted in Tromsø to investigate the optical effects caused by powerful HF pumping of the ionosphere. During the time interval 18:32 to 18:36 UT, when the heating beam illuminated a region of an upward field-aligned current, sudden appearance of an auroral arc was observed by the ALIS cameras. Strong temporal variations of the intensity of the arc were coincident with the HF pumping modulation period. Analysis of the optical data and the ionospheric parameters measured by the UHF ESCAT radar shows that the observed auroral arc was triggered by Alfvén waves excited by modulated HF heating of the ionosphere.

## **ULF electromagnetic noise due to random variations of background atmospheric current**

V. V. Surkov (*Moscow Engineering Physics Institute, Kashirskaya road, Moscow 115409, Russia*)

A mechanism for ULF electromagnetic noise due to random fluctuations of the atmospheric conductivity and background currents was examined. The conductivity fluctuations similar to the flicker-noise or  $1/f$  noise can develop inside the electric environment of a mesoscale convective system in the vicinity of the thunderstorm or hurricane and at the front of atmospheric disturbance. In the model the spectral densities of the random electromagnetic and current fluctuations are coupled via transfer functions. The random process is assumed to be steady and uniform and isotropic in space, which in turn implies that the spectral density of the process is delta-correlated. A spatio-temporal correlation of the conductivity variations at different points and a correlation radius of the random process is supposed to be dependent on gas transfer and the acoustic wave propagation due to pressure and temperature gradients in the atmosphere. A spectral amplitude of correlation matrix of the electromagnetic perturbations in the frequency range of 0.01-0.001 Hz was estimated. It was shown that the large-scaled random fluctuations of the atmospheric background current are capable to sustain generation of the ULF magnetic noise that can be detected by ground magnetometers.

## **Response of the lower polar ionosphere to X-class solar flares in January 2005**

V.D. Tereshchenko, E.B. Vasiljev, O.F. Ogloblina, V.A. Tereshchenko, A.P. Osepian, S.M. Chernyakov (*Polar Geophysical Institute, Murmansk, Russia; E-mail: vladter@pgi.ru*)

The observations by the partial reflection method of the lower polar ionosphere above the settlement Tumanny in the Murmansk region (69.0° N, 35.7° E) during strong X-class solar flares from 15 to 20 January are presented. In

## ***Ionosphere and upper atmosphere***

these events significant variations of the vertical structure of the polar ionosphere were revealed. The variations displayed in decrease of an altitude of the ionosphere bottom by 25 km and in increase of electron concentration at the heights of 50-60 km by two orders of magnitude. Ionospheric effects of the flares were accompanied by the strengthened absorption of middle and short radiowaves as well as by splashes of cosmic radioemission. It was shown experimentally that the sources of the observed ionospheric disturbances were solar proton fluxes with energy up to 80 MeV and powerful flares of X-ray solar emission.

### **Change of the polar ionosphere structure during solar flares. Experiment and model**

V.D. Tereshchenko, A.P. Osepian, O.F. Ogloblina, E.B. Vasiljev, V.A. Tereshchenko (*Polar Geophysical Institute, Murmansk, 183010, Russia; E-mail:vladter@pgi.ru*)

The response of the lower ionosphere to variations of the solar hard X-ray flux produced by the powerful solar flares on 5 and 6 April 2004 is examined. With this aim we use experimental data (electron density profiles measured with the partial reflection method at geographic latitude  $\varphi=69.0^\circ\text{N}$ , longitude  $\lambda=35.7^\circ\text{E}$ ) together with a theoretical model of the lower ionosphere. The model contains the following parts: computation of the ionization rates by the solar EUV, Lyman -  $\alpha$  and Lyman -  $\beta$  radiation, scattered Lyman -  $\alpha$  and Lyman -  $\beta$  radiation, solar X-ray fluxes in the different wavelength ranges and galactic cosmic rays and the D-region ion chemistry model describing the cluster ions formation from the simple ions, the processes of the negative ion formation and loss, the ion-molecular and ion-ion reactions and the recombination processes. The theoretical model of the ionization-recombination cycle in the D-region allows us to calculate the electron densities, densities of the main positive and negative ions and effective recombination coefficients both in the quiescent conditions and during solar flares.

The results of theoretical calculations of the electron density at the altitudes of 50-90 km in the sunlit ionosphere ( $\chi < 90^\circ$ ) are compared with experimental data. It is shown that during the quiet conditions the modeled  $N_e(h)$  – profiles are the closest to the experimental  $N_e(h)$  – profiles at altitudes exceeding 70-75 km. During the solar flares, the calculated values of electron density are in a good agreement with the measured  $N_e$  – values at the altitudes  $h \geq 55$ -60 km. Note, that during the powerful solar flare on 5 April, when intensity of hard X-rays ( $\lambda=0.5$ -8.0Å) increased by about 2 orders of magnitude, the ionisation in the D-region was entirely due to X-rays and electron density at altitudes 55-90 km increased by a factor 5-10 compared to quiet conditions. A good agreement between calculated and experimental values of electron density permits to use the theoretical model for the investigation of the changes of ion composition and effective recombination coefficient in the D-region caused by solar flares.

### **An ionospheric effect of a lunar echo from a space gamma-splash**

V.D. Tereshchenko, E.B. Vasiljev, O.F. Ogloblina, V.A. Tereshchenko, S.M. Chernyakov (*Polar Geophysical Institute, Murmansk, 183010, Russia; E-mail:vladter@pgi.ru*)

Based on the method of partial reflections (PRM), the behaviour of the polar bottom ionosphere above the settlement Tumanny (Murmansk region) is studied during registration of a powerful gamma-splash from the repeater of soft gamma-rays SGR 1806-20. A huge gamma-flash and its ionospheric effect have been found out on satellites and by ground means of VLF-measurements on December, 27, 2004 approximately at 21:31 UT. At this time the settlement Tumanny was in the shadow of the Earth and the ionosphere above it was well shined with the full Moon. The moon passed through the meridian, on which there was a point of observations, at 21:53 UT.

It was shown that there was a big similarity in time variations of amplitudes of partial reflections and reflections of radiowaves at the very low frequencies which were observed in the lighted hemisphere of the Earth. At that time, the amplitude of partially reflected signals from the ionosphere pulses with the period of 7.5 s, which is commensurable with the period of rotation of the neutron star – a source of the gamma-splash.

The reason of ionospheric disturbances observed with PRM can be a stream of the strong X-ray radiation of  $2 \cdot 10^{-5}$  erg/cm<sup>2</sup>. This value is 26 times more than the value measured by the Russian satellite "Koronas-F" which has found out a lunar reflection of the flash. It is possible to explain the distinction of measurements by the presence of a very intensive stream of gamma-photons with energy of 3-10 keV, which is not registered at this extra-atmospheric solar observatory. Thus, it is possible to consider, that the sudden disturbance of the polar ionosphere which was detected by PRM was caused by X-ray radiation from SGR 1806-20.

## **Исследование зависимости параметров резонансной структуры спектра (РСС) фонового шума от направления на источник для плоскослоистой модели ионосферы с наклонным магнитным полем**

Е.Н. Ермакова, Д.С. Котик, С.В. Поляков (*Научно-исследовательский радиофизический институт, Нижний Новгород, Россия*)

Выполнено моделирование резонансной структуры спектра фонового шума для плоско-слоистой модели ионосферы с наклонным магнитным полем. Для моделирования выбирались реальные профили ионосферных параметров на базе международного стандарта ионосферы (International Reference Ionosphere - IRI-2001), атмосферы (MSIS-E-90 Atmosphere Model) и геомагнитного поля (DGRF/IGRF Geomagnetic Field Model 1945 - 2). Исследована зависимость частотного масштаба, основных частот и других параметров РСС от направления на источник. Результаты моделирования показывают, что РСС даже на средних широтах может проявляться в обеих компонентах магнитного поля, при этом частотный масштаб и основные частоты могут различаться в компонентах  $H_{\rho}$  и  $H_{\varphi}$ . Это различие зависит от угла между плоскостью магнитного меридиана и направлением на источник. Наиболее сильно РСС выражено в компоненте  $H_{\varphi}$  при углах близких к 0 и  $\pi/2$ , а наиболее слабо - при углах, близких к  $\pi/4$ . Таким образом, параметры РСС несут в себе информацию не только о локальных свойствах ионосферы, но и о направлении на источники низкочастотного фонового шума.

Выполнено моделирование РСС при наличии одновременно нескольких источников, расположенных под разными углами к плоскости магнитного меридиана, а также для периодов максимума и минимума солнечной активности.

Работа выполнена при финансовой поддержке гранта РФФИ N 04-02-17333.

## **Механизм формирования широкополосного максимума в спектре фонового шума на частотах 2-6 Гц**

Е.Н. Ермакова, Д.С. Котик, С.В. Поляков (*Научно-исследовательский радиофизический институт, Нижний Новгород, Россия*)

В работе исследуется механизм формирования широкополосного низкочастотного максимума в спектре фонового шума, основанный на наличии сильно неоднородной области для показателя преломления нормальных волн в ионосфере на высотах до (250-300) км. Такая пространственная структура может приводить к осцилляциям интенсивности компонент магнитного поля с частотным масштабом, определяемым интегральной оптической толщиной нижних слоев ионосферы для низкочастотных электромагнитных волн. Этот частотный масштаб существенно больше аналогичного масштаба традиционной резонансной структуры. Увеличение интенсивности спектральных компонент магнитного поля на частотах 2-6 Гц соответствует первой основной частоте этой "крупномасштабной" структуры. Величины частот максимума сильно зависят от параметров нижних слоев ионосферной плазмы. Выполненное моделирование этого спектрального максимума для плоскослоистой модели ионосферы позволяет объяснить многие особенности этой структуры, наблюдаемые экспериментально:

- максимум наблюдается практически всегда в ночное время суток;
- максимум наблюдается в спокойных геомагнитных условиях;
- максимум может наблюдаться, как в компоненте С-Ю, так и в компоненте В-З, при этом, как правило, максимум более ярко выражен только в одной из компонент;
- поляризация на частотах максимума (отношение право - и лево - поляризованных компонент магнитного поля) сильно зависит от частоты;
- возможность существования в периоды, когда отсутствует РСС (например, в годы максимальной солнечной активности);
- дрейф частоты максимума после захода солнца с частот (2-3)Гц до (5-5.5)Гц;
- влияние локальных свойств ионосферы на параметры максимума (частоту и относительную амплитуду);
- пространственный масштаб широкополосного максимума сопоставим с пространственным масштабом шумановских спектральных максимумов.

Работа выполнена при финансовой поддержке гранта РФФИ N 04-02-17333.

## **О механизмах взаимодействия литосфера-атмосфера-ионосфера**

О. А. Молчанов, А. Ю. Щекотов (*Институт физики Земли РАН, Москва, Россия*)

Обсуждаются два механизма воздействия литосферных процессов на ионосферу:

1. Показано, что одним из источников ионосферной турбулентности (ИТ) являются акусто-гравитационные волны (АГВ). Влияние процессов подготовки землетрясений на ионосферу может быть объяснено АГВ накачкой.
2. Эффекты от электрических полей, связанных с сейсмичностью, слишком слабы для объяснения литосферно-ионосферных связей.

## **Исследование параметров высокоширотной ионосферы методом разнесенного приема**

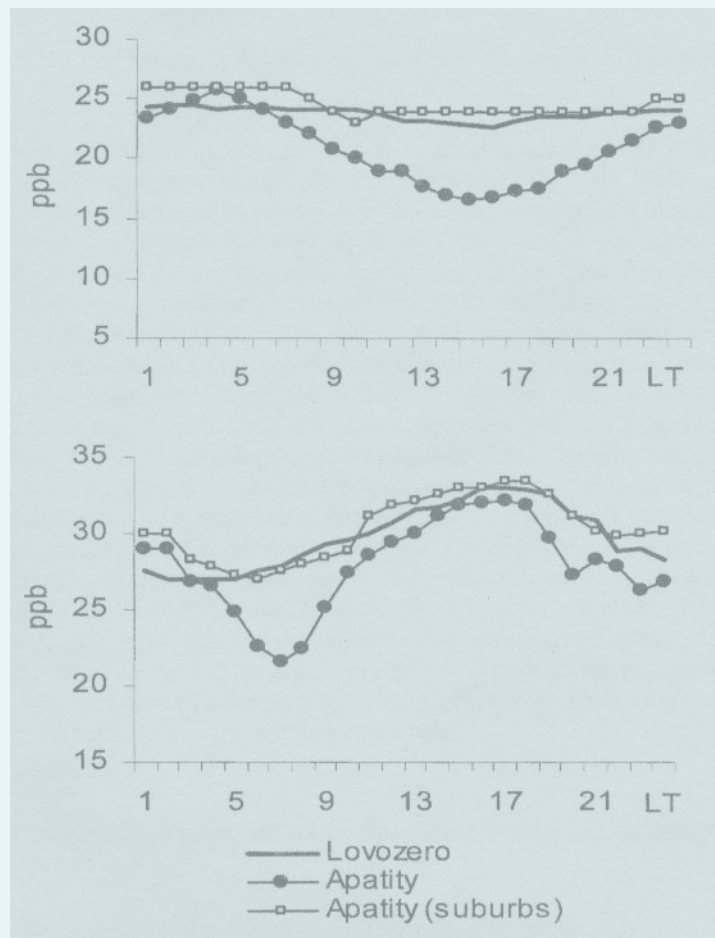
Н.Г. Сергеева, Е.Б. Васильев, О.Ф. Оглоблина (*Полярный Геофизический Институт, КНЦ РАН, Мурманск, Россия*)

В данной работе исследуются характеристики движения ионосферной плазмы в динамо-области (в E-слое) в возмущенные дни (22.03.04, 21.09.03, 24.09.03). Исследования горизонтального движения неоднородностей высокоширотной ионосферы проводятся СВ-КВ радаром в п.Туманный (69.0° N, 35.7° E) методом разнесенного приема.

Исследованы суточные вариации дрейфовой скорости, углов отклонения вектора дрейфовой скорости от северного направления и электрического поля для разных высот. Углы отклонения вектора дрейфовой скорости мало изменяются с высотой. Векторы дрейфовой скорости имеют в основном юго-восточное направление или юго-западное направление. Максимальное значение электрического поля наблюдается на высотах 100, 110 км в 0-3 UT и в 17-23 UT (22.03.04). Направление дрейфовой скорости 21.09.03 сменилось с юго-восточного на северо-западное в 3.40 UT на всех рассматриваемых высотах, а 24.09.03 в 13.30 UT с юго-восточного на северо-восточное. При смене направления в первом случае величина дрейфовой скорости и электрического поля не изменяется. Во втором случае величина дрейфовой скорости и электрического поля увеличилась в 2.5 раза. Неустойчивость направлений дрейфовой скорости наблюдается в периоды равноденствия. Электрическое поле в E-области, вычисленное по измерениям дрейфовых скоростей, в основном определяется ионосферным ветром.

Величины дрейфовой скорости сравнивались с распределением конвекции, полученной системой Н-Ф радаров (SuperDARN), которая использует информацию о доплеровской скорости когерентного эха. Величины дрейфовых скоростей, измеренных в Туманном, согласуются с величинами доплеровской скорости когерентного эха в E-области.

## Low Atmosphere, Ozone





## **Some results of atmospheric currents and acoustic-gravitational waves measurements in Apatity**

A.I. Akhmetov, Yu.V. Fedorenko, M.I. Beloglazov, V.A. Shishaev (*Polar Geophysical Institute, Apatity, Russia*)

We report the preliminary results of joint measurements of atmospheric current, acoustic-gravitational waves and meteorological parameters performed on the PGI range in Apatity. A brief description of atmospheric pressure gauge developed on the basis of small-size liquid microbarograph and its electronic circuit is given. Such two gauges are installed spaced apart by  $\sim 3$  kilometers. A system of registration of atmospheric electric current and a block diagram of system and data stream are also discussed. It is shown that there are intervals, when the forms of signals from microbarograph and antenna of atmospheric currents are nearly coincident at the frequencies of  $\sim 0,001$  Hz. Thus, under 'good weather' conditions (the wind velocity of  $\sim 1$  m/s), the duration of similarly shaped signals can reach 2,5 hours, whereas in windy weather only 30-40 minutes.

## **On the influence of geomagnetic activity on atmospheric intensity at the Kola Peninsula**

M.I. Beloglazov, L.A. Pershakov, G.P. Beloglazova (*Polar Geophysical Institute of the Kola Science Centre RAS, Apatity*)

Some results of low-latitude atmospheric intensity measurements made at PGI atmospheric range in Apatity are presented. The measurements started in 2003 at frequencies 1-300 Hz. This range covers practically the entire spectrum of resonant frequencies of the globe. It is found that in quiet conditions the atmospheric intensity has two maxima – the morning maximum about 03-06UT and the evening one about 16-20UT. From Apatity neutron supermonitor data for the whole previous observational period, i.e. from July 2003 to September 2005, 10 events of significant Forbush-decrease (reduction of galactic cosmic rays intensity by 4 % and more) were selected. The observations at the Kola Peninsula indicated that in all chosen events, in the mentioned above frequency range, a reduction of intensity and advent frequency down to complete vanishing is observed.

In addition, the period from November 2004 to October 2005 has been considered. For each month, both the most disturbed and quietest days (database of the global Kp-index got out: U.S. Dept. of Commerce, NOAA, Space Environment Center, [http://jro.igp.gob.pe/database/kpindex/html/kpjoin\\_online.htm](http://jro.igp.gob.pe/database/kpindex/html/kpjoin_online.htm)), which were not covered by Forbush-periods, were selected. It is revealed that for most part of the year, an increase in geomagnetic activity is accompanied by a reduction of atmospheric intensity. Only in June and July the atmospheric intensity, registered in high latitudes in geomagnetically disturbed periods keeps nearly the same as in the quiet periods. However, even in the summer period, on 22 July 2004, the Forbush-effect resulted in an essential reduction of atmospheric intensity. Besides, on 09 May 2005, which was a day of "good" weather, the evening maxima in atmospheric intensity were absent. We relate this fact to the increase of geomagnetic activity: on this day the Kp-index increased from 2 in the morning up to 4-5 in the evening (see <http://jro.igp.gob.pe/database/kpindex/html/kpjoin.htm>). Therefore, it can be concluded that the atmospheric intensity registered in high latitudes is much more dependent on geomagnetic conditions than on meteorological factors.

## **On the atmosphere stratification effect in the ground-level ozone concentration in the Kola Peninsula**

V.I. Demin, M.I. Beloglazov (*Polar Geophysical Institute, Apatity, Russia*)

The difference of hourly mean ozone concentration in Lovozero and on top of the Lovchorr Mountain exhibits a positive correlation with the difference in temperature observed in these two points during summer period. The correlation coefficient is 0.72 for all summer months. However, the correlation coefficient made 0.88 during the period from 31 July to 06 August 2004 when a slow-moving anticyclone settled down above the Kola Peninsula and the atmospheric fronts did not pass. The reason is as follows. The air temperature on top of the Lovchorr Mountain and that at the altitude of 1095 m in the free atmosphere (according to sounding data in Kandalaksha) differ insignificantly (the correlation coefficient is more than 0.95; the mean temperature difference is less than 3°C for 00 UT and less than -1°C for 12UT during summer months). Hence, we can assume that the difference in the temperatures on top of the Lovchorr Mountain and in Lovozero and vertical air temperature gradient in the free atmosphere in the layer of 160-1095 m are insignificant. The positive correlation is caused by the close relation of turbulent mixing and atmosphere stratification. Unstable atmosphere stratification and, as a consequence, an intensive turbulent mixing cause smoothing of the vertical ozone profile within the mixed layer, so that the maximum ground-level ozone concentration is close to that at its upper boundary. For the case of stable stratification (at night or in winter), the turbulent exchange is caused by the dynamic turbulence, and the difference in ozone

## ***Low atmosphere, ozone***

concentrations in Lovozero and on top of the Lovchorr Mountain depends on wind velocity.

### **Changes in the ozone contents at the Kislovodsk mountain observatory during the foehns caused by the air crossing of the Big Caucasian ridge**

V.I. Demin<sup>1</sup>, N.F. Elansky<sup>2</sup>, I.A. Senik<sup>2</sup>

<sup>1</sup>*Polar Geophysical Institute, Apatity, Russia,*

<sup>2</sup>*Institute Physics of Atmosphere, Moscow, Russia*

The Big Caucasian ridge is stretched hundred kilometers from the North-West to the South-East. The large extent and significant altitudes make difficult a horizontal airflow around the mountain range and the air is forced to cross over the ridge. There is a southwest or southern air current toward cyclone center when cyclones are moving northward of the Caucasus Mountains. These air currents have a descending component on the northern (leeward) slope of the mountain ridge.

The rising air is enriched with ozone in the upper atmosphere levels. This air causes an increase of ozone concentration in the foothill regions when it is lowering. We detected this effect at the Kislovodsk mountain observatory of the Institute of Atmospheric Physics. The observatory is located on the northern slope of the Caucasian ridge (2070 m asl, the Shadzhatmaz Plateau).

The air crossing of the Big Caucasian ridge and subsequent lowering were detected by the technique of the backward trajectories [<http://www.arl.noaa.gov>]. The time when the descending air appears at the station level was established by the characteristic foehn effects. The ozone concentration increases are 15-25 ppb in the present synoptical state.

### **Monitoring of stratospheric ozone in Arctic from a board icebreaker «Kapitan Dranitsyn»**

A.A. Krasilnikov, Y.Y. Kulikov, V.G. Ryskin (*Institute of Applied Physics, Nizhny Novgorod, Russia*)

In this paper we report on ozone perturbations in Arctic stratosphere observed in August 2005 with a microwave spectrometer. The device (new mobile ozonometer) was used in observations of stratospheric ozone in polar latitudes from a board of the icebreaker «Kapitan Dranitsyn» on the route Murmansk-Severnaya Zemlya-Murmansk (the extent of the route is ~ 7500 km) in the period from 9 August to 24 August 2005. The purpose of the trip was a research of the vertical structure of ozone layer. Extraordinary low total content of ozone with the large space of a covering was observed. In the observations of stratospheric ozone in Arctic (70°N - 81°N) from a board of icebreaker an unexpected result was revealed, namely, low maintenance of O<sub>3</sub> at altitudes 22-60 km, three times smaller than the average monthly value for these latitudes. Thus the vertical structure of ozone distribution was broken at heights 22-35 km.

*Acknowledgments.* We thank general director Aleksey Mironov «Poseidon Arctic Voyages Ltd» for financial support of the present work. We express deep gratitude Murmansk Shipping Company in person Nikolay Rumyantsev, and also to the captain of ice-breaker Alexander Zaerko and a team for assistance in performance of research work.

### **On the influence of the non-spherical form of the Earth on the global neutral wind system in the lower and middle atmosphere**

I.V. Mingalev and V.S. Mingalev (*Polar Geophysical Institute, Apatity, Russia*)

Recently, we have developed two versions of the mathematical model of the global neutral wind system in the lower and middle atmosphere. In the first version of the model, the surface of the Earth is supposed to be a sphere. In the second version, the Earth's surface is assumed to approximately coincide with an oblate spheroid, with the radius at the equator being larger than that at the pole. In the present study, these two modifications of the model are employed in order to clear up how the non-sphericity of the Earth influences on the formation of the planetary circulation of the lower and middle atmosphere. The steady-state distributions of atmospheric parameters are calculated using two versions of the model for conditions when summer is in the Northern Hemisphere. The simulation results indicate that the non-sphericity of the Earth affects noticeably the formation of the global neutral wind system in the lower and middle atmosphere.

## Impact of dry deposition on the surface ozone variability

O.A. Tarasova<sup>1</sup>, G.I. Kuznetsov<sup>1</sup>, N.F. Elansky<sup>2</sup>

<sup>1</sup>*Atmosphere Physics Dept., Faculty of Physics, Lomonosov Moscow State University, Moscow, Russia*

<sup>2</sup>*Institute of Atmosphere Physics RAS, Moscow, Russia*

Dry deposition on the surface is a well-known sink of surface ozone under unpolluted conditions. It defines the vertical gradients of ozone concentration in the surface layer, depending on meteorological conditions, in particular, on atmospheric boundary layer stratification and on the surface type. Several field experiments, namely, the measurements above the ground and sea surfaces in the Crimea and above different surfaces in Zvenigorod, have been performed to study the role of deposition in surface ozone levels. It is confirmed that in the rural conditions in Zvenigorod, a pronounced vertical gradient is observed in the surface layer, with the concentrations being of ~ 20 ppb higher at 10 m altitude than at 1.5 m above the grass surface. At the same time, the measurements set from the platform, sited 650 m away from the shore at the Black Sea, did not reveal such gradients. Ozone concentration above the sea exceeded the one over the land, which is in agreement with the findings of INDOEX campaign (Lal and Lawrence, 2001). Previously, the costal horizontal gradient had been detected by our group while analyzing surface ozone measurements at European network of EMEP project ([www.emep.int](http://www.emep.int)).

The field experiments performed by our group in summer 2005 showed that the ozone concentration inside an enclosure made of ozone compatible material (polyethylene) of 1 m<sup>3</sup> volume, decreases exponentially with a characteristic time of about 3 minutes over asphalt and wood and 3.2 minutes over grass (this for a transparent polyethylene sheet). This time scale increases when the frame is covered by a second layer of black polyethylene and a third white polyethylene layer (to prevent thermal heating), and reaches 7.2 minutes for wood surface, 3.7 minutes for grass and stinging nettle and 4.9 minutes for asphalt. These estimates are rather qualitative but they can serve as an example that clears up the contribution of dry deposition to surface ozone variability.

The formation of the temperature inversion creates favorable conditions for pollutant accumulation in the PBL. Moreover, stable temperature inversions can play in the case of ozone the same role as "a box" in the experiments described above. By preventing ozone mixing with higher ozone-rich layers of the free troposphere, it leads to strong ozone depletion. Estimates obtained for several TROICA expeditions showed that in average, in all expeditions ozone concentration is lower under inversion (between 2.4 ppb for spring condition to 11.6 ppb for summer conditions) which confirms stronger ozone deposition on the earth's surface in summer.

With regard to the highlighted effects of vertical ozone gradient formation in the surface layer, it is of great importance to unify the methodology of surface ozone concentration measurements to avoid systematical shifts in data.

## Synchronous manifestations of 160-min pulsations of the ground pressure in the area of Russia

V.Ye. Timofeev<sup>1</sup>, L.I. Miroshnichenko<sup>2</sup>, S.N. Samsonov<sup>1</sup>, N.G. Skryabin<sup>1</sup>

<sup>1</sup>*Yu.G. Shafer Institute of Cosmophysical Research and Aeronomy, 31 Lenin Ave., 677980 Yakutsk, Russia*

<sup>2</sup>*N.V. Pushkov Institute of Terrestrial Magnetism, Ionosphere and Radio Wave Propagation, 142190 Troitsk, Moscow Region, Russia*

The oscillations of ground pressure with a period of ~ 160 min in December, 2003 and March, 2004 relative to the zeroth meridian are studied from 5-min data of 4 stations separated in longitude in the area of Russia. The choice of time is stipulated by the fact that in December the area of Russia is closest to the direction towards the Galaxy center under such a choice of the reper point (through the Earth). The most removal of the zeroth meridian from this direction is in March. If we suppose that the 160-min pulsations come from the Galaxy center, then they should synchronously manifest in the area of Russia most distinctly in December.

Indeed, as our analysis proves, in December these oscillations synchronously manifest in Moscow, Yakutsk, Apatity and Tixie, mainly in the form of "packets" (quanta) in 2-5 impulses. The mean amplitude of synchronous variations in the area of Russia is ~ 0.0115 mb. In other seasons, the observed synchronism and manifestation of oscillations in the form of packets are much worse.

We suppose that 160-min pulsations of the ground pressure are not associated with the pulsations of Sun brightness, for they are most pronounced in the time when the station is near the direction towards the Galaxy center.

## **Regression relations of surface ozone and meteorological parameters and possibilities of surface ozone forecasting**

A.M. Zvyagintsev<sup>1</sup> and I.N. Kuznetsova<sup>2</sup>

<sup>1</sup>*Central Aerological Observatory, Dolgoprudny, Russia*

<sup>2</sup>*Hydrometeorological Research Center of Russia, Moscow, Russia*

The importance of surface ozone forecasting in the Central Russia Region is obvious and confirmed by several strong surface ozone episodes in the Moscow region for the last 10 years. The episodes in Moscow region in 2002 were among the most severe ones in the whole Europe. Similar episodes were also observed in other Russian regions (Novosibirsk, Tomsk region, etc.). All surface ozone episodes were associated with so-called adverse meteorological conditions. We have found that surface ozone episodes are observed only in some meteorological situations characterized by a definite values of “meteorological pollution potential”, which is calculated in the Hydrometeorological Research Center. Earlier we found that the surface ozone anomalies are strongly related to the meteorological ones and their regression relations can be obtained. Among the most significant predictants of surface ozone, we can name temperature, relative humidity, wind speed (we suppose that for ordinary nonmountain stations the most suitable is the mean wind speed in the planetary boundary layer). So we develop an empirical model for surface ozone forecasting that uses actual meteorological parameters and their forecasting values. Our forecasting model was testified for observations in the Moscow region and at German stations which send their data to the WDCGG in Japan. Such model is better than “climatic” and “inertia” ones and can ensure determination coefficient ca. 50%.

## **On climatic variations in the Khibiny mountains**

Yu. L. Zyuzin<sup>1</sup>, V.I. Demin<sup>2</sup>

<sup>1</sup>*Center of Avalanshe Sufety OAO „Apatit“, Kirovsk, Russia*

<sup>2</sup>*Polar Geophysical Institute, Apatity, Russia*

The results of analysis of meteorological observations that have been performing at the mountain-avalanche station "Central" of the OAS "Apatit" from 1962 up to present time are shown.

The temperature increase is detected. The trend is the most appreciable in the last 15 years. Thus the increase of the mean summer temperature is about 2°C. There are also trends in winter temperatures and precipitations. However, we cannot state unambiguously that this increase is caused by the Global Warming. So, the data of the meteorological station “Yukspor” (1932-1980) indicate that an appreciable negative temperature trend was in the region from 1930 to 1960. In this connection, the current temperature increase can also be considered as a recovery to “the climatic normal” of the thirtieth years.

The data of the nearest flat stations have not eliminated this uncertainty.

## **Планетарные волны в общем содержании озона южной полярной области**

А.В. Агапитов, А.В. Грицай, А.М. Евтушевский, Г.П. Милиневский (*Киевский национальный университет имени Тараса Шевченко, Украинский антарктический центр*)

На материалах измерений общего содержания озона (ОСО) комплексом TOMS, установленного на борту КА серии Nimbus рассмотрены вариации ОСО в широтном поясе 50°–70° ю. ш. во время существования зимней озоновой в аномалии. Изменения ОСО на краю озоновой дыры представляют собой баротропные волны Россби, распространяющиеся на высотах нижней стратосферы, где находится максимум высотного профиля содержания озона. Определяющую роль для скорости их распространения играет меридиональный профиль атмосферного давления.

Табл. 1. Скорость движения гармоник волн Россби: теоретическая и наблюдаемая

Номер гармоники	1	2	3
Скорость движения без учета градиента давления и зонального потока, м/с	-37,63	-19,24	-10,6
Наблюдаемая скорость движения, м/с	1,7	9,53	13,85

Табл.2. Параметры волн Россби теоретические и восстановленные по данным TOMS и NOAA

Дата, широта	теоретические		восстановленные	
	$r_R$ , км	$V_R$ , м/с	$r_R$ , км	$V_{\text{зонального потока}}$ , м/с
60 ° ю.ш.	2177	54	2010±300	49,4
65 ° ю.ш.	2081	42	1850±280	36,5
70 ° ю.ш.	2007	32	1780±260	25

На основе анализа измерений TOMS космических аппаратов серии Nimbus и базы данных по атмосферному давлению NOAA показано, что:

- в широтном диапазоне 60° ю. ш. - 70 ° ю. ш. ОСО является хорошим индикатором волновой активности планетарного масштаба;
- широтная структура ОСО в широтном диапазоне 60° ю. ш. - 70 ° ю.ш. описывается в приближении первых трех гармоник с точностью до 5%;
- меридиональный профиль давления в широтном диапазоне 60° ю. ш. - 70 ° ю. ш. имеет определяющее влияние на возможность существования волн Россби планетарного масштаба и их пространственно-временные характеристики – зависимость фазовой скорости от широты
- численное моделирование динамики волн Россби в линейном приближении показало устойчивость волны-1 в широтном диапазоне 60° ю. ш. - 70 ° ю. ш.. Характерное время существования волны-2 и волны-3 несколько дней, что соответствует данным наблюдений.

### Многолетние вариации приземной концентрации озона и их возможные причины

Белан Б.Д. (Институт оптики атмосферы СО РАН, 634055, г. Томск, пр.Академический, 1, e-mail: bbd@iao.ru)

Измерения счетной концентрации аэрозоля, вначале с самолета-лаборатории над территорией Западной Сибири, а затем приземные измерения аэрозоля в районе Томска, выполненные сотрудниками ИОА СО РАН в 80-х – 90-х годах, выявили, что эта компонента воздуха испытывает многолетнюю изменчивость, близкую к периоду 11 лет. Оказалось, что в период с 1983 по 1988 г.г. счетная концентрация аэрозоля уменьшалась, а с 1990 года начала возрастать. Затем был перерыв в измерениях. Следующий падения концентрации начался в 1994 году (ровно через 11 лет) и завершился в 1999 году, после чего концентрация аэрозоля снова начала нарастать. Таким образом, в течение почти 20 лет наблюдалось два многолетних цикла уменьшения и увеличения концентрации аэрозоля. Причем изменение концентрации произошло в 80-х годах в 5 раз, а в 90-х годах – почти в 20 раз, что многократно превышает возможные ошибки измерений.

Концентрация озона начала измеряться позже. Сейчас имеется ряд продолжительностью 16 лет. Однако и она выявляет подобный аэрозолю многолетний ход. Исключение составляет 1995 год. Причина падения концентрации озона в этом году пока не установлена.

Сопоставление полученных результатов с данными измерений в других регионах показало, что подобные многолетние изменения зафиксированы и в других районах.

Д. Хоффман по баллонным измерениям счетной концентрации аэрозоля выявил над США в период с 1983 по 1989 год падение счетной концентрации в слое 5-10 км почти на порядок и примерно в 3 раза в слое 2-5 км, что по времени и величине близко к вышеприведенным данным. Анализ аэрозольной оптической толщи за период с 1980 по 1996 год в Польше, показал, что в те же периоды, как и в Томске, наблюдалось медленное ее падение ~7.4 % в год и быстрое восстановление в период роста. Близкую картину получила для аэрозольной толщи в Москве и Г.М. Абакумова.

Тренды концентрации озона, близкие по времени к нашим, обнаружены для Кисловодска, для Греции, в Финляндии, в Дании .

Следовательно, многолетние вариации аэрозоля и озона имеют не случайный и не региональный характер. Более того, они отражают проявление каких-то закономерностей, имеющих, по крайней мере, полушарный характер.

Для нахождения причин этого явления последовательно были проанализированы озоновый механизм, последствие вариаций прихода УФ-радиации, которые вывели на промежуточный вариант. Этот механизм обусловлен взаимодействием усиливающейся УФ-радиации с растительностью. В начале процесса роста УФ-радиации происходит угнетение растений, после 1-2 годичного процесса адаптации, у них усиливается продуктивность, что приводит к выбросу в атмосферу дополнительного количества озон- и аэрозолеобразующих веществ. Эта гипотеза проверена с помощью нормализованного индекса вегетации и дала хорошие результаты.

## **Самолетные технологии в исследовании окружающей среды и их применение на примере Норильска**

Б.Д. Белан (*Институт оптики атмосферы СО РАН, 634055, г. Томск, пр. Академический, 1, e-mail: bbd@iao.ru*),

Сложная экологическая ситуация, возникшая в ряде районов в результате активного вмешательства человека в природную среду, требует адекватных действий по стабилизации состояния, созданной из природной, окружающей среды. Чтобы действия имели целенаправленный и положительный характер необходима полная и достоверная информация о ее состоянии. В настоящее время разработано достаточно много разных методов, которые применяются для определения характеристик окружающей среды. Одним из них является метод самолетного зондирования атмосферы и подстилающей поверхности. Описанию применения этого метода и некоторых результатов, полученных с его помощью, и посвящена данная работа. Методология самолетного зондирования атмосферы применительно к оценке качества состояния воздушного бассейна крупных промышленных центров, включает несколько схем маршрутов «крест», «квадрат», «галсы», пересечение шлейфов, что позволяет определять состав и объем выбросов основных источников примесей, баланс различных соединений, поступающих и выходящих из города, оценивать потоки, осаждающиеся на поверхность.

Города и территории, в которых эта методология была ранее реализована: Павлодар, Усть-Каменогорск, Хабаровск, Комсомольск-на-Амуре, Амурск, Кемерово, Нижний Тагил, Нижневартовск, Улан-Удэ; Норильск; месторождениях: Мегион, Самотлор; на полуострове Камчатка, в Прибайкалье. В ходе самолетного зондирования были получены оригинальные результаты, многие из которых не имеют аналогов в мире.

Работа выполнена по программе СО РАН 24.3.3, при поддержке междисциплинарного проекта СО РАН №130, программы Президиума РАН №13.4, грантов РФФИ 04-05-64559 и 04-05-08010.

## **О контроле содержания озона в приземном слое на территории Российской Федерации**

В.И. Демин<sup>1</sup>, А.М. Звягинцев<sup>2</sup>, И.Н. Кузнецова<sup>3</sup>, О.А. Тарасова<sup>4</sup>

<sup>1</sup>*Полярный геофизический институт, г. Апатиты, Россия*

<sup>2</sup>*Центральная аэрологическая обсерватория, г. Долгопрудный, Россия*

<sup>3</sup>*Гидрометеорологический научный центр России, г. Москва, Россия*

<sup>4</sup>*Московский Государственный университет, г. Москва, Россия*

По санитарно-гигиеническим нормативам (см, например, ГН 2.2.5.1313-03 от 15.06.03) озон отнесен к группе наивысшей опасности, подлежащих непрерывному контролю,

В настоящее время в России нормируются две характеристики приземного озона: максимально разовая (средняя за 20-30 минутный промежуток времени) и среднесуточная концентрации. В качестве ПДК для максимально разовой концентрации озона установлено значение 160 мкг м-3 и для среднесуточной - 30 мкг м-3 (что для равнинных станций соответствует 80 и 15 млрд-1).

В России длительные и регулярные измерения проводятся сетевыми подразделениями и учреждениями Росгидромета в 7 федеральных центрах, организациями РАН в Москве, Томске, Улан-Удэ, Кисловодске и в Ловозеро (Мурманская область).

Результаты наблюдений приземного озона показывают, что случаи превышения максимальной разовой ПДК происходят нечасто. Их нигде не было зарегистрировано более 10 раз в году и они наблюдаются не каждый год. В ряде регионов (например, Северо-Западном федеральном округе) таких случаев не было зарегистрировано вовсе.

Что же касается превышения нормы среднесуточной ПДК, то здесь ситуация совершенно иная. В Москве, среднесуточная концентрация озона ежегодно превышает ПДК около половины дней в году. По данным СибНИГМИ, аналогичный показатель имеет место и в Новосибирске. В Ловозеро (район фонового мониторинга) среднесуточные концентрации озона превышают ПДК в течение около 95 % дней в году, в то время как максимальные разовые концентрации озона к ПДК даже не приближаются. Это обстоятельство, несомненно, указывает либо на недостаточную обоснованность российского норматива для среднесуточной концентрации озона и требует его пересмотра или отмены, либо на необходимость принятия мер с целью защиты здоровья населения. Следует отметить, что вышеуказанный российский норматив для максимально разовой ПДК озона близок к установленному Европейским Союзом уровню 180 мкг м-3, в то время как

среднесуточные концентрации озона за рубежом не ограничиваются.

Результаты многолетнего мониторинга приземного озона в фоновых районах указывают на целесообразность обращения в Минздрав РФ с предложением отказаться от нормирования среднесуточной концентрации озона, либо, в крайнем случае, пересмотреть ее значение.

### **Решение фундаментальных и прикладных задач по изучению околоземного космического пространства с помощью воздухоплавательной техники**

Т.И. Сысоева, С.П. Черников (*ФИАН, Москва, Россия*)

В докладе будут рассмотрены следующие эксперименты по измерениям:

1. КЛ сверхвысоких энергий (эксперимент "Сфера");
2. градиента магнитного поля;
3. высотного хода содержания озона;
4. вредных выбросов в атмосферу;
5. солнечных нейтронов;
6. нейтрино (эксперимент RADICAL на ст. Восток Антарктида).

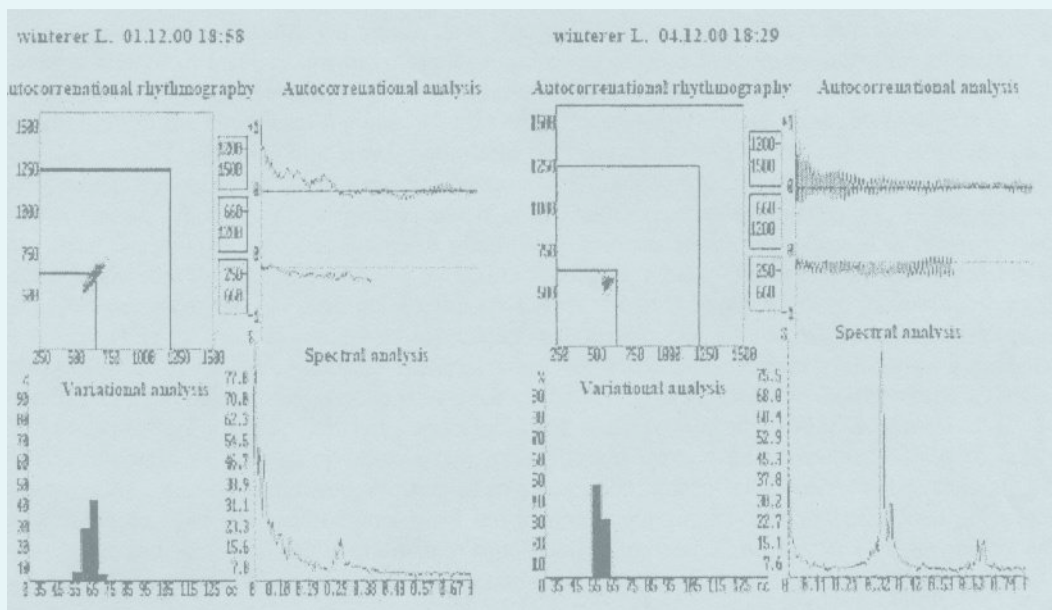
Далее будет представлен обзор средств отечественной воздухоплавательной техники различного назначения, в том числе и разработанных в последнее время для научных исследований, задач военного назначения и других целей (защита окружающей среды от вредных выбросов в атмосферу, реклама, голография, воздухоплавательные шоу и прочее).

Кроме того, будут рассмотрены поисковые работы по стартам отечественных аэростатов в высоких широтах, вокруг северного и южного полюсов, средней полосе (озеро Байкал) и на полигоне Хайдеабат (Индия).

Также представлен большой фото и видео материал о последних стартах аэростатов в Вольске и Антарктиде.



# Heliobiosphere





## How can geomagnetic reversals be related to biological evolution?

Natalia K. Belisheva<sup>1</sup>, Helfried K. Biemat<sup>2</sup>, Helmut Lammet<sup>2</sup>, Charles S. Cockell<sup>3</sup>

<sup>1</sup>*Polar-Alpine Botanical Garden Institute, Kola Scientific Centre, Russian Academy of Sciences,*

<sup>2</sup>*Space Research Institute, Austrian Academy of Sciences, Graz, Austria*

<sup>3</sup>*Planetary and Space Sciences Research Institute, Open University, Milton Keynes, UK*

Through paleomagnetism, scientists now have solid proof that the Earth's magnetic field, and thus the geomagnetic north and south poles, have reversed themselves many times in the past. How could reversing polarity be related to evolution and development of living systems? We have studied the connection between a number of insect and terrestrial tetrapods families and duration of periods with normal and reverse polarities from early Cenozoic period (84 Mya) towards Neogene (23-0 Mya). It was found that duration of periods of the normal and reverse polarities decreased from Paleogene to Neogene. In concordance with the rate of changes of the magnetic polarity, the number of living families are increasing.

Following each revitalization, the dipole field strength is fluctuating. This means that the geomagnetic cut-off (the minimum energy of primary cosmic particles required to reach a specific point on the planetary surface) should be also fluctuating during changes of polarity from a minimum (theoretically zero) to maximum (as for actual dipole field strength in the equatorial regions, where vertical cosmic ray cut-off is about 13-17 GeV). In the present time, the influence of the Earth's dipole magnetic field configuration results in a better protection against high energetic particles near the equator than in the polar areas, which leads to lower dose of irradiation in equatorial than in polar regions. Hence, when the geomagnetic cut-off is low, the exposure to cosmic rays of living systems is high. The more often the polarity changes, the more often living systems should be exposed to high intensity of cosmic rays, and, consequently, the rate of biological evolution should be higher. This is that we can see in Neogene.

Our experiments carried out during a great solar events, when the solar particle fluxes increase in  $10^5$  in near-earth space and when such an increase was associated with an increase of secondary cosmic rays near Earth's surface, multiple lesion of DNA containing material were revealed. Such research allow to assess the significance of secondary cosmic rays on the genetic substance of the cell systems near the Earth's surface (Belisheva et al., 1994; Belisheva and Popov 1995; Belisheva and Gak 2002; Belisheva et al., 2002; Belisheva et al., 2003). During and after the increase of secondary cosmic rays near Earth's surface simultaneously in such cell lines cell fusion, gigantic nuclei, nuclei association, chromatin fragmentation, micro-cells, micronuclei, separate chromosomes were found. Such sorts of phenomena could had led to producing multi-cellular structures, polyploidy, multiplication gene copies and etc., that are evolutionary significant materials. This means, that secondary cosmic rays on the Earth's surface potentially are a powerful source of genetic diversity, supplying by material for evolutionary process.

However, the intensity of cosmic ray fluxes and the area impact are modulated by magnetosphere structure and magnetic field strength. When the magnetic strength decreases, that should be during the polarity reversal, the effect of cosmic ray impact can be increasing. We suppose that the Earth's magnetosphere not only protects of living systems to the exposure of cosmic rays, but also promotes damage reparation in opposite of irreparable damages on the Earth's orbit (Akoef et al. 1989), where the magnetic field strength is low.

We believe that cosmic rays and geomagnetic field can be the driving forces of biological evolution.

## Investigation of sensitivity and noise characteristics of the bioeffective UV radiation sensors in field conditions

S.Chernouss<sup>1</sup>, N.Perevozchikov<sup>2</sup>, V.Shishaev<sup>1</sup>, O.Antonenko<sup>1</sup>, A.Mikhaylov<sup>3</sup>, N.Belisheva<sup>4</sup>

<sup>1</sup>*Polar Geophysical Institute KSC RAS, Apatity, Murmansk region*

<sup>2</sup>*Moscow Institute of Physics and Technology, Dolgoprudniy, Moscow region*

<sup>3</sup>*Kola Branch of the Petrozavodsk State University, Apatity, Murmansk region*

<sup>4</sup>*Polar-Alpin Botanical Garden-institute KSC RAS, Apatity, Murmansk region*

There are described optical equipment to measure ultra violet (UV) and photosynthetically active radiation (PAR) of Sun by different methods. Absolute calibration of the devices is under consideration. First measurements of the Solar radiation in spectral ranges of UV-A ( 320 - 400 nm ) , UV- B (290 - 320 nm ) and PAR ( 400 - 700 nm ) carried out at PGI Apatity range by the Eldonet dosimeter are presented. Testing of the Physics and Technology Institute (FTI) optical sensor on the basis of gas filled photocell (I) was provided. Comparison of measurements produced by the FTI sensor with the Eldonet dosimeter simultaneous measurements demonstrates a good correlation of data in the UV spectral ranges. Temporal dependences of the FTI sensor noise during several months

## *Heliobiosphere*

are presented and discussed. Attempt of estimation of some sources of noise was done. Bioeffectivity of Solar UV radiation in different spectral ranges is under discussion. It seems to be possible to use the FTI sensor in field measurements as indicator of bioeffective Solar radiation.

Authors thanks to RFBR grants: 05-04-97511\_r-sever-a and 06-04-90603- BNTS-a for support of this work.

(1) N.F.Perevozchikov, V.F. Sharikhin // *New kind of electromagnetic radiation of the Sun as one of the mechanisms of Solar-Terrestrial Relations*// in "Cosmic Weather and its connection with geophysical and meteorological processes", publ. by Internatiomnal Crimean Conference "Cosmos and Biospere Partenit", Crimea, Ukraine, 2003, p. 57-58.

## **A measuring complex for tree-rings analysis**

A.G Kanatjev<sup>1</sup>, O.I. Shumilov<sup>1</sup>, E.A. Kasatkina<sup>1</sup>, I.Yu. Kirtsideli<sup>2</sup>

<sup>1</sup>*Institute of North Industrial Ecology Problems, Kola Science Center RAS, Fersmana str. 14, 184209 Apatity, Russia*

<sup>2</sup>*Botanical Institute RAS, St.-Petersburg, Russia*

A special complex has been designed for the annual tree-ring widths measurement and analysis. it consists of professional scanner Epson Perfection 4990, computer system and software. This complex allows processing of juniper samples having got a complex structure (a lot of missed, light and false rings). The created complex in many aspects does not yield the similar system WinDENDRO, designed on the West, but in comparison to manual measurement systems, it offers a number of advantages: productivity gain, possibility of archiving the results of the measurements at any stage of the processing, operator comfort. For the first time in Russia (or may be independently) it has been developed a new software, allowing processing of samples of different types (cores, saw cuts), including those which is difficult to process, having got a complex wood structure (inhomogeneity of growing in different directions, missed, light and false rings etc.). This software can analyze pictures made with optical scanners, analog or digital cameras. The complex software program was created on programming language C++, being compatible with modern operating systems like Windows XP. Annual ring widths are measured along paths traced interactively. These paths can have any orientation and can be created so that ring widths are measured perpendicular to ring boundaries. A graphic of ring-widths in function of the year is displayed on a screen during the analysis and it can be used for visual and numerical cross-dating and comparison with other series or master-chronologies. Ring widths are saved to the text files in a special format, and those files are converted to the decadal (Tucson) format accepted for data conservation in the International Tree-Ring Data Bank. The created complex is universal in application that will allow its use for decision of the different problems in biology and ecology. With help of this complex it has been reconstructed a long-term (1328-2004) tree-ring chronology on the base of juniper and pines samples collected at Kola Peninsula in 2004. These juniper trees seem to be the oldest ones (one tree is 676 years old) found in Europe up to date.

The work was partially supported by Russian Foundation for Basic Research (grant N 05-04-97528).

## **Some contemporary patterns in long-term global dynamics of terrestrial biota suggesting geophysical mediation**

P.A. Kashulin, N.V. Kalachveva (*Polar-Alpine Botanical Garden-Institute, Apatity, Russia*)

The some contemporary features of temporal patterns in year-to-year population dynamics of both terrestrial flora and fauna at various Earth regions are considered under point of view of exogenous geophysical driving hypothesis. Of especial interest findings are related to prevalence of 2-3 year span periods in the dynamics at the definite geographical regions. The biological population parameters were as follows: small mammal abundance, annual gross bio productivity, arboreal plant seeds masting phenomenon, multiannual and seasonal pattern of indicator plant species flowering. In attempts to find out the reasons for the new appeared trends the comparison of those with geophysical indices was carried out. Under the definite environmental conditions and within some geographical areas the year-to-year dynamics of the population parameters found to be either chaotic or cyclic to a various extent. The parameters of the cyclic regimes with 2-3 and 4-5 years period span are considered in comparison with quasi-biennial oscillations (QBO), Northern Atlantic oscillation (NAO) and other geophysical indices. QBO presumably can affect stratospheric ozone, and consequently assumed have been of higher weight at equatorial and temperate zones of the Earth as a factor influencing ambient bio active UV-B. Respectively, the larger relative changes of UV-B irradiance are expected at higher latitudes.

On the other hand, in turns, as it were shown (Björn et al., 1997), for northern and arctic ecosystems the ambient UV-B irradiance showing the relative significant fluctuations have a greater importance for the resident biota as compared to absolute level of one. Thus, the new patterns in multiannual productivity of *Vaccinium myrtillus* etc. appeared since 1990 at the Kola Peninsula and neighboring areas with 2 yr span recurrence of extremely large fluctuations can be caused or mediated by QBO. The same explicit two years cycles are pronounced in the between year flowering onset pattern in various boreal and arctic plant species. A number of indicator species including representatives of *Sorbus* and *Vaccinium* genera between five remote each other monitoring points of the Northern Fennoscandia also exhibit pronounced brief cycles occurred with high synchronicity. The hypothesis for geophysical provenance of the new patterns in biota dynamics is supported by homology of the bio and geophysical cycles and by the presence of regional scale synchronicity which were closely linked to cyclicity.

### **Quantitative description of geomagnetic activity for study of heliogeomagnetic factors influence on the biosphere**

A.E. Levitin, L.I. Gromova, L.A. Dremukhina, E.G. Avdeeva, D.I. Korzhan (*Institute Terrestrial Magnetism, Ionosphere and Radio Wave Propagation, Troitsk, Moscow region, Russia*)

It is presented a brief review of current state of quantitative assessment of geomagnetic activity based on classic indices of geomagnetic activity used for study of heliogeomagnetic factors influence on the biosphere. Geomagnetic activity is the most visible description of state and dynamic of many physical processes in the Earth's space environment caused by energy of the solar radiation and corpuscular effect. Namely these processes rather than the geomagnetic field variations more often may generate mechanism of specific influence of magnetospheric substorms and magnetospheric storms (magnetic substorm and magnetic storm are only elements of these events) on biological objects. Therefore quantitative description of geomagnetic activity must be different for solving geophysical problems and for problems of space weather influence on human health, animals or another biological objects. Positive and negative properties of classic indices of geomagnetic activity AE(AU, AL), Kp (ap), aa, Dst, PC are analyzed. It is shown resources for more correct assessment of the Earth's magnetic field state for specific problems of space weather influence on biosphere also.

### **Reconstruction of natural water ionic composition, forming within Khibiny massif**

S.I. Mazukhina, D.B. Denisov (*Institute of the North Industrial Ecology Problems, 184209, Murmansk region, Apatity, Fersman st., 14a*)

One of the problems of present-day ecology is to estimate anthropogenic impact on water systems of the Kola Peninsula. Thus it is necessary to know natural water ionic composition as well as formation conditions. By means of paleoecological approach, based on stratigraphic investigations of diatom complexes in Goltzovoe Lake (Khibiny massif) sediments, it has been determined that the lake ecosystem has not suffered any changes since industrial development of the region started. The lake waters are, evidently, forming because of «water-rock- atmosphere» interaction, practically without technogenic factors. Such problem can be solved by thermodynamics equilibrium method (program complex (PC) «Selector»). In the model for fresh water chemical composition investigations (under temperatures from +10 to +25°C), a wide range of possible values of pH (from 1 to 12) and Eh (from 1.2 to – 0.8) was used. The component enumeration corresponded to real natural water and mineral composition of Khibiny massif. Starting enumeration of base multisystem consisted of 233 individual substances (in water solution – 92, in gas phase – 13, number of solid phase – 113). The independent components inscribe in: Al-Ar-C-Ca-Cl-F-Fe-K-Mg-Mn-N-Na-Ne-P-S-Si-Ti-Sr-H-O-e (e-electron). The solid phases of the multisystem taking into account typical Khibini mountains minerals. Based on analytical data of Goltzovoe Lake chemical composition (superficial and ground) in making the equilibrium condition of the «water solution- atmosphere» system, thermodynamics models of natural waters, including ionic composition, complex compounds formation and attenuated gases concentrations were developed. The study of «water-rock- atmosphere» system indicates low dredge contents in the lake waters and amorphous silica forming under low temperatures, which is verified by monitoring results.

As a result of investigations, the conclusion is: Goltzovoe Lake waters can be serve as natural ionic composition standard attached to comparison with lake and streams waters, forming within Khibini massif under technogenic pollution conditions.

## **Mortality dynamics assessment during 22<sup>nd</sup>-23<sup>d</sup> 11-year solar cycles in the North European region**

I.N. Peminova<sup>1</sup>, V.S. Krestov<sup>2</sup>, A.L. Kosova<sup>1</sup>, M.V. Shulina<sup>2</sup>

<sup>1</sup>*Polar Geophysical Institute, Apatity, Russia*

<sup>2</sup>*Hospital of the Kola scientific center*

The mortality essentially depends on the heliogeophysical factors in the course 11-year solar cycle. This was first described by Chizhevsky in 1930-50s, who revealed synchronous changes in the dynamics of total mortality of the world population and of the mortality from epidemic infections, and 11-year solar activity cycle. Nowadays, this finding requires a new approach from the point of view of the up-to-date interdisciplinary investigations in the fields of heliobiology, chronomedicine and chronopatology. Our analysis of North European population mortality revealed a relationship between some heliogeophysical parameters in the 22<sup>nd</sup>-23<sup>d</sup> cycles and the main causes of deaths among different age-sex population groups.

Statistical analysis of death cases has been performed for the period from 1992 to 2004 on the basis of death statements and international classification for diseases and causes of death (ICD X).

The data were provided from general observations and cover the whole set of death cases of Apatity population.

Based on data analysis, the following conclusions can be made:

- the main contribution to population mortality structure in the North European area proceeds from heart and blood circulation system diseases (49,4-62,5%), traumas, poisonings (14,6-19,7%), malignant neoplasm (9,6-15,4%);
- significant age-sex peculiarities are revealed in the dynamics and levels of both total mortality and mortality from the main death causes: heart and blood circulation system diseases and malignant neoplasm;
- the dynamics of population deaths from heart and blood circulation system diseases and malignant neoplasm is clearly related to cosmic ray dynamics; no correlation with the solar spot numbers is found.

## **Influence of geomagnetic fields on ability of human cells to repair DNA damage**

I.N. Perminova, E.V. Perminova, M.N. Yakovleva (*Polar Geophysical institute, Kola Science Center, RAS, Apatity, Russia*)

The problem of estimation of magnetic disturbance effects in human health remains one of the least investigated and at the same time the most interesting and acute for today. The investigations on human genome stability are recognized as the most informative under permanent low intense influence of geomagnetic activity. However, at present, only a small number of researches are exploring this problem. The study of one of the basic links of genome protective system, namely, of DNA repair system, provides an important information both about genotoxic effects of the influence and ability to repair DNA damage. Changes in repair activity result in accumulation of mutations which, in their turn, enhance risk of development of the oncological pathology and other diseases.

Estimating of unscheduled DNA synthesis (UDS) has been performed on whole blood cells from practically healthy volunteers (their number n was 7 at paired comparison). The results obtained in November 2004 ('the quiet period') (n=18) were compared with the data obtained in September 2005 (n=9), three days after a flash on the Sun (the Forbush-effect was observed). The specific features characterizing the life style of volunteers, which also can essentially modify the UDS index, were taken into account.

The results obtained evidence DNA repair processes inhibition during the solar flash and associated changes in geomagnetic parameters (UDS index=0,85 (av. geom.)), with the average level for the population in the Far North is 1,0-1,2. Clear distinctions in individual sensitivity to geomagnetic factor influence are observed and reflected in the increase in variability of UDS values over the whole group, which is stipulated by volunteer genotype.

## **Dendroclimatic potential of the oldest juniper trees at Kola Peninsula**

O.I. Shumilov<sup>1</sup>, E.A. Kasatkina<sup>1</sup>, N.V. Lukina<sup>2</sup>, I.Yu. Kirtsideli<sup>3</sup>, A.G Kanatjev<sup>1</sup>

<sup>1</sup>*Institute of North Industrial Ecology Problems, Kola Science Center RAS, 184209 Apatity, Russia; e-mail:*

<sup>2</sup>*Centre for Forest Ecology and Productivity RAS, 117997 Moscow*

<sup>3</sup>*Botanical Institute RAS, St.-Petersburg, Russia*

During the summer-autumn season 2004 at the remote central part of Kola Peninsula behind the polar circle at the northern timberline several tens samples of juniper (*Juniperus Siberica* Burgsd) were collected, These juniper trees

seem to be the oldest ones (one tree is 676 years old) found in Europe up to date. In spite of very hard processing procedure on account of a large amount of very thin, missing and false rings, it was possible to make a chronology and get some conclusions on past climatic variations at Kola Peninsula mainly caused, as we assume, by extraterrestrial agents (solar activity and galactic cosmic ray variations). It was obtained that:

- 1) There is a rather good agreement between long-term climatic variation in Europe and at Kola Peninsula.
- 2) The minima of solar activity Sporer (1416-1534 AD), Maunder (1645-1715 AD) and Dalton (1801-1816 AD) were accompanied by temperature decreases. Cooling at Wolf minimum end (up to 1350) seem to be seen at Kola Peninsula juniper series and is absent at European temperature trend.
- 3) Some recent decreases of solar activity around 1900 and 1960 are as well accompanied by tree growth decrease.
- 4) Kola Peninsula tree-ring chronologies don't show any great warming at the end of the XX century.
- 5) Spectral and wavelet analysis of juniper tree-ring records showed:
  - a) pronounced 22- and 80-100-year periodicities;
  - b) the main cycle of solar activity (11-year Schwabe cycle) don't reveal itself in juniper tree-ring chronologies;
  - c) 20-22-year periodicity appeared not always, but during some time intervals: 1328-1550, 1710-1800, 1985 up to present.

The work was partially supported by Russian Foundation for Basic Research (grant N 05-04-97528)

## AUTHOR INDEX

### A

Agapitov A.V.	21, 61, 78
Akhmetov A.I.	75
Alexeev I.I.	15, 31
Andreev M. Yu.	61
Antonenko O.	85
Artamonov I.V.	15, 65
Aso T.	62
Avdeeva E.G.	26, 32, 33, 87

### B

Baishev D.G.	28
Balabin Yu.V.	51, 57
Balikhin M.A.	44, 45
Balogh A.	16
Barkhatov N.A.	21, 31, 51
Baumjohann W.	16
Belakhovsky V.B.	54
Belan B.D.	79, 80
Belisheva N. K.	85
Beloglazov M.I.	75
Beloglazova G.P.	75
Belov A.V.	53
Belyaev G.	67
Besser B.P.	16
Biernat H.K.	27, 33, 54, 64, 85
Biktash L.	21, 61
Blomberg L.G.	32
Borovkov L.P.	22
Boroyev R.N.	22, 28
Bösinger T.	46
Brändström U.	62, 69
Bryukhanov V.V.	24

### C

Cao J.	47
Chebrov V.	67
Chernikov S.P.	81
Chernouss S.	85
Chernyaev A.B.	52
Chernyakov S.M.	70
Chugunova O.M.	41, 47
Cockell C. S.	85
Cornilleau-Wehrlin N.	44
Cristea E.	34
Crosby N.	46
Cumnock J.A.	32

### D

Danielides M.A.	35
Demekhov A.G.	41, 44, 46
Demin V.I.	75, 76, 78, 80
Denisov D.B.	87
Despirak I.V.	22, 41, 54
Dmitrieva N.P.	31
Doronina E.N.	66
Dremukhina L.A.	15, 16, 26, 32, 33, 87
Du A.	22, 36

### E

Efishov I.I.	27
Elansky N.F.	76, 77
Engebretson M.J.	36, 41
Erkaev N.V.	34, 54
Ermakova E.N.	71
Evtushevski A.M.	78

### F

Farrugia C.J.	27, 54
Fedorenko Yu.V.	23, 75
Fedorov E.N.	42, 46, 67
Feldstein Y.I.	15, 32, 37
Förster M.	66

### G

Getselev I. V.	52
Gladkikh M.M.	65
Golovchanskaya I.V.	42, 43
Gordeev E.	67
Gratton F. T.	27, 54
Gritsai A.V.	78
Gromova L.I.	15, 16, 26, 32, 33, 37, 87
Gubchenko V.M.	33
Gurnett D.	46
Gushchina R.T.	53
Gustavsson B.	62, 69
Gvozdevsky B.B.	51

### H

Hausieitner W.	34
Hayakawa M.	67
Heyn M.F.	27
Honary F.	43
Hviuzova T.A.	57

### I

Ishanov S.A.	62
Ismaguiov V.S.	42, 64
Ivanov I.B.	27
Ivanova T.A.	55
Ivanova V.V.	27

### K

Kalachveva N.V.	86
Kanatjev A.G.	86, 88
Karpov S.N.	52
Karpova Z.M.	52
Kasatkina E.A.	86, 88
Kashulin P.A.	86
Kat'kalov Yu. V.	23
Kauriste K.	23
Khodachenko M.L.	33
Kirchner G.	34
Kirillov A.S.	63

Kirtsideli I.Yu.	86, 88
Kleimenova N.G.	23, 25, 45
Klimenko M.V.	24
Klimenko V.V.	24
Knyazeva M.A.	63
Kopytenko E.A.	64
Kopytenko Yu.A.	42, 64
Kornilov I.A.	23, 24, 38
Kornilov O. I.	24
Kornilova T.A.	23, 24, 38
Korovinskiy D.B.	34
Korzhan D.I.	26, 32, 33, 87
Kosova A.L.	88
Kotik D.S.	71
Kotikov A.L.	64
Koustov A.V.	37
Kozelov B.V.	22, 25, 35, 38, 43, 44, 46, 67
Kozelova T.V.	35
Kozlovsky A. E.	35
Kozyra J.U.	15, 32
Kozyreva O.V.	23, 25, 45
Krainev M.B.	53
Krasilnikov A.A.	76
Krestov V.S.	88
Kulikov Y. N.	64
Kulikov Y.Y.	76
Kuznetsov G.I.	77
Kuznetsov S.N.	26, 35, 55
Kuznetsova I.N.	78, 80

## L

Lammer H.	64, 85
Lazutin L.L.	25, 35
Leitner M.	54
Levitin A.E.	15, 16, 21, 26, 31, 32, 33, 87
Leyser T.	69
Lichtenegger H. I. M.	16, 64
Lotova N. A.	54
Lubchich .A.A.	22, 41, 54
Lukina N. V.	88

## M

Macusova E.	44, 46
Malova H.V.	38
Manninen J.	23
Marples S.	43
Martynenko O.V.	15, 65
Mazukhina S.I.	87
Medvedev V.V.	62, 65, 66
Meredith N.	35
Meshalkina N. S.	55
Mikhaylov A.	85
Milinevski G.P.	78
Mingalev I.V.	38, 76
Mingalev O. V.	38, 42
Mingalev V.S.	61, 76
Mingaleva G.I.	61
Miroshnichenko L.I.	52, 57, 77
Mochalov A.	67
Moiseyev A.V.	28, 36
Molchanov O.A.	67, 72
Morente J.A.	16
Muravieva E.A.	26, 55
Musatenko S.I.	61
Myagkova I.N.	26, 55

## N

Nakamura R.	16
Namgaladze A.A.	15, 63, 66
Nozawa S.	37
Nunn D.	41

## O

Obridko V. N.	54
Ogloblina O.F.	69, 70, 72
Okhlopov V. P.	52
Onishchenko O.G.	44, 45
Osepian A.P.	69, 70
Ostapenko A.A.	45

## P

Panasyyuk M.I.	55
Parrot M.	44
Pashin A.B.	64, 67
Pellinen-Wannberg A.	62
Penz T.	27, 64
Perevozchikov N.	85
Perminova E.V.	88
Perminova I.N.	88
Pershakov L.A.	75
Pesec P.	34
Petrukovich A.A.	16
Pickett J.	46
Pilipenko V.A.	41, 42, 46
Plotnikov I.Ya.	28
Podgomy A. I.	55, 56
Podgorny I.M.	55, 56
Podzolk M. V.	52
Pokhotelov O.A.	44, 45
Polyakov S.V.	17, 45, 71
Popov V.A.	32
Prigancova A.	15, 32

## R

Ranta A.	23
Revunov S.E.	31, 51
Rietveld M.	62, 69
Rodger A.	41
Roldugin A.V.	45
Roldugin V.C.	45, 67
Romanova N.	46
Romanova N. Yu.	38
Rubinshtein I.A.	55
Rucker H.O.	33
Runov A.	16
Ruzhin Yu.Ya.	27
Rycroft M.J.	41, 46
Rypdal K.	25
Ryskin V.G.	76

## S

Sakharov Ya. A.	23
Samsonov S.N.	77
Sandahl I.	62, 69
Santolik O.	44, 46
Schekotov A. Yu.	67, 72
Schur L.I.	51

Semenov A.I.	67, 68
Semenov N.A.	42
Semenov V.S.	27, 34
Semenova N.V.	69
Senik I.A.	76
Sergeeva N.G.	72
Sergienko T.	62, 69
Shagimuratov I.I.	27
Shefov N.N.	67, 68
Shibkov S.A.	64
Shishaev V .A.	75, 85
Shukhtina M.A.	27
Shulina M.V.	88
Shumilov O.I.	86, 88
Sinitin V.	67
Sisoeva T.I.	81
Skryabin N.G.	28, 77
Solovyev S.I.	22, 36
Starkov G.V.	37
Starostin L.I.	55
Steen Å.	62
Struminsky A.B.	56
Sünkel H.	34
Surkov V. V.	69

## T

Tarasova O.A.	77, 80
Tepenitsyna N.Yu.	27
Tereshchenko V .A.	69, 70
Tereshchenko V .D.	69, 70
Timofeev V. Ye.	77
Titova E.E.	43, 44, 46
Tokar V.G.	62
Tolochkina S.V.	57
Trakhtengerts V.Y.	41, 44, 46
Treumann R.A.	44, 45
Tserkovniuk O.M.	21
Tsurutani B.T.	15, 32

## U

Uspensky M.V.	37
---------------	----

## V

Val'chuk T.E.	56
Vashenyuk E.V.	51, 52, 57
Vasiljev A.N.	45
Vasiljev E.B.	69, 70, 72
Vasilyeva E.V.	15
Vedenkin N.N.	55
Velichko V.A.	22, 28
Vinnikov V.V.	64
Vladimirsky K. V.	54
Vlasova N.A.	55
Volkov M. A.	38
Vorobjev V.G.	28, 37, 38
Voronin A.N.	46
Vovchenko V.V.	42

## Y

Yagodkina O.I.	28, 37
Yagova N.	46
Yahnin A.G.	22,46, 69
Yahnina T.A.	46
Yakovleva M.N.	88
Yanke V.G.	53
Yevlashin L. S.	28
Yumoto K.	36
Yushkov B. Yu.	55

## Z

Zalesskaya V.A.	62
Zelenyi L.M.	38
Zhang T.-L.	16
Zharkova Y.S.	62, 65, 66
Zolotukhina N.A.	47
Zverev V.L.	57
Zvyagintsev A.M.	78, 80
Zyuzin Yu. L.	78